

Physical and Numerical modelling of hybrid monopiled-footing foundation systems

By
H. Arshi

A Thesis submitted in partial fulfilment of the requirements of the
University of Brighton for the degree of Doctor of Philosophy

Declaration

This thesis is the work of Harry Arshi and presents the results and findings of a programme of experimental and numerical modelling of hybrid monopiled-footing foundation systems. This posthumously submitted thesis is unfortunately incomplete, but as Harry's supervisor I have compiled and amalgamated papers into the thesis which present a more complete picture of the research work undertaken.

The report of the examiners is presented overpage.

A handwritten signature in black ink that reads "Kevin Stone". The signature is written in a cursive style with a large, sweeping flourish at the end.

Dr Kevin Stone
August 2016

Examiners Report Post Discussion.

The examiners agreed the topic was original and the way in which the science conducted ensures an original contribution to knowledge.

The outcome of the research evidenced the usability of the tested hybrid monopiled-footing foundation system and the potential to apply this new knowledge to the industry.

The methodology deployed 3 sets of different investigative methods where normally it would be two. This adds robustness and confidence in the findings. In particular the numerical modeling after the laboratory and centrifuge testing illuminates the potential performance of the hybrid system.

Although the discussion chapter is missing from the thesis, the papers presented at the end of the thesis discuss the results and recommendations adequately.

Offshore wind farm research is relatively new concept and this work demonstrates the potential application to other offshore structures for example offshore platforms. The results were so positive that they can inform subsequent collaborative research between industry and academia to determine the transferrability of the findings from this original piece of research.

The thesis was commended for its robust reporting and thorough evidence of the outcomes of the testing procedures. This identifies clearly where further research may be directed.

The examiners wish to commend the candidate on the scope of the research and the professional manner by which the thesis was presented.

Finally, the examiners wish to comment on the effort of the supervisor in supporting Shahryar Arshi throughout the research and in the compilation of the various parts that form the final thesis submitted for examination.

To my family

 CONTENTS

1.	INTRODUCTION	1
1.1	Aims and Objectives	4
2.	LITERATURE REVIEW	6
2.1	Introduction	6
2.1.1	Offshore Pile Foundations	6
2.1.2	Parametric Definitions of the Structural System	8
2.2	Pile Foundations.....	9
2.2.1	Axial Pile Capacity.....	9
2.2.2	Laterally Loaded Pile Foundations	11
2.2.3	Failure under Lateral Loads	12
2.2.4	Ultimate Lateral Resistance & Lateral Deflection	18
2.3	Hybrid Monopile-Footing Foundation Systems.....	32
3.	MATERIALS AND EXPERIMENTAL METHODOLOGY	36
3.1	Introduction	36
3.2	Materials.....	36
3.3	Experimental methodology	37
3.3.1	Introduction	37
3.4	Single gravity testing apparatus	37
3.5	Model preparation.....	38
3.5.1	Single gravity models	39
3.6	Centrifuge tests	40
3.6.1	Introduction	40
3.6.2	University of Brighton Geotechnical Centrifuge Testing Facility.....	42
4.	SINGLE GRAVITY TESTS	44
4.1	Introduction	44
4.2	Single gravity test programme	44
	Series 1 : Lateral load bearing capacity of monopiles	44
	A summary of the series 1 tests are presented in Table 4.1.....	44
	Series 2: Vertical load bearing capacity of footings.....	44
	Series 3: Vertical load bearing capacity of skirted footings.....	45
	Series 4: Lateral load bearing capacity of monopiled-footings.....	45

4.3	Results	46
4.3.1	Monopile Tests	46
4.3.2	Footing Tests	48
4.3.3	Hybrid Monopile-Footing Tests	50
4.3.4	Skirted Hybrid Monopile-Footing Test	52
4.4	Discussion and analysis of single gravity tests	54
5.	CENTRIFUGE MODEL RESULTS	57
5.1	Introduction	57
5.2	Vertical load response.....	57
5.3	Lateral response.....	59
5.4	Discussion of centrifuge model tests	67
6.	NUMERICAL MODELLING.....	69
6.1	Introduction.....	69
6.2	Aims and objectives	70
6.3	The ICFEP model	70
6.3.1	Constitutive Model Calibration	71
6.4	ICFEP Results	71
6.4.1	Displacements.....	72
6.5	Lateral capacity	75
7.	DISCUSSION AND CONCLUSIONS	77
8.	REFERENCES	
9.	TABLES	

1. INTRODUCTION

Offshore wind farms are becoming more and more popular as a source for producing more renewable energy. The offshore wind energy industry is gaining increased momentum as many countries such as The Netherlands, Denmark and UK are considered to be the lead in terms of technology used for the design, construction and maintenance of wind turbines. (EWEA, 2004). It is thought that the potential for the offshore production of electricity in Europe is considered to be more than its consumption. (Beurskens and Jensen, 2005)

During the recent years in the UK alone, the number of wind turbines designed and installed per year has increased and this rate is to grow to an impressive number of 2.5 new turbines installed per day by the year 2020, as shown in Figure 1. This is based on the current government plans for the next round of wind farms (round 2 and 3) to be constructed 65 km from shore, illustrated in Figure 1.1. (Carbon trust analysis, 2010)

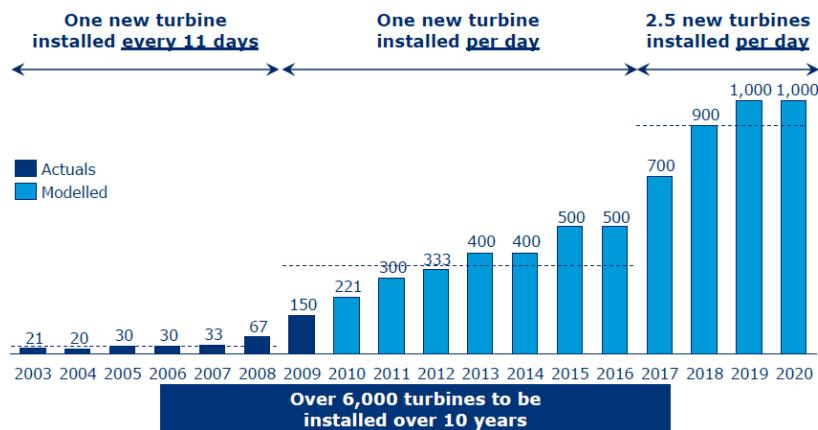


Figure 1.1 Dramatic increase on the number of wind turbines installed (Carbon trust analysis, 2010)

The types for foundations used for offshore structures are divided into four categories (Illustrated in Figure 1.3);

- Pile foundations used to the water depths ranging from 5m to over 120 m (Westage and DeJong, 2005)
- Gravity base foundations used to the depth of up to 25 m
- Suction caissons used for the depth of up to 20 m (Houlsby and Byrne, 2000)
- Floating foundations usually used for depth of greater than 50 m (DNV-OS-J101, 2004)

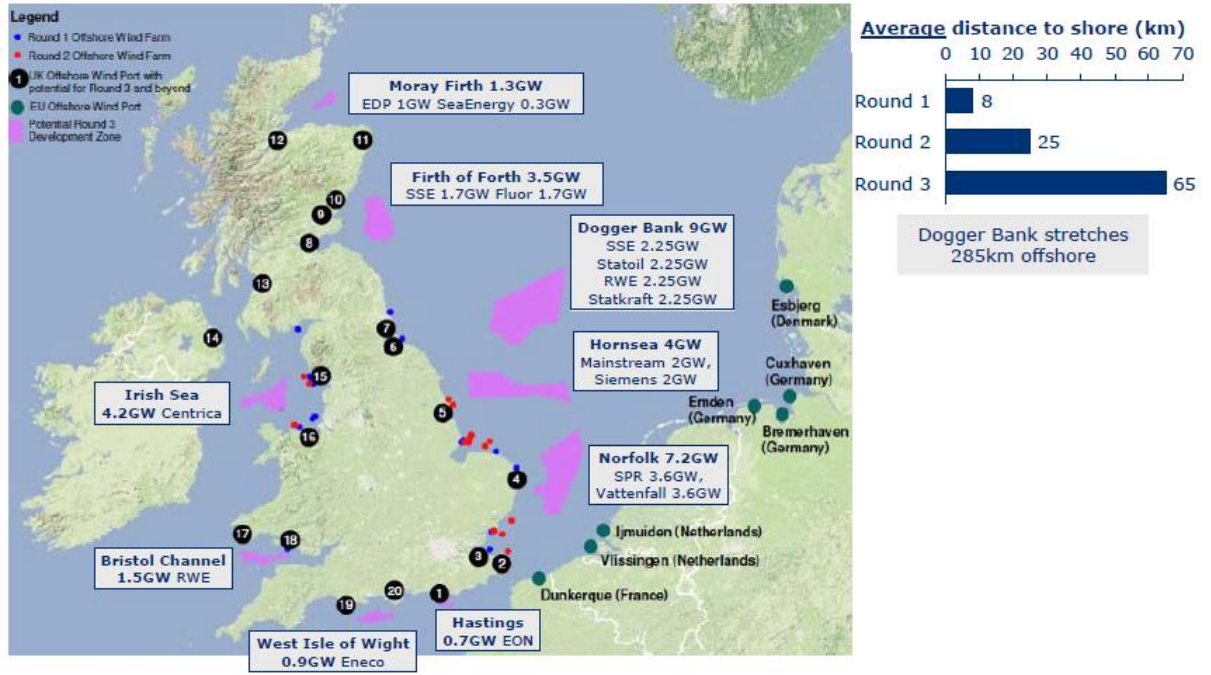
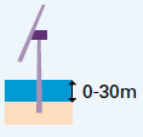
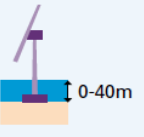
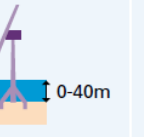
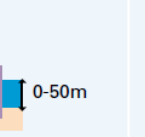

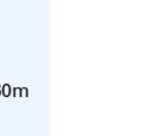


Figure 1.2 Next round of wind farms to be constructed (Carbon trust analysis, 2009)

Pile foundations transferred both compressive and tensile forces to from the structure and water above to the seabed and are the most common and preferred design solution. Operational wind turbines in the UK have monopile foundations and this popularity is due to the fact that they are simple to construct (using large steel tubing) and economical to manufacture compared to the other type of foundations available (Westage and DeJong, 2005).

	Monopile	Concrete Gravity Base	Tripod	Tri-pile	Jacket	Floating
Design	 0-30m	 0-40m	 0-40m	 0-50m	 0-50m	 >60m
Examples	Greater Gabard (UK) Egmond ann Zee (NL)	Nysted (DK) Thornton Bank (BEL)	Borkum West (DE)	Bard Offshore 1 (DE)	Beatrice (UK)	None Although used in oil & gas
Pros	<ul style="list-style-type: none"> Simple design Extended offshore tower 	<ul style="list-style-type: none"> Cheap No drilling required 	<ul style="list-style-type: none"> More stability than basic monopile 	<ul style="list-style-type: none"> Can be installed by traditional jack-up barge Piles can be built at any dock or steel mill 	<ul style="list-style-type: none"> Stability Relatively light 	<ul style="list-style-type: none"> Allows deep water use Uses less steel
Cons	<ul style="list-style-type: none"> Diameter increases significantly with depth Drilling difficulties 	<ul style="list-style-type: none"> Seabed preparation required 	<ul style="list-style-type: none"> More complex installation 	<ul style="list-style-type: none"> Cost 	<ul style="list-style-type: none"> Cost 	<ul style="list-style-type: none"> Cost

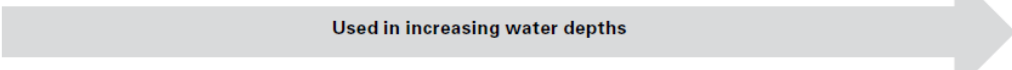
Used in increasing water depths 

Figure 1.3 Some examples of offshore foundation design

Monopile foundations, however, cannot currently be used for depths of beyond 30m with 3MW or heavier turbines. Moreover monopile diameters are limited to 5-6m and so are not economical for larger 5MW turbines for depth of over 20ms. The only feasible way for the monopile foundations to achieve the economical standards in deep water is by reducing their mass/MW ratio. Furthermore, the feasibility of using monopile foundations in deep water is further compromised by (i) the cost of installing piles in significant water depths, and (ii) the compliant nature of the structure. With regard to the latter issue much promise had been shown by theoretical studies of a guyed monopile system (Bunce and Carey, 2001a and 2001b) however such an approach remains to be fully exploited. An alternative to the guyed system is to incorporate a bearing plate at the mudline such a degree of restraint is added to resist lateral loads. As a consequence the penetration depth of the monopile may also be reduced but the performance of the foundation system is maintained. The performance of a ‘hybrid’ foundation system comprising a monopiled-footing is the subject of the research presented in this thesis.

1.1 Aims and Objectives

The aim of this research is to achieve a good understanding of the complex phenomena behind soil-structure interaction of the hybrid monopile-footing foundation system under static loading. Specifically the research aims to answer the following series of questions.

- Does the addition of a bearing plate improve the lateral capacity of a monopile
- Does the addition of a skirt to the footing improve the capacity of the hybrid system
- What is the relationship between the footing diameter, skirted footing diameter, skirt length, pile diameter and pile length with the lateral capacity of the hybrid foundation system
- Is the connection between the footing and the monopile play any part in improving the lateral capacity of the hybrid system
- What is the most efficient way of designing the connection between the footing and the monopile
- Does the distribution of vertical load (dead loads) effect the performance of the hybrid system
- What is the relationship between loading (vertical and horizontal) and the elements comprising the hybrid foundation

The answers to the above will be achieved via modelling, both experimentally and numerically, the behaviour of the foundation system under static loading.

The objectives of the research are as follows:

- To conduct 1g model tests on the hybrid foundation system and its comprising elements (i.e. pile, footing and skirted footing) under combined axial and lateral static loading
- To obtain 1g data on the performance of the foundation system under combined axial and lateral static loading
- To conduct centrifuge model tests on the hybrid foundation system and its comprising elements (i.e. pile, footing and skirted footing) under combined axial and lateral static loading

- To obtain centrifuge data on the performance of the foundation system under combined axial and lateral static loading
- To carry out a comprehensive series of analytical as well as numerical (2D) model tests on the foundation system under different geometries under combined axial and lateral static loading
- To carry out a series of 3D numerical analysis, on a selected number of models, under combined axial and lateral static loading
- To use the results of the physical and numerical model tests to formulate a design guidelines/methodology for the foundation system

2. LITERATURE REVIEW

2.1 Introduction

This chapter covers principles of offshore pile foundations from the perspective of hybrid monopile-footing foundation systems. As previously described in chapter 1, the hybrid monopile-footing foundation system comprises of two main elements; the monopile and the footing. Hence, it is essential to have an understanding of the principles and mechanics of these two foundation elements individually.

2.1.1 *Offshore Pile Foundations*

Offshore pile foundations are usually hollow tubular steel sections and typically vary in diameter from about 0.75m to over 4m for large monopile foundations. Generally the diameter to wall thickness ratio varies from 25 to 100 (Randolph and Gourvenec 2011). Deep pile foundations are normally preferred over shallow foundations in situations where very high lateral loads are present, or when the sea bed upper layer soil lacks the required stiffness. The type of pile foundation used at a particular site solely depends on the geotechnical characteristic of the soil.

Offshore piles foundations are either driven to the ground, or drilled and grouted. Driven steel piles are the most common method for supporting offshore oil platforms and offshore wind turbines. The smaller size offshore jackets usually have one pile at each corner of the structure and the offshore wind turbines have one monopile to support the structure. Moreover, monopiles can be used to anchor offshore floating structures (usually a preferred type of structure for deep water conditions) such as tension-leg platforms.

The two main types of pile foundations used offshore are driven piles, and drilled and grouted piles. The preferred and most commonly used type is the driven steel piles, which is due to its cost and ease of installation. The drilled and grouted piles are usually used in cemented sediment and rock ground conditions.

2.1.1.1 *Driven Piles*

This type of pile foundation is usually a hollow and open ended tubular steel section which is the most preferred types of pile foundation used for offshore platform and offshore wind turbines.

The method of installation is via driving the section into the seabed using a hydraulic hammer. This is done with above-water hydraulic hammers in shallow water and underwater hydraulic hammers. The length of the piles could be up to 100 m. Due to the nature of open ended pile, soil could flow through the pile and form a 'plug' during driving. In order to minimise and prevent this, a thickened wall is often used at the bottom of the pile. In some case, a steel plate could be welded to the bottom of the pile and consequently prevent the flow of soil through the pile (De Mello et al. 1989, De Mello and Galgoul 1992). Once pile is driven to the required depth, the pile head is then welded or grouted to the structure above.

Issues such as tip damage and refusal could limit or slow down the process of driving the pile. Sometimes the required penetration cannot be reached due to the damage sustained to the pile head which results in the buckling of the tip of the pile (Barbour and Erbrich 1995). The damage caused as a result of buckling could then lead to pile driving refusal.

2.1.1.2 *Drilled and Grouted Piles*

These types of piles are a hybrid of steel tubular piles and grouted pile, where the steel section is inserted to a drilled hole and then filled with grout (Rickman and Barthelemy 1988). Drilled and grouted piles are used as an alternative to driven piles in situations where pile driving is not an option, for instance when the ground where the foundation needs to be installed is hard rock or calcareous sediments. The process of installation is as follows:

A primary pile is first driven into the ground.

A drilling rig is then sent down to the excavated hole in order to create the required depth for the pile.

The main pile is then inserted into the hole and then filled with grout.

The design of drilled and grouted piles must consider issues such as hole stability, the necessity for using primary piles and grouting process. Due to the long construction process and delays that may occur, these types of foundations are more expensive.

2.1.2 *Parametric Definitions of the Structural System*

Throughout this chapter the following components will be used in describing the pile load, pile resistance and pile geometry:

2.1.2.1 *Applied Loads*

The load acting on the head of the pile (at mudline) comes from three different sources:

2.1.2.2 *Self weight of the structure:*

The weight of the structure above the water surface (i.e. platform or wind turbine) as well as the weight of the structure between the water surface and seabed (i.e. jacket supporting a platform, or column supporting a wind turbine).

2.1.2.3 *Working loads:*

The loads created as a result of working dynamic and cyclic loading. This is created by the operational activities in the case of a platform and rotation of the pillar in the case of a wind turbine.

2.1.2.4 *Environmental loads:*

This is created by the loads exerted to the structure above the water as a result of wind or storms as well as the loads acting on the structure between the water surface and seabed as a result of wave and current loading. Moreover if the structure is located in an active earthquake zone, earthquake induced loads will also be applied to the structure in form of dynamic pseudostatic accelerations.

All of the loads stated above will eventually be transferred to the foundations. The resultant components will act at the pile head in form of bending moments (denoted M), vertical loads (denoted V) and lateral loads (denoted H). The vertical and lateral loads could be applied in monotonic (static), cyclic and/or dynamic forms.

2.1.2.5 *Displacements and Rotations*

The response of the foundation to the applied loads will be in form of displacements (or translations) which could take place along the length of the pile (denoted δ) and/or rotations at the pile head (denoted θ).

2.1.2.6 *Axial Resistance*

This is a form of resistance (denoted Q_a) that a pile shows to axial load which is generated through the generation of frictional resistance (shear stress) between the surrounding soil and pile (denoted τ_s) and resistance at the base of the pile (denoted q_b).

2.1.2.7 *Lateral Resistance*

The lateral resistance of the pile (denoted P_{ult}) is generated through the normal and shear stresses acting laterally on the pile. This is, in other words, the lateral resistance of the soil to the lateral loads induced to the pile. The stresses around the circumference of the pile are not uniform and vary in a very complex manner. In practice, this is treated as a disturbed load varying along the length of the pile which is a force per unit length of the pile.

2.1.2.8 *Bending Strength / Plastic Moment Capacity*

This is the capacity of the pile to induced loads and is denoted as M_p . This is purely a measure of the properties of the structural materials used to fabricate the pile.

2.2 **Pile Foundations**

2.2.1 *Axial Pile Capacity*

2.2.1.1 *Governing Equation*

There are two components that contribute to the axial strength, or capacity of a pile; the friction at the soil/pile interface or the ultimate shaft resistance, and the resistance at the base of the pile or the ultimate base resistance. The total pile capacity is then calculated through the following equation:

$$Q_t = Q_s + Q_b \quad 2.1$$

Where Q_t is the total pile capacity, Q_s is the total shaft capacity and Q_b is the total base capacity.

In cohesionless soils, the shaft capacity is the product of the resistance at the soil-pile interface τ . This is produced as a result of the horizontal effective stress acting at the pile shaft at failure σ'_f and the mobilised coefficient of friction $\tan \delta$ (Randolph and Gourvenec 2011). This resistance at the soil-pile interface is acting along the length of the pile and

calculating the total shaft capacity needs to include the integration over the surface area of the pile. Hence:

$$Q_s = \pi D \int_0^L \tau_s dz = \pi D \int_0^L \sigma'_f \tan \delta dz \quad 2.2$$

Where D is the pile diameter, L is the total pile length, τ_s is the resistance at soil-pile interface and σ'_f is the horizontal effective stress acting at pile shaft at failure.

In cohesive soils, the general approach is to correlate the shaft capacity to the in situ undrained strength. This is defined by:

$$\tau_s = \alpha s_u \quad 2.3$$

Where α is the friction factor and s_u is the in situ undrained strength. It is important to note that there is no direct relationship τ_s between s_u . This is due to the fact that the ratio between these two parameters are affected by the angle of friction at the soil-pile interface as well as the changes of soil strength and stress caused by loading, remoulding and consolidation of the soil. The friction factor takes this into account and has been adapted into design via introducing empirical relationship (Tomlinson 1957).

The total base capacity is the maximum stress that can be mobilised at the pile base in contact with soil, i.e. the pile area. Hence:

$$Q_b = \frac{\pi D^2}{4} q_b \quad 2.4$$

Where q_b is the base resistance of the pile and needs to be multiplied by the pile area at the base. In the case of an open ended or tubular pile, as the axial load is mobilised. Hence, the soil within the pile the base resistance is calculated from the two components acting on the pile wall as well as on the soil plug.

There are different methods that could be employed for designing the piles of which five are widely accepted and used in the industry. The bases for design are the equations presented above (2.1 to 2.4) however each method suggests a different method for introducing the variables, mainly τ_s . The primary input parameter employed by all methods is the Cone Penetration Test (CPT) end resistance (q_c).

It is not necessary here to present in detail axial design methods, but the reader is referred to the following methodologies currently used in practice.

Method	Main reference
2.2.1.2 <i>American Petroleum Institute Method</i>	API 2006
2.2.1.3 <i>Fugro Method</i>	Kolk <i>et al.</i> 2005; Fugro 2004; Bustamante and Gianceselli 1982
2.2.1.4 <i>Imperial College Pile Design Method</i>	Jardine <i>et al.</i> 2005a
2.2.1.5 <i>Norwegian Geotechnical Institute Method (NGI-05)</i>	Clausen <i>et al.</i> 2005; Aas <i>et al.</i> 2004
2.2.1.6 <i>University of Western Australia Method (UWA-05) method</i>	Lehane <i>et al.</i> 2005c; Lehane <i>et al.</i> 2005a

2.2.2 *Laterally Loaded Pile Foundations*

Of more significance in this study is the lateral response of single piles. The response of the single free headed pile forms the main foundation system for a conventional monopiled wind turbine. The development of a head moment through partial of full fixity is also of interest in this study and as a consequence the design of free and fixed headed piles under lateral loading is reviewed in the following sections.

2.2.2.1 *Response to Lateral Loads*

As discussed previously, lateral loads on piles could come from different sources. The effect of the loads on piles could be characterised into two different groups (De Beer 1977):

Active loading: May come from wind, waves, ice, current, ship impact, traffic and mooring forces which are all live and time dependent.

Passive loading: Derived from earth pressures and moving soil which are all dead or time independent.

Assuming that a laterally loaded pile is infinitely rigid, the response of the pile is solely dependent on the nature of the loading and the properties of the surrounding soil. Four different types of active loading can occur at the pile head area which are static or monotonic

(short term), cyclic, sustained and dynamic. Passive loading takes place along the length of the pile.

Due to the nature of offshore conditions, static and dynamic loading are the most common types of lading that piles experience. Monotonic loading, on the other hand, which the gradual increase of the lateral loads until the piles or the soil reach the ultimate capacity, rarely takes place in practice. However, monotonic curves are extremely important they are the baseline demonstrating the nature and effect of other types of loading (Reese and Van Impe 2011).

A typical p - y curve for a particular case of a monotonic is illustrated in Figure 2.1, where a monotonically increasing load is applied to the pile head. From the investigation's point of view, a typical load versus lateral deflection of a pile head forms the basis for the analysis where these curves may be utilised to find the initial stiffness, the ultimate lateral resistance, and errors that may have been taken place in the process of conducting the tests.

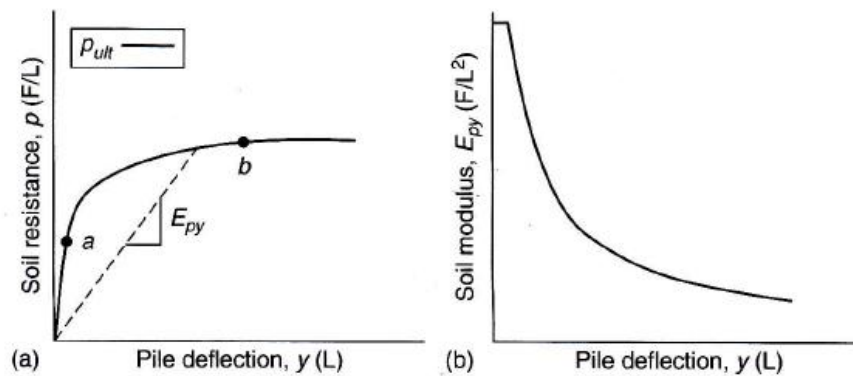


Figure 2.1. Typical p - y curve and resisting soil modulus (Reese and Van Impe 2011)

2.2.3 Failure under Lateral Loads

When a pile fails under lateral loads, two different scenarios are possible namely (i) the ultimate lateral soil resistance has been exceeded in which case the pile fails as a rigid body (this is also referred to as geotechnical failure) or (ii) the plastic moment capacity of the pile is exceeded which results in the failure of the pile in bending (this is also referred to as structural failure).

2.2.3.1 Failure Modes

The head restraint conditions as well as the length of the piles have a dominant influence on the way piles behave and fail under lateral loads. Hence, the failure modes tend to be divided into two different categories as follows:

2.2.3.2 Fully Free Head Condition

When the lateral load is increased to failure, the net lateral force acts against the load direction. For short piles the failure mode involves failure for the soil only and takes place by rigid rotation of the whole pile about the point of rotation at a particular point along the length of the pile (Z_{crit} which is at 70% to 80% of the pile length from the top of the pile) (Randolph and Gourvenec 2011). This is further illustrated in Figure 2.2.

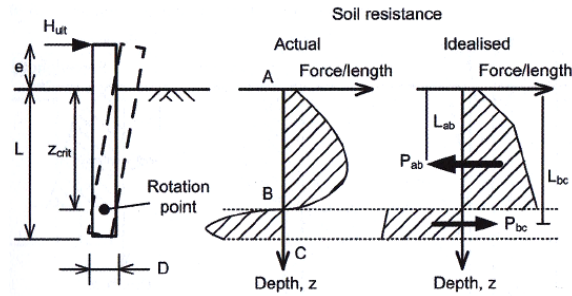


Figure 2.2 Failure mechanism for free headed short piles under lateral loads (Randolph and Gourvenec 2011)

The first step in calculating the lateral pile capacity H_{ult} at an eccentricity e , is to determine the profile of limiting soil resistance along the length of the pile. Then assuming a value for the Z_{crit} the values of positive and negative soil resistances P_{ab} and P_{bc} (positive above the rotation centre and negative below it) as well as the lengths of the lines of action L_{ab} and L_{bc} may be calculated. The lateral pile capacity then could be obtained using the following equilibrium equation:

$$H_{ult} = P_{ab} + P_{bc} \quad 2.5$$

$$H_{ult}e = -P_{ab}L_{ab} + P_{bc}L_{bc} \quad 2.5$$

Furthermore, by expressing the above equations by recalling P_{ab} , P_{bc} , L_{ab} and L_{bc} , in terms of Z_{crit} it is possible to solve the above equations simultaneously in order to calculate H_{ult} .

In the case of a long pile (as shown in Figure 2.3), the failure mode involves the formation of a plastic hinge at one or two points along the length of the pile. The location of the plastic hinge is at the distance Z_{crit} from the free surface. The location where the plastic hinge is

forms is at the point where the maximum bending moment takes place (i.e. zero shear force). This implies that the lateral forces above and below the plastic hinge are in horizontal equilibrium.

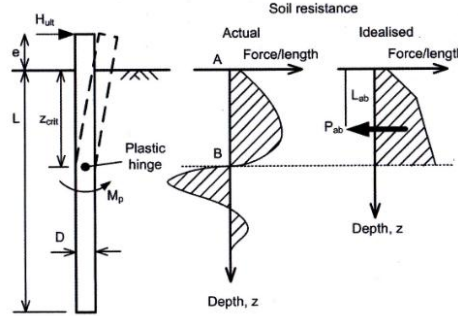


Figure 2.2 Failure mechanism for free headed long piles under lateral loads (Randolph and Gourvenec 2011)

Since the soil below the point where the plastic hinge forms are in self equilibrium, only the positive soil resistance above the location of the plastic hinge needs to be taken into account for the calculation of the lateral capacity H_{ult} . In order to satisfy the equilibrium conditions, above the location of the plastic hinge the maximum soil resistance must equal the lateral capacity, hence by taking a moment about the top of the pile:

$$H_{ult} = P_{ab} \quad 2.7$$

$$M_P = P_{ab}(L_{ab} + e) \quad 2.8$$

Similar to the equilibrium equations for short piles, equations 2.7 and 2.8 could be expressed in terms of Z_{crit} . Once, using this iterative process the value of Z_{crit} and P_{ab} are found, H_{ult} could be calculated using equation 2.7.

2.2.3.3 Fully Fixed Head Condition

For both short and long piles, in the presence of a fully fixed head condition where the pile head is restraint against lateral translations and rotation, three different possible failure modes could take place.

Failure of the pile due to lateral translation and in the absence of any rotations at pile head or along the length of the pile. In this condition no hinges form.

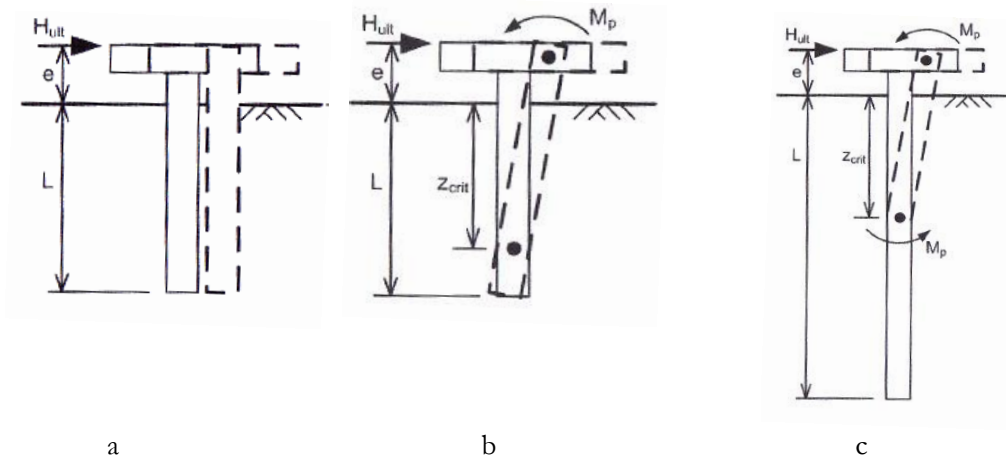


Figure 2.3a Failure mechanism for fixed headed piles with lateral translation, b) with the formation of one hinge and c) Failure mechanism for fixed headed piles with the formation of two hinges (Randolph and Gourvenec 2011)

Failure of the pile by formation of a hinge at the pile head and rotation of the pile about the point of rotation at Z_{crit} and as well as the plastic hinge at the pile head. Analysis such piles are exactly in the same manner as fully free short pile with an additional M_p term in the moment equilibrium equation (equation 2.8).

Failure of the pile by formation of a hinge at the pile head as well as the point of maximum bending moment (Figure 2.3), and rotation of the pile about the plastic hinge at Z_{crit} and as well as the plastic hinge at the pile head. Analysis of such piles is exactly in the same manner as fully free short pile with an additional M_p term in the moment equilibrium equation (equation 2.8).

2.2.3.4 Limiting Lateral Resistance

For cohesive soils, the lateral resistance is related to the undrained shear strength. This is done through failure mechanisms that are related to the behaviour of the soil around the pile. Close to the surface the failure mechanism takes place via failure of a wedge of soil in front of the pile. This leads to a lower limiting resistance compared to at depth. Generally, for cohesive soils, the value of limiting lateral resistance has been taken as $P_f = 2DS_u$ which is the lower bound limit (passive failure in front of the pile, Figure 2.4) that takes place near the surface. This value increases with depth to an upper bound value of $P_f = 9DS_u$ at depths larger than 3 times the pile diameter (Broms 1964a). For longer piles the nature of flow around the piles changes and less resistance is provided by the flow at the horizontal plane. This leads to the

creation of concentric shells immediately adjacent to the direction of the flow where the soil flows in a circular manner in the fan zone (Figure 2.5). The design value of $P_f = 9DS_u$ is believed to be conservative for this type of failure mechanisms (Broms 1964a).

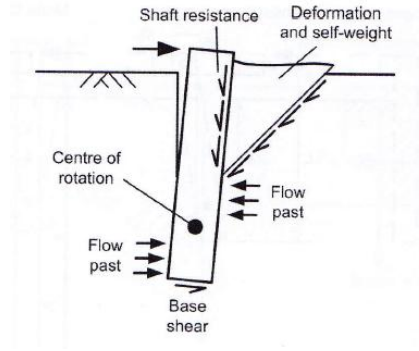


Figure 2.4 Mechanism of lateral resistance of piles in cohesive soils

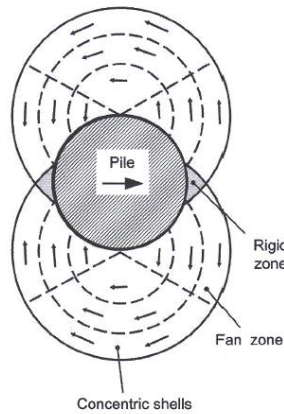


Figure 2.5 Flow around mechanism for laterally loaded piles cohesive soils

Since the plasticity mechanisms cannot be constructed in cohesionless soils, methods for estimating the variation of P_f with depth are empirical (where the estimations are checked against field data). These imperial relationships tend have a dimensionless factor N (by dividing the lateral resistance by the in situ vertical effective stress) that depends on the angle of friction ϕ , where:

$$N = \frac{P_f}{D\sigma'_v} = \frac{P_f}{D\gamma'z} \tag{2.9}$$

Since the pile wall will behave similarly to a retaining wall at shallow depths. The value of N is very likely to be close to the value of the coefficient of the earth pressure, K_p at the soil surface (Barton 1982). Propose by Reese et al. (1974), at shallow depths some kind of wedge failure mechanics will take place (similar to wedge failure mechanism for cohesive soils shown in Figure 2.4). Hansen (1961) and Mayerhof (1995) have developed charts showing the variations

of N with depth, illustrated in Figure 2.6. These graphs also compare the proposed value with the previous findings of Broms (1964b) and Barton (1982). Prasad and Chari (1999) developed the relationship which shows a good agreement between the previous findings where P_f is increasing linearly with depth (variation further illustrated in Figure 2.7).

$$P_f = DK_P^2 \sigma'_v = DK_P^2 \gamma' z \quad 2.10$$

Where
$$K_P = \frac{1 + \sin \phi}{1 - \sin \phi} \quad 2.11$$

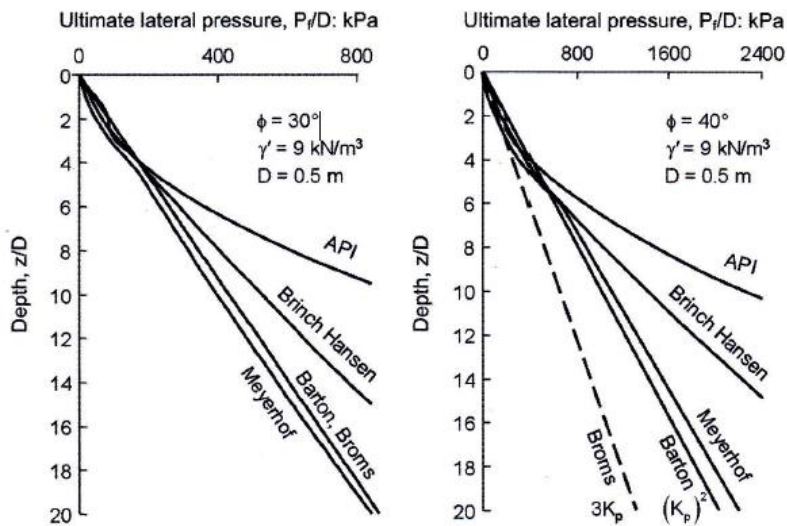


Figure 2.6. Lateral resistance variation with depth using different approaches (Randolph and Gourvenec 2011)

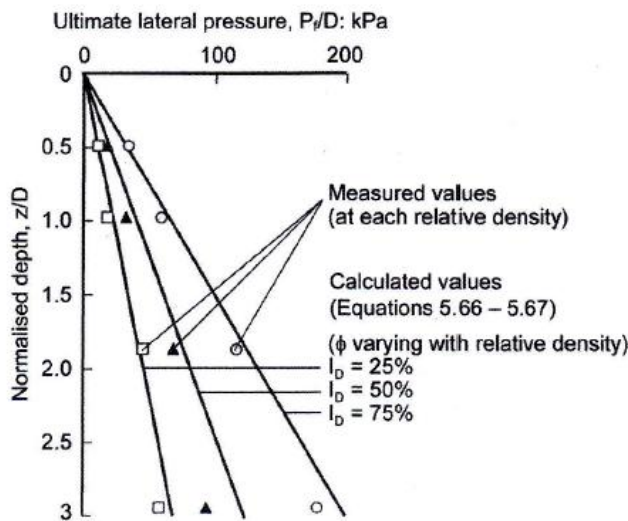


Figure 2.7 Lateral resistance variation with depth after Prasad and Chari (1999)

2.2.4 *Ultimate Lateral Resistance & Lateral Deflection*

2.2.4.1 *Introduction*

Generally the ultimate lateral resistance of a pile is calculated by assuming a distribution of maximum lateral resistance in the pile and treating the pile as a beam under the distributed load along the length of the pile and a point load at the pile head. The magnitude of the maximum load that could be applied at the pile head could then be found via solving for equilibrium. This will be followed by checking that the deflections are within the acceptable limits and that the plastic moment capacity of the pile has not been exceeded (Poulos and Davis 1980). This is all done with an expectable applied factor of safety.

Analysing the ultimate lateral resistance of a pile is a complicated in that the behaviour of the pile under load and its relative lateral deflection involves the interaction between the pile and the soil.

2.2.4.2 *Static Approach*

The starting point in estimating the ultimate lateral resistance of a pile is to consider the statics of the pile. For the case of a pile where there is no head restraints (i.e. free headed pile), under the normal offshore loading conditions, the forces exerted on the pile are the lateral load H , the moment M and the ultimate soil resistance P_u (illustrated in Figure 2.8).

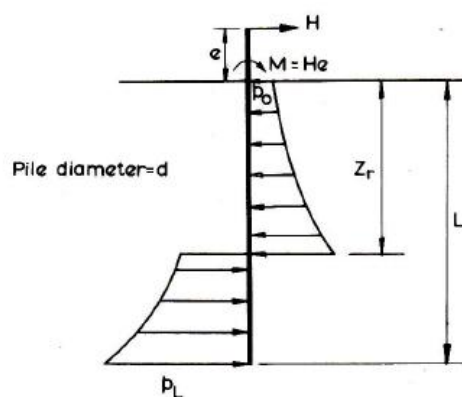


Figure 2.8. Free headed laterally-loaded pile

Assuming that the pile is rigid (i.e. the soil will reach its ultimate capacity before the pile) the limiting combination of the forces, i.e. M_u and H_u which will lead to the failure of the pile, may be obtained by applying the equilibrium of horizontal forces. Solving the resultant

equilibrium equations for the unknown depth of rotation Z_r , and the ultimate lateral load H_u will give the equation of the ultimate bending moment M_u (Poulos and Davis 1980). Taking M_u as He , where e is the eccentricity of loading, and solving the equilibrium equations leads to the following equations.

$$Z_r = \frac{1}{2} \left(\frac{H_u}{P_u d} + L \right) \quad 2.12$$

For the case of a uniform distribution of soil resistance with depth:

$$\frac{H_u}{P_u d L} = \sqrt{\left(1 + \frac{2e}{L}\right)^2 + 1} - \left(1 + \frac{2e}{L}\right) \quad 2.13$$

And for the case of a linear variation of soil resistance with depth:

$$\frac{H_u}{P_u d L} = \left(1 - \frac{P_o}{P_L}\right) \left(\frac{Z_r}{L}\right)^2 + \left(2 \frac{P_o}{P_L}\right) \left(\frac{Z_r}{L}\right) - \frac{1}{2} \left(1 + \frac{P_o}{P_L}\right) \quad 2.14$$

The variation of $\frac{H_u}{P_u d L}$ against $\frac{e}{L}$ are shown the Figures 2.9 and 2.10 for both case under different failure load and moment combinations.

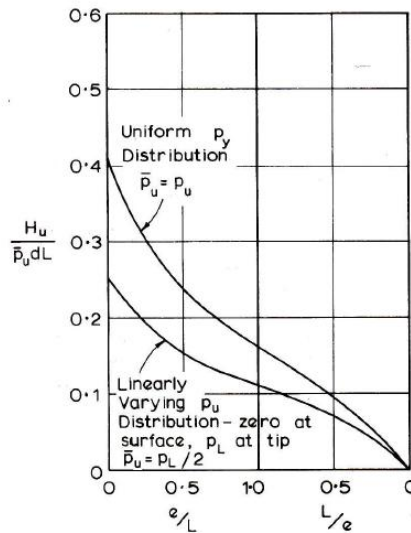


Figure 2.9. Ultimate lateral resistance of free headed rigid piles based on factor $\frac{e}{L}$

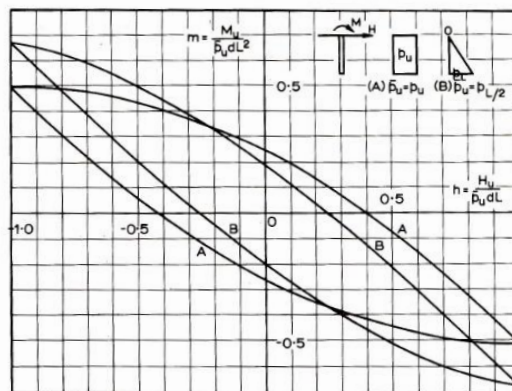


Figure 2.10. Ultimate lateral resistance of free headed rigid piles based on factor m

An alternative method was also proposed by Hansen (1961) where a trial an error method is suggested for the calculation of the depth of rotation such that the resultant moment taken about the centre of location equals to zero. Once the depth of ration is calculated, the ultimate lateral resistance may be calculated using the horizontal equilibrium equations.

Generally, for the case of a purely cohesive soil, it is suggested (Poulos and Davis 1980) that the ultimate lateral resistance of soil increases from the surface down to the depth of about three times the pile diameter and remains constant below that (illustrated in Figure 2.11). Lateral failure involved the plastic flow of the soil at the horizontal plane the pile around the pile below this depth and the value of P_u may be calculated using plastic theory. The value of lateral resistance factor K_c depends on the pile adhesion c_a to cohesion c , and shape of the pile or the aspect ratio $\frac{a}{d}$. The relationship between aspect ratio and lateral resistance factor is illustrated in Figure 2.12.

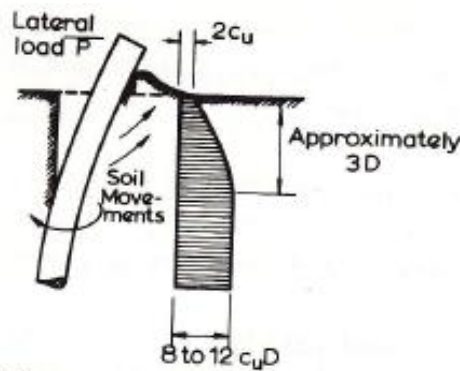


Figure 2.11 Lateral resistance distribution in cohesive soils

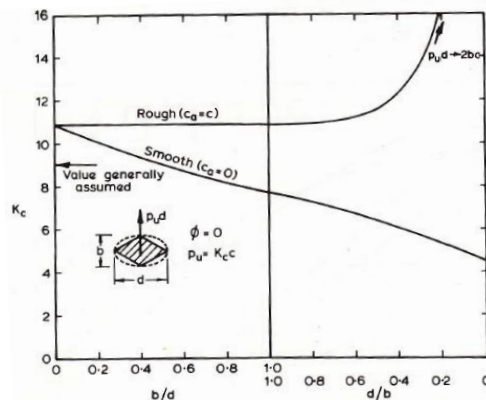


Figure 2.12 Effect of adhesion and aspect ratio on lateral resistance in cohesive soils

In the case of a $c - \phi$ soils, Hansen (1961) suggested an alternative derivation of the ultimate lateral resistance of soil that was based on the earth pressure theory. He also considered the variation of the soil resistance with depth which may be calculated by:

$$p_u = qK_q + cK_c \quad 2.15$$

where q is the vertical overburden pressure, c is cohesion and K_c and K_q are the factors that are a function of ϕ and $\frac{z}{d}$. The value of these factors may be obtained from Figures 2.13 and 2.14.

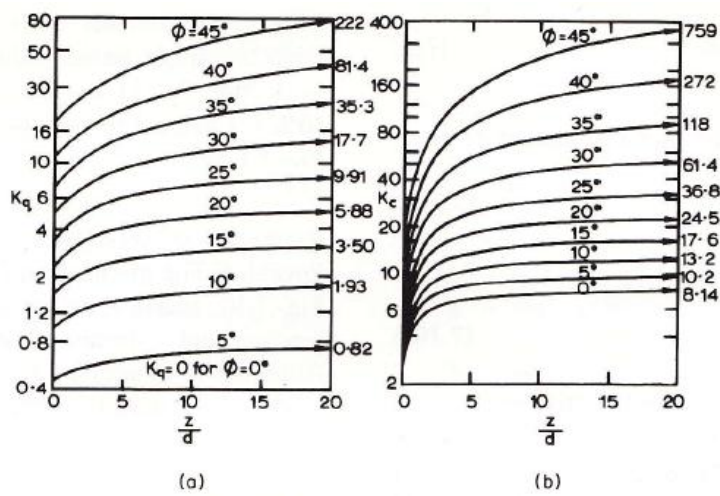


Figure 2.13. Lateral resistance factors K_q and K_c

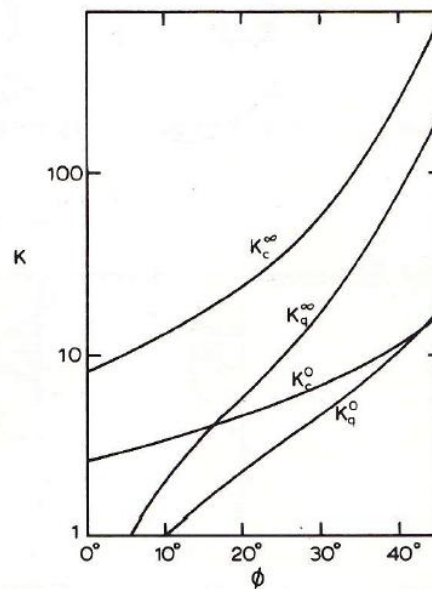


Figure 2.14. Lateral resistance factors at ground surface (0) and infinite depth (∞)

2.2.4.3 Broms's Method

Broms's theory is essentially based on the static approach with the difference that some simplifications have been applied to the load distribution profiles along the length of the pile. Moreover this approach studies the behaviour of the pile in cohesive and cohesionless soils with different head restrained conditions separately. This method was published in two separate papers (Broms 1964a and b) for cohesive and cohesionless soils respectively. A brief review of the method for cohesionless soils is presented below.

Broms analysis for laterally loaded piles in cohesionless soils (Broms 1964b) were carried out assuming that the active earth pressure acting at the back of the pile is neglected, the distribution of passive pressure along the front of the pile is equal to three times Rankine passive pressure and that the shape of the pile section has no influence on the distribution of ultimate soil pressure or the ultimate lateral resistance.

Broms's assumption on the value of ultimate lateral resistance, P_u , being three times Rankine passive pressure was based on limited empirical evidence on the comparison between predicted and observed values. Further comparisons suggest that the factor 3 is rather conservative in some case. Moreover, the average ratio of predicted to observed ultimate lateral loads was found to be about two thirds (Poulos and Davis 1974) which leads to the distribution of soil resistance being as:

$$P_u = 3\sigma'_v K_p \quad 2.16$$

where

σ'_v is the effective vertical overburden pressure

$$K_p = \frac{1+\sin\phi'}{1-\sin\phi'} \quad 2.17$$

ϕ' is the angle of internal friction

The two possible failure modes for the case of free-headed piles are shown in Figure 2.15. Similarly to free headed piles in cohesive soils, the pile is classified as short if the maximum moment acting on the pile is less than its yield moment. As illustrated in Figure 2.15(a), assuming that the point of rotation is very close to the tip of the pile, the high pressures are replaced by a single point load acting at the pile tip. Taking moments about the toe and

resolving it for H_u results in the equation below, further illustrated graphically in Figure 2.16(a) in terms of dimensionless parameters $\frac{L}{d}$ and $\frac{H_u}{K_p \gamma d^3}$.

$$H_u = \frac{0.5 \gamma d L^3 K_p}{e + L} \quad 2.18$$

The maximum moment takes place at a distance f below the surface where:

$$H_u = \frac{3}{2} \gamma d K_p f^2 \quad 2.19$$

$$f = 0.82 \sqrt{\left(\frac{H_u}{d K_p \gamma}\right)}$$

$$M_{max} = H_u \left(e + \frac{2}{3} f\right) \quad 2.20$$

If M_{max} exceeds M_y the pile will act as a long pile and the H_u may be obtained by replacing M_{max} by M_y in the above, the results of which have been illustrated graphically in Figure 2.16(b) in terms of dimensionless parameters $\frac{H_u}{K_p \gamma d^3}$ and $\frac{M_y}{d^4 \gamma K_p}$.

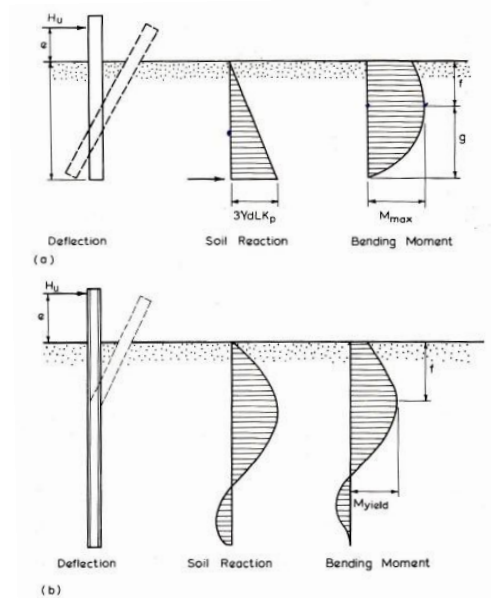


Figure 2.15 Failure mode and behaviour of free headed piles in cohesionless soils for (a) short (b) long piles

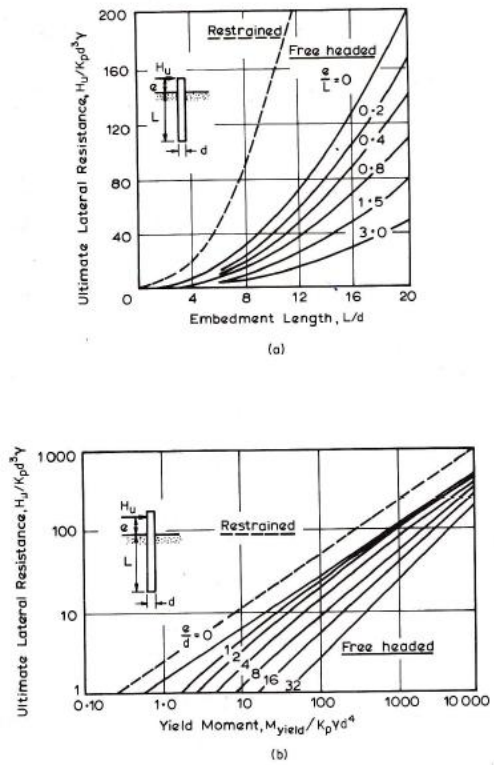


Figure 2.16 Ultimate lateral resistance in cohesionless soils for (a) short piles (b) long piles

For fixed headed condition, it is assumed that the moment resistance M_y is present at the pile cap. The failure modes are categorised as short, intermediate and long, illustrated in Figure 2.17.

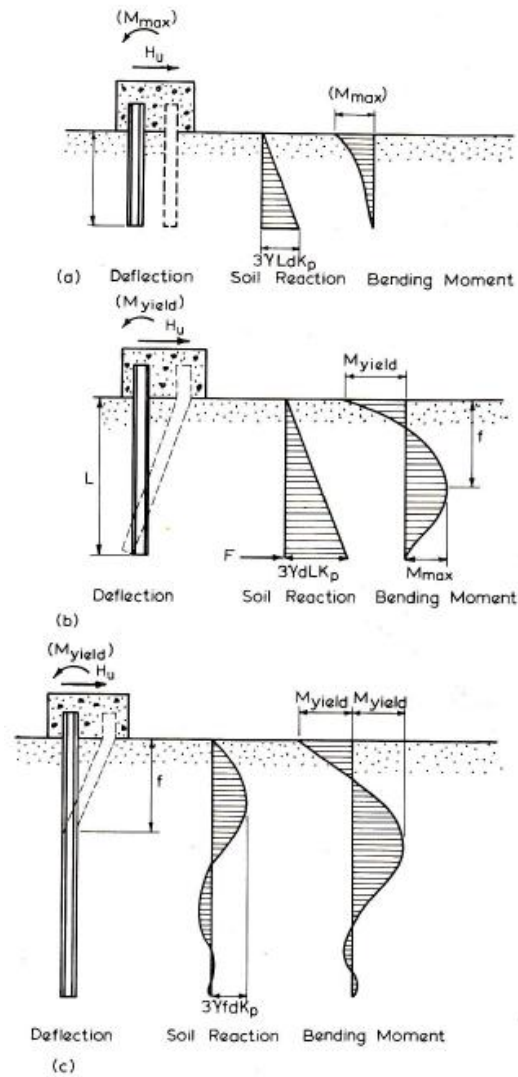


Figure 2.17 Failure mode and behaviour of fixed headed piles in cohesionless soils for (a) short (b) intermediate and (c) long piles

For short piles, applying the horizontal equilibrium, resolving it for H_u and M_{max} leads to:

$$H_u = 1.5\gamma L^2 d K_p \quad 2.21$$

$$M_{max} = \frac{2}{3} H_u L \quad 2.22$$

In the case of M_{max} exceeding M_y , the pile is classified as intermediate, and applying the horizontal equilibrium, resolving it for F and taking moments about the top of the pile leads to where H_u may be calculated.

$$F = \left(\frac{3}{2}\gamma L^2 K_p\right) - H_u \quad 2.23$$

$$M_y = (0.5\gamma d L^3 K_p) - H_u L \quad 2.24$$

Moreover, if the maximum bending moment reaches M_y at two locations leads to the equation below from which H_u may be calculated (Figure 2.17(c)).

$$H_u \left(e + \frac{2}{3}f \right) = 2M_y \quad 2.25$$

Dimensionless solutions are all illustrated in Figure 2.16.

2.2.4.4 Laterally loaded Plates: Plain Strain Solution

Assuming that the pile rotates about an arbitrary point along the length of the pile, Tomlinson and Woodward (2008) suggest the following equations as a simple method of calculating the lateral deflections. The equations could be applied to both free headed and fixed headed pile head conditions (illustrated in Figure 2.18).

$$y = \frac{H(e+zf)^3}{3EI} \quad (\text{free head condition}) \quad 2.26$$

$$y = \frac{H(e+zf)^3}{12EI} \quad (\text{fixed head condition}) \quad 2.27$$

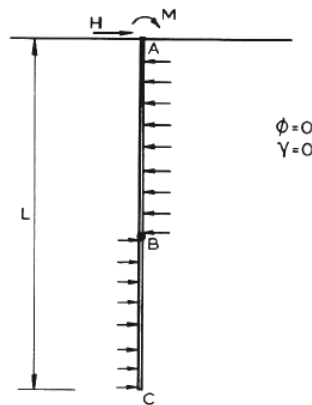


Figure 2.18 Pile under horizontal load simplified as a cantilever (Tomlinson and Woodward 2008)

2.2.4.5 Elastic Continuum Theory

This theory is based on the continuum model for soil which has been generated using finite element and boundary element analysis. The results for this solution were analysed and normalised where simple relationships were fitted by Randolph (1981). The notations for his analysis are illustrated in Figure 2.19.

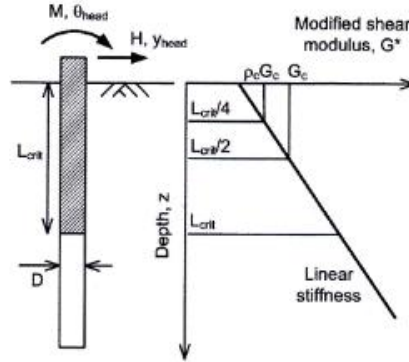


Figure 2.19 Notations for elastic continuum analysis

Based on this approach, the critical pile length, L_{crit} is expressed in terms of pile-soil stiffness ratio, $\frac{E_p}{G_c}$ where E_p is Young's modulus of a solid pile of equivalent bending rigidity, G_c is the characteristic shear modulus, G^* is the modified shear modulus used to normalise the results for different values of Poisson's ratio ν and ρ_c is a parameter introduced to quantify the degree of non-homogeneity. So for a circular pile:

$$E_p = \frac{(EI)_p}{I_{solid}} = \frac{(EI)_p}{\frac{\pi D^4}{64}} \quad 2.28$$

$$G^* = G \left(1 + \frac{3\nu}{4}\right) \quad 2.29$$

$$\rho_c = \frac{G_{z=L_{crit}/4}^*}{G_c} \quad 2.30$$

$$L_{crit} = D \left(\frac{E_p}{G_c}\right)^{\frac{2}{7}} \quad 2.31$$

The following equations were then suggested to be used in order to calculate the lateral deflections and rotation at pile head. These equations are based on the foregoing parameters above as well as the applied load H and M .

$$y = \frac{(E_p/G_c)^{\frac{1}{7}}}{\rho_c G_c} \left[0.27 \frac{H}{L_{crit}/2} + 0.3 \frac{M}{(L_{crit}/2)^2} \right] \quad 2.32$$

$$\theta = \frac{(E_p/G_c)^{\frac{1}{7}}}{\rho_c G_c} \left[0.30 \frac{H}{(L_{crit}/2)^2} + 0.80 \sqrt{\rho_c} \frac{M}{(L_{crit}/2)^3} \right] \quad 2.33$$

The above expressions represent the lateral response at the pile head when the pile is free at the surface. In the case of a fixed headed pile, the following equations may be used:

$$M_{max} = -\frac{0.375HL_{crit}}{2\sqrt{\rho_c}} \tag{2.34}$$

$$\theta = \frac{(E_p/G_c)^{\frac{1}{7}}}{\rho_c G_c} \frac{H}{L_{crit}/2} \left[0.27 - \frac{0.11}{\sqrt{\rho_c}} \right] \tag{2.35}$$

Furthermore, the displacement and bending moment expressions can be normalised in order to extend this to any depth along the pile. Hence, the normalised displacement at any given depth along the pile length is:

$$\bar{y} = \frac{yDG_c}{H} \left[\frac{E_p}{G_c} \right]^{\frac{1}{7}} \tag{2.36}$$

The results are graphically illustrated in Figures 2.20 for free headed piles and in Figure 2.21 for fixed headed piles. The results are presenting three different soil modulus and the bending moments are normalised by HL_{crit} .

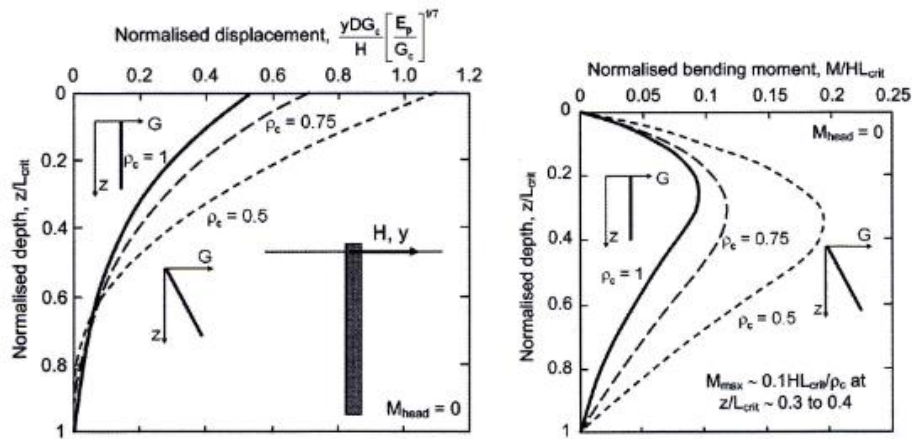


Figure 2.20 Normalised lateral displacement and bending moment profiles for free headed piles using elastic continuum theory

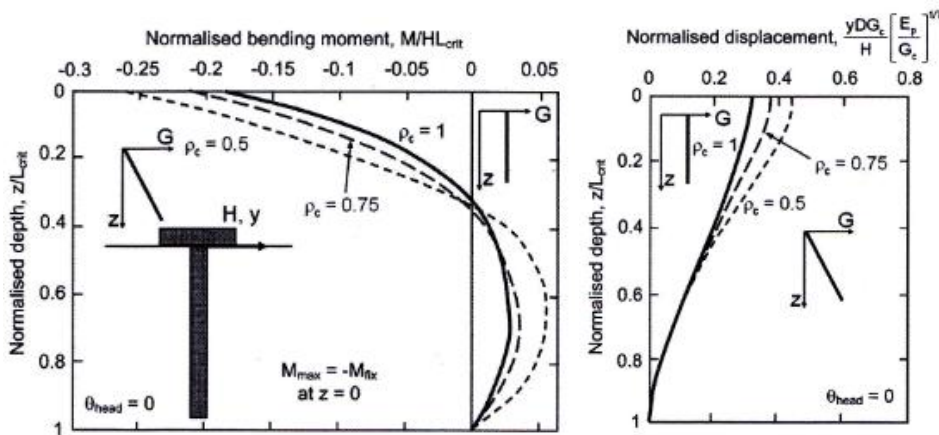


Figure 2.21 Normalised lateral displacement and bending moment profiles for fixed headed piles using elastic continuum theory

For free headed piles, the maximum bending moment occurs at a depth of about 30% to 40% of L_{crit} which is where the plastic hinge would be expected to occur for long piles. For fixed piles, however, this would occur at the point of fixity or the piles head. Generally, the values of maximum bending moments are about 30% to 80% greater, and the maximum lateral displacement reduces by a factor of 2, for fixed headed piles. Also the maximum bending moment are for soil stiffness proportional to depth ($\rho_c = 0.5$).

2.2.4.6 Subgrade Reaction Method (Elastic Pile - Elastic Soil)

This method, which is also known as Winkler idealisation, models the response of pile to lateral loads by treating the soil as a series of springs along the length of the piles, where the springs behave linearly (schematically illustrated in Figure 2.22) .

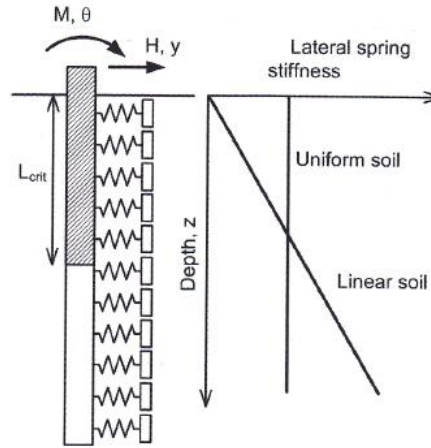


Figure 2.22 Winkler idealisation of laterally loaded piles

Initially this model was used to analyse the behaviour of thin vertical elastic strips where Terzaghi (Elson: 1955) defined the stiffness of the springs as:

$$k = \frac{p}{u} \text{ (kN/m}^3\text{)} \quad 2.37$$

Where k is the modulus of subgrade reaction, p is the vertical load and u is the vertical deflection. For piles this relationship is expressed to:

$$K = k_h B = \frac{p}{u} = n_h B \left(\frac{z}{B}\right)^n \quad 2.38$$

Where k_h is the horizontal coefficient of subgrade reaction, B is the breadth of the pile, n_h is the rate of increase or gradient of subgrade reaction with depth (which commonly varies from 0 to 2) and z is depth. The differential equation governing the behaviour of a pile subjected to axial, lateral and moment is governed by:

$$E_p I_p \frac{d^4 u}{dz^4} + P \frac{d^2 u}{dz^2} + K u = 0 \quad 2.39$$

$$I = \int y^2 dA \quad 2.40$$

Where I_p is the moment of inertia of the pile section and $E_p I_p$ represents the bending rigidity of the pile. Since for laterally loaded pile the axial load has a negligible effect on its lateral behaviour, term containing P may be taken out, so for the moment, rotation and stiffness along the length of the piles may be calculated using:

$$E_p I_p \frac{d^4 u}{dz^4} + Ku = 0 \quad 2.41$$

$$E_p I_p \frac{d^3 u}{dz^3} + \theta = 0 \quad 2.42$$

$$E_p I_p \frac{d^2 u}{dz^2} + M = 0 \quad 2.43$$

For both cases of stiffness of the springs being constant or linearly increasing with depth, Matlock and Reese (1960) have developed closed form solutions for the calculation of deflection and rotation at pile head u and θ induced by the applied lateral load H and moment M .

The relationship between k_h or n_h with depth z has been reported (Randolph and Gourvenec 2011) as $k_h \sim 4G$ or $n_h \sim 4\left(\frac{dG}{dz}\right)$, where G is the operative shear modulus of the soil. It has also been proven that the exact link between k_h and G is also influenced by stiffness and deformed shape of the pile (Baguelin et al. 1977).

For the case of the stiffness remaining a constant along the pile length (Randolph and Gourvenec 2011), the critical length beyond which the pile acts as infinitely long which is also the depth to which the lateral load is transferred is given by:

$$L_{crit} = 4\left(\frac{(EI)_p}{k_h}\right)^{\frac{1}{4}} \quad 2.44$$

Where the subgrade reaction solution gives:

$$y = \sqrt{2} \frac{H}{k_h} \left(\frac{L_{crit}}{4}\right)^{-1} + \frac{M}{k_h} \left(\frac{L_{crit}}{4}\right)^{-2} \quad 2.45$$

$$\theta = \frac{H}{k_h} \left(\frac{L_{crit}}{4}\right)^{-2} + \sqrt{2} \frac{M}{k_h} \left(\frac{L_{crit}}{4}\right)^{-3} \quad 2.46$$

For the case of stiffness linearly increasing with depth, from zero at the ground surface (Reese and Matlock 1956), the critical length as well as the deflection and rotation at pile head are given by:

$$L_{crit} = 4 \left(\frac{(EI)_p}{n_h} \right)^{\frac{1}{5}} \quad 2.47$$

$$y = 2.43 \frac{H}{k_h} \left(\frac{L_{crit}}{5} \right)^{-2} + 1.62 \frac{M}{n_h} \left(\frac{L_{crit}}{4} \right)^{-3} \quad 2.48$$

$$\theta = 1.62 \frac{H}{n_h} \left(\frac{L_{crit}}{4} \right)^{-3} + 1.73 \frac{M}{n_h} \left(\frac{L_{crit}}{4} \right)^{-4} \quad 2.49$$

In all cases the above derivations are valid when $L > L_{crit}$. Based on this theory, since there is no transfer of shear stress, the model does not represent a continuum, which is indicative of the fact that the springs are discrete. This as a result, leads to an overestimation of the deformations (Elson 1984). The main difficulty with this method is choosing an appropriate value for k. The difficulty arises as it is unknown whether or not the pile diameter has any influence on the value of k (Elson 1984). The limitation of this method is in cases where soil at ground surface goes through the cycle of overstressing which results in yielding. When this happens the load per unit length of pile is not proportional to deflection, hence the Winkler analysis is no longer accurate. It is suggested (Elson 1984) that the Winkler analysis should be limited to cases where the maximum reaction on the pile does not exceed one half the passive resistance of the soil.

2.2.4.7 **Nonlinear p-y Method**

Methods presented earlier are based on the theory of elasticity which results in having a constant value of soil-pile stiffness. This is not the most accurate way of representing the actual interaction between the soil and the pile. In practice as the lateral resistance approaches the failure load P_f , strain levels increase and leads to degradation of the initial stiffness. The nonlinear $p-y$ method is an extension to the subgrade reaction approach where the laterally loaded pile is treated as a beam with a series of discrete springs whereby including these nonlinear springs, the response of the deforming soil around the pile is also taken into account. This is shown schematically in Figure 2.23.

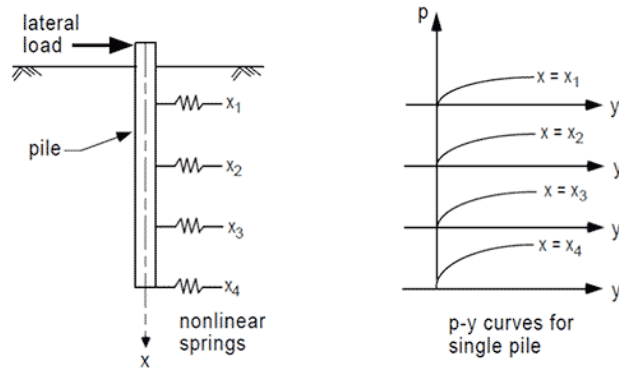


Figure 2.23 Illustration of non-linear p-y curves for laterally loaded piles

2.3 Hybrid Monopile-Footing Foundation Systems

The hybrid monopiled-footing concept is not dissimilar to that of a retaining wall with a stabilising base, in that the stabilising base acts to generate a resisting moment from the underlying soil enhancing the lateral stiffness of the retaining wall. This problem has been studied in detail and is well reported, see for example Carder (1993) and Carder et. al. (1999), Powrie and Daly (2007).

Single gravity tests on a monopiled-footing (Chalkdis 2005, Ward 2006, Stone et al 2007) have been widely reported. Figure 2.24 shows a typical set up for a single gravity model test with a monopiled circular foundation plate rigidly connected to the pile.

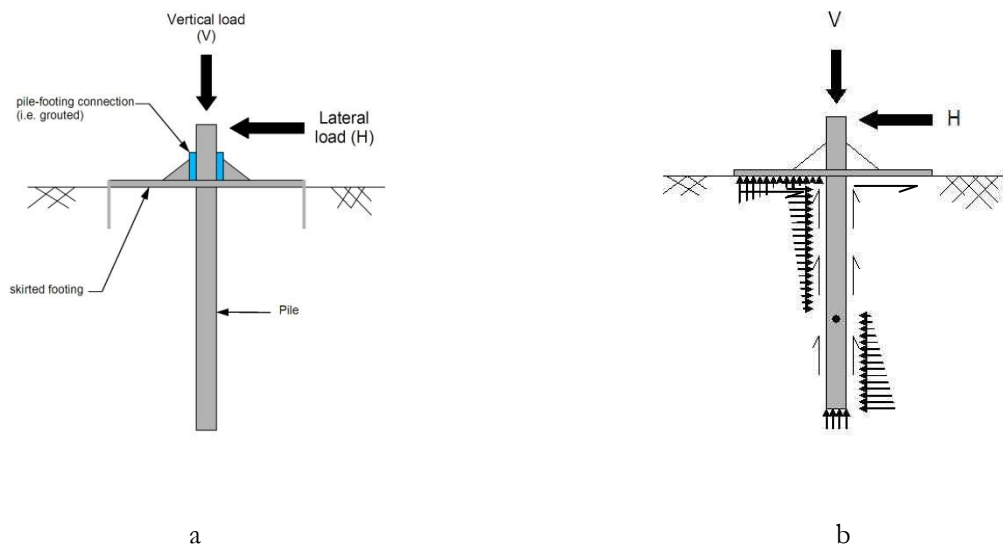


Figure 2.24: Schematic representation of a) hybrid foundation system consisting of a mono-piled footing and b) schematic representation of induced soil stressed.

A typical set of single model test data is shown in Figure 2.25 where it is apparent that the bearing plate significantly enhances the lateral capacity of the monopile for these tests conducted in dense dry sand.

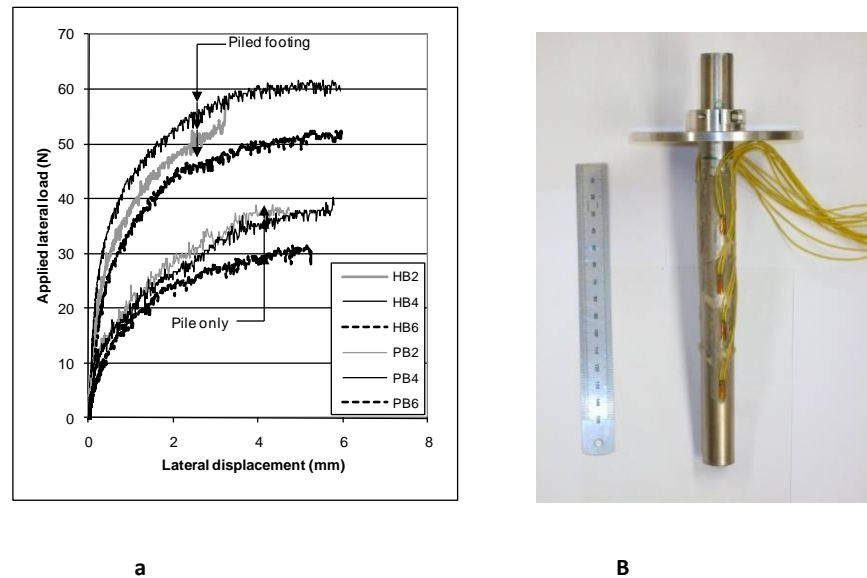


Figure 2.25a: Typical set of single gravity test data (after Stone et al 2007) and b) instrumented model pile and footing after (Stone et al 2010)

A series of centrifuge model tests were also reported by Stone et al 2010a, 2010b, where an instrumented monopile (refer to Figure 2.25b), and more recently by Lehane et al (2014). All these test concerned a hybrid system where the bearing plate was rigidly fixed to the pile. From the single gravity and centrifuge tests reported to date the following summary of findings can be made;

- i) the vertical capacity of the hybrid system is essentially the sum, or slightly greater than the sum, of the individual components (pile and footing)
- ii) the lateral stiffness and load capacity of the hybrid foundation is improved over that of the pile alone and,
- iii) that the initial contact stress between the footing and the soil has a significant influence on the lateral stiffness of the system response.

More recent single gravity tests have been reported by Arshi (2011), and Arshi and Stone (2011, 2012a, 2012b) where further investigations on the influence of the footing size and in particular the connection between the footing and the pile have been investigated. As identified in the early studies referred to above (e.g Stone et al 2007) the requirement for the plate to exert a positive contact with the soil at the onset of loading significantly enhances the initial lateral response of the system. This can be achieved in one of two ways. In the first approach the plate and pile are fixed together and sufficient vertical load is applied such that the axial capacity of the pile is exceeded and the remaining applied vertical load provides a positive pre-stress bearing pressure with the soil. The other approach is to allow vertical movement of the plate to occur such that the footing may act independently from the pile. The positive contact between the footing and the soil underneath is solely controlled by the vertical load acting on the footing.

There are thus two different arrangements that can be configured for the hybrid system. The first relates to the system where the bearing plate or footing is rigidly attached to the pile, and the second to the case where the bearing plate is uncoupled from the pile and free to slide relative to the pile shaft. The two configurations are referred to as ‘coupled’ and ‘decoupled’ hybrid systems respectively and shown schematically in Figures 2.26a to 2.26c.

In the coupled system all the vertical loading is shared between the pile and the bearing plate, and in order to achieve a contact pre-stress between the plate and the ground the loads applied to the system must be such that the axial capacity of the pile is exceeded such that settlement and contact of the plate with the underlying soil will be maintained. This arrangement would appear to offer significant savings in the size and/or length of the monopile and is essentially analogous to a pile raft with a single pile.

In the decoupled configuration vertical loads applied to pile are carried independently from the plate and vice versa, with the only vertical load transfer occurring as the result of frictional contact at the plate/pile connection. The bearing plate is capable of supporting significant vertical loads, for example the entire superstructure weight of a wind turbine and tower may be supported by the bearing plate with little or no vertical load acting on the pile (Ashri 2012).

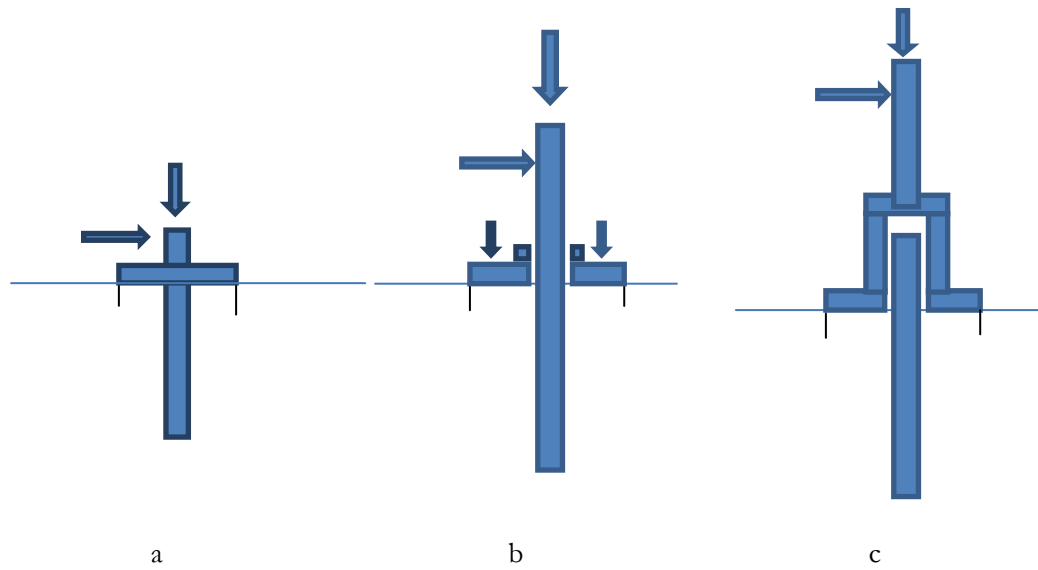


Figure 2.26 a) Typical arrangement for coupled system, b) decoupled system with ballast loading applied to bearing plate and, c) decoupled arrangement with superstructure load carried by bearing plate..

Only a single set of centrifuge tests performed on clay samples is currently reported in the literature (Lehane et al 2010). These tests did not indicate much improvement in the lateral performance of a coupled monopole due to the presence of the bearing plate. However, this was a limited study and thus it is difficult to draw conclusions. It is suggested here that the rather poor performance of the system tested was due to the system geometry in that length of the pile was long and the diameter of the plate relatively small, and hence little vertical load was applied to the soil such that it is likely that there was little positive bearing stress between the plate and the pile since all the vertical load was being taken by the pile. However, further testing is required to investigate the performance of hybrid foundations on clay soils.

The study reported in this thesis is a continuation and expansion of the single gravity and centrifuge tests referenced in this section. In particular the centrifuge test data is somewhat limited and this research is undertaken to considerably enhance the test database of hybrid foundation systems.

3. MATERIALS AND EXPERIMENTAL METHODOLOGY

3.1 Introduction

The single gravity and centrifuge model tests used essentially the same materials and as such that the centrifuge tests can almost be considered as a repeat of the single gravity tests. However in the centrifuge the response of the soil to perturbation (strength and stiffness) is more correctly modelled and can be more directly related to a prototype response. There is thus much commonality between the single gravity and centrifuge models with regard to materials and test methodology.

3.2 Materials

All the single gravity and centrifuge tests were conducted in samples prepared from medium dense dry sand. The sand used was a David Ball fraction C with d_{50} of 0.5 mm. The sand is generally classified as a fine grained, rounded to sub-rounded, uniformly graded quartz sand. The maximum and minimum void ratios were 1.1 and 0.68 respectively, corresponding to dry unit weights of 12.9 and 17.0 kN/m³.

Direct shear box tests were conducted to establish the critical state friction angle of 32 degrees. It was also of interest to establish the interface friction between the sand and the aluminium used for the pile and plate. A simple modification to the direct shear box test was made by placing an aluminium plate in the lower half of the direct shear box. Interface friction values are tabulated below.

Table 3.1. Interface friction from direct shear box tests

Normal stress (kPA)	Interface friction (degrees)	Mobilisation displacement (mm)
49	20	~1.75
98	15	~1
147	15	~1

The model piles, footings and skirted footings used were all fabricated from aluminium with density of 2,700 kg/m³ and Young's modulus of 70,000 MPa. The pile was threaded through the bearing plate which in turn was clamped to the pile. Thus the location of the bearing plate

on the pile shaft could be adjusted for the ease of installation. Tables 3.1 to 3.3 and Figure 3.1 show details of the model foundation system and all of its comprising elements.

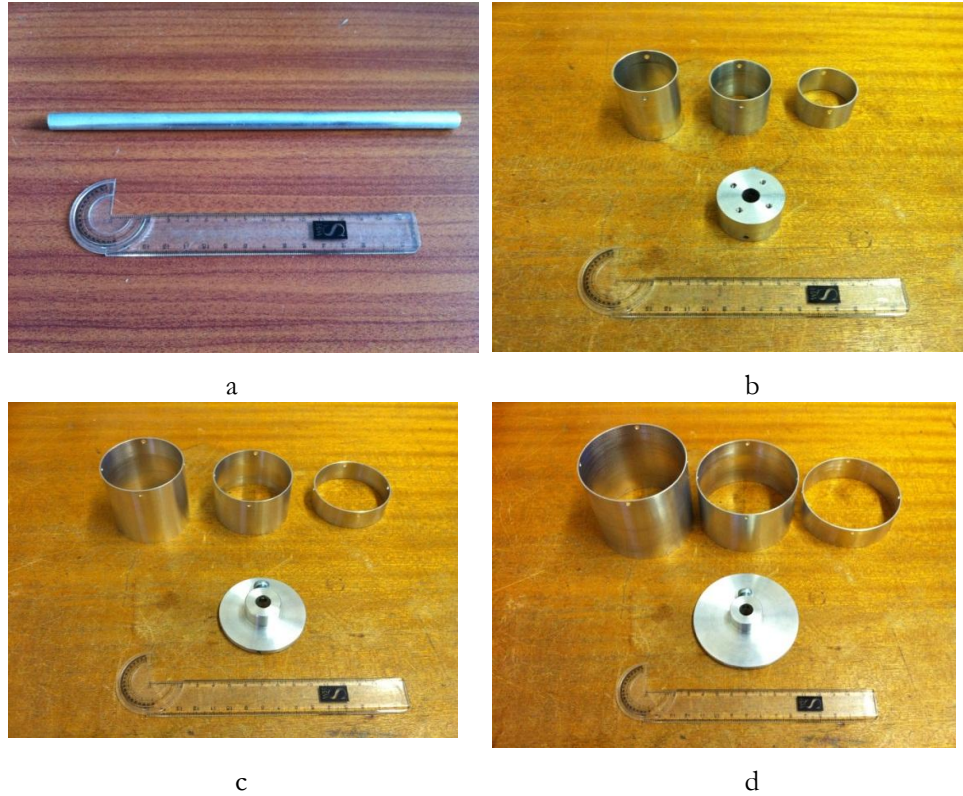


Figure 3.1. Model hybrid foundation system; (a) Pile (b) F40 footing and skirts (c) F60 footing and skirts (d) F80 footing and skirts.

3.3 Experimental methodology

3.3.1 Introduction

In this section the apparatus used to conduct both the single gravity and centrifuge tests is presented together with descriptions of the test procedures. It is noted that there is much similarity in the method of preparation and testing since the centrifuge tests are essentially a replication of the single gravity testing methodology only the tests are undertaken in the enhanced acceleration field induced by the centrifuge.

3.4 Single gravity testing apparatus

A single gravity tests were conducted in a sandbox with internal cross sectional dimensions of 310 mm by 220 mm and a depth of 240 mm. All tests were carried out in a Wykeham-Farrance 1D testing rig, as shown in Figure 3.2. The rig comprised of a 1D actuator located at the top of the rig, with the capability of being able to driving the shaft up or down. The loads

were measured in two different ways; for loads with a relatively low range a digital load cell was used where it could read loads of up to 250 N. For higher magnitudes, a proving ring was used with a capacity of reading loads of up to 700 N.

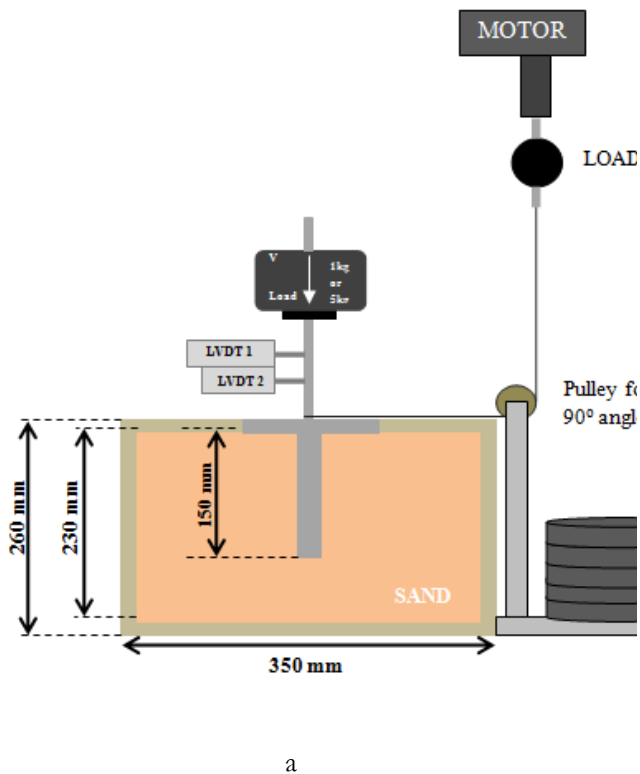


Figure 3.2 a) Schematic diagram and b) photograph of single gravity test arrangement

Deflections were measured using LVDT's (linear variable differential transformers) attached to the piles at two points above the soil surface, at a distance of 20 mm vertically apart (Figure 3.2b). All load and displacement data was continuously monitored and logged throughout the duration of each test using an instruNet data acquisition system.

3.5 Model preparation

Sand was poured into the sandbox in three different stages. First a third of the sandbox was filled by sand by puvlation, the sandbox was then placed on the vibrating table for 20 seconds and then removed. This process was repeated three times until sand reached the sandbox surface. The surface was then scraped carefully tin order to get a levelled surface.

The installation process began with pile driving. The tip of the model pile was positioned in the desired location and was hammered in at a rate of 2 mm/s until the pile reached the

desired penetration depth. The footing was then lowered to the soil surface. In the case of skirted footing, the skirted footing was first lowered until the bottom of the skirts reached soil surface. Then the skirted footing was hammered in at the same rate as the pile (2 mm/s) until the footing reached a soil surface. Once a good contact between the soil and the footing/skirted footing was made, the clamp was secured (fully coupled/fixed pile-footing connection) or was left unsecured (decoupled/slipping pile-footing connection). Figure 3.6 shows a typical foundation installation process.



Figure 3.6. Installation of skirted footings following the completion of pile driving

3.5.1 *Single gravity models*

Several combinations of pile diameter and embedment length, together with combinations of footing diameter and plate length were used in the single gravity test programme. The tables below summarise the component elements used in forming the test combinations.

Table 3.2. Summary of model pile geometries

ID	Pile length, L (mm)
P1	40
P2	60
P3	80
P4	120
P5	160
P6	180
P7	200

Table 3.3. Summary of model footings

ID	Footing thickness, t (mm)	Footing diameter, d (mm)
F1	5	40
F2	5	60
F3	5	80

Table 3.4. Summary of model skirted footings

ID	Skirt thickness, t_s (mm)	Skirt length, L (mm)	Footing diameter, D (mm)	Skirt length (L) / footing diameter (D)
S1.F1	1	12	40	0.3
S2.F1	1	24	40	0.6
S3.F1	1	36	40	0.9
S1.F2	1	18	60	0.3
S2.F2	1	36	60	0.6
S3.F2	1	54	60	0.9
S1.F3	1	24	80	0.3
S2.F3	1	48	80	0.6
S3.F3	1	72	80	0.9

3.6 Centrifuge tests

3.6.1 Introduction

It is well known that the behaviour of most geomechanical materials, such as soil and rock, is very dependent on stress level. In conventional small scale model tests, performed in the Earth's gravitational field, it is not always possible to maintain similarity with prototype situations, and to ensure that stress levels in areas of interest reach prototype values. A geotechnical centrifuge can subject small models to centripetal accelerations which are many times the earth's gravitational acceleration. By selecting a suitable acceleration level the unit weight of the soil being tested can be increased by the same proportion by which the model dimensions have been reduced. Thus stresses at geometrically similar points in the model and

prototype will be the same. In other words, if a $1/N$ scale model of a prototype is spun at $N \times g$ on the centrifuge, then the model's behaviour is thought to be similar to the prototype's behaviour. For this to hold true three assumptions must be satisfied. Namely: 1) that the model is a correctly scaled version of the prototype: 2) that the $1/N$ scaled model when subjected to an ideal gravity field behaves like the prototype at $1g$; and 3) that the centrifuge produces this ideal gravitational field. These assumptions are briefly examined below.

To satisfy this first assumption, that the model is an exactly scaled version of the prototype, requires that the scaling relationships between the model and prototype are met. The establishment of correct scaling relationships is crucial if the prototype response is to be correctly modelled and specific problem may have a unique set of scaling relationships which may be derived by either of the two methods outlined above. Some of the more common relationships are given below in Table 3.5.

Table 3.5: Useful scaling relationships

Parameter	Scaling factor
Acceleration	N
Seepage velocity	N
Length	$1/N$
Stress	1
Strain	1
Force	$1/N^2$
Time (diffusion)	$1/N^2$
Time (creep)	1

The second assumption that the $1/N$ scale model under an ideal Ng gravity field will behave like a prototype at $1g$ is satisfied if the material properties of the model and prototype are the same. Consequently, the use of in-situ materials is often preferred where difficulty in producing an equivalent material with the same prototype properties occurs. However, care must be employed to ensure that grain size effects will not be important when using prototype material.

Finally, the third assumption, that the centrifuge can supply an ideal Ng gravity field, cannot be completely satisfied. This condition would require that the acceleration at any point

throughout the model would not change in magnitude or direction. However, since the acceleration at a point in the model is directly proportional to the radius of that point from the centre of rotation, there must be a variation in imposed acceleration from the surface to the base of the model. This variation in acceleration level also leads to a non-linear stress gradient through the model. This stress level error can be quantified and is deemed a minimum when the gravity scaling factor linking the model with the equivalent prototype corresponds to the gravitational acceleration generated at a depth one third the depth below the model surface (Taylor, 1984).

3.6.2 *University of Brighton Geotechnical Centrifuge Testing Facility*

Figure 3.7a and 3.7b shows the University of Brighton's Geotechnical Centrifuge. The centrifuge was designed and constructed by Broadbent and Sons Ltd and is a 7g/tonne centrifuge capable of reaching 300g.

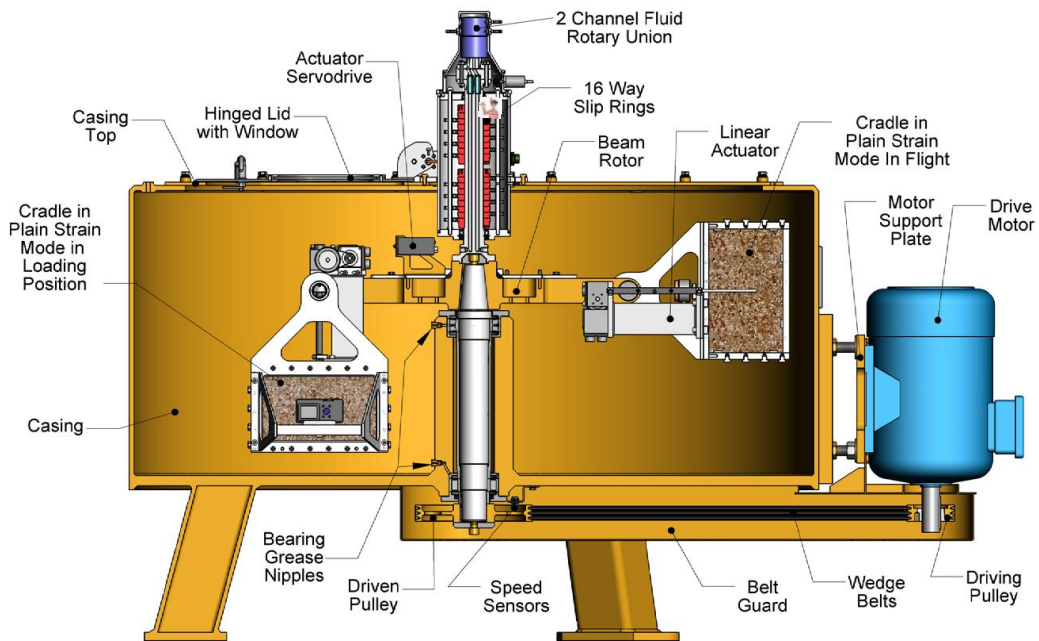


Figure 3.7a - University of Brighton's geotechnical centrifuge



Figure 3.7b - University of Brighton geotechnical centrifuge

The Centrifuge is a balanced beam configuration (Figure 3.7b) and the model, complete with instrumentation are placed in the two swinging cradles suspended on pivots from the ends of a beam rotor. As the speed increases, the cradles swing from the honing position towards horizontal, subjection the models to a centrifugal acceleration.

The experimental procedure for the centrifuge tests is virtually identical to that presented for the single gravity tests. The only difference being that the model once prepared is then placed on the centrifuge and the test performed at an enhanced acceleration of 50 gravities. Continuous recording of load and displacement data is undertaken for the duration of the test.

4. SINGLE GRAVITY TESTS

4.1 Introduction

As mentioned previously the single gravity tests were conducted to obtain a significant database of behavioural response of the hybrid system and to investigate the many variables in a relatively rapid manner. The results of this extensive test programme were then used to design a centrifuge test programme to investigate the more important factors which influence the response of the hybrid system.

4.2 Single gravity test programme

The testing programme was divided into four distinct series. Each series focussed on a different element that contributes or affects the overall behaviour of the foundation system. The sections below present the programme of tests undertaken in each series.

Series 1: Lateral load bearing capacity of monopiles

This series investigates how single monopiles behave under lateral loads to derive a basis for comparison to the response of the hybrid foundation system. The following parameters are investigated:

- The effect of vertical load on the lateral load bearing capacity of the monopile.
- The effect of pile embedment depth on the lateral load bearing capacity of the monopile.
- The effect of the location of point of applied load on the lateral load bearing capacity of the monopile.

A summary of the series 1 tests are presented in Table 4.1.

Series 2: Vertical load bearing capacity of footings

The development of the bearing capacity under the footing is essential in understanding and analysing the behaviour of hybrid foundation system. For the purpose of this investigation and analysis, the following will be looked at:

- The effect of footing size on the vertical load bearing capacity
- The vertical load bearing capacity of centrally loaded footings
- The vertical load bearing capacity of eccentrically loaded footings

A summary of the single gravity footing tests is presented in Table 4.2.

Series 3: Vertical load bearing capacity of skirted footings

The addition of skirts provides a potential beneficial impact to further enhance the bearing capacity of soil under the footing. Hence the development of the bearing capacity under the skirted footings is of interest. For the purpose of this investigation and analysis, the following will be investigated:

- The effect of skirt length on the vertical load bearing capacity of the skirted footings
- The vertical load bearing capacity of centrally loaded skirted footings

The series 3 skirted footing tests undertaken is summarised in Table 4.3

Series 4: Lateral load bearing capacity of monopiled-footings

The investigation of the constituent element of the hybrid system in the previous test series are brought together when the behaviour of the hybrid monopile-footing, both skirted and unskirted, is investigated in detail. This study will investigate the following:

- The effect of footing size
- The effect of connectivity between the bearing plate and the pile
- The effect of vertical load applied by the bearing plate
- The effect of pile embedment depth
- The effect of the point of applied lateral load
- The effect of skirt length

A summary of the unskirted monopile-footing tests is presented in Table 4.2 and the skirted monopile-footing tests in Table 4.3.

4.3 Results

As is evident from Tables 4.1 to 4.4 that a considerable number of single gravity test were undertaken as part of this study. However, these tests are considered as a thorough preliminary assessment of the monopiled-footing system and are essentially a precursor to the centrifuge tests reported later in Chapter 5. Consequently, a limited presentation of the single gravity tests is presented here to illustrate the more significant findings.

The data are generally presented through plots of applied lateral load, H (N) versus measured lateral deflection at the mudline, δ (mm). This graph represents the lateral response of the foundation system from which the lateral stiffness and ultimate lateral capacity can be derived. The pile is assumed to rotate as a rigid body and the horizontal displacement at the mudline is derived from the following expressions where φ is the tilt of the pile as derived from the LVDT readings.

$$\varphi = \text{Tan}^{-1}\left(\frac{\delta_{LVDT1} - \delta_{LVDT2}}{\text{Distance between the two LVDTs}}\right) \quad 3.1$$

$$\delta = \delta_{LVDT1 \text{ or } 2} - \left(\frac{\text{Distance from LVDT1 or 2 to the pile tip}}{180 - 90 - \varphi}\right) \quad 3.2$$

4.3.1 Monopile Tests

The lateral response of the monopile is of interest since it forms the baseline for comparing the performance of the hybrid system. The single gravity tests were principally designed to investigate the effect of applied vertical load and pile embedment depth on the lateral capacity of the pile although the effect of the point of load application was also investigated.

4.3.1.1 The Effect of Vertical Load

The effect of the vertical load on the lateral response of the pile was investigated for axial loads of 0, 10 and 50N. The pile embedment depth was constant at 150 mm for all the tests. Figure 4.1 summarises the results through plots of lateral load (H) versus horizontal mudline displacement (δ). It is apparent from this plot that the lateral response is significantly enhanced by the magnitude of the vertical load. It is noted that this response is consistent with other studies (see for example Karthigeyan et al 2007). The increase in lateral stiffness

and capacity is significant for the 10N increment in vertical load but less so for the following increment from 10 to 50N.

The results suggest that for the given pile geometry, there may be a critical vertical load after which the lateral load capacity and its stiffness remains relatively invariant to further vertical loading.

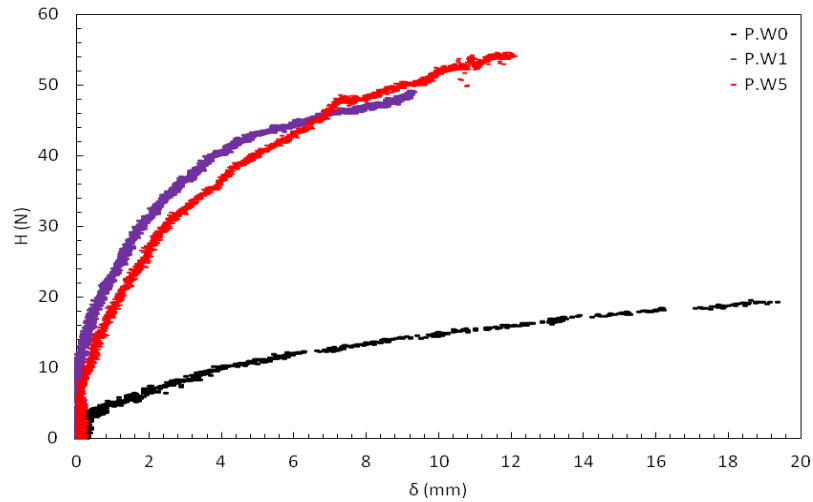


Figure 4.1. H vs. δ graph for the monopile under different vertical loads

4.3.1.2 The Effect of Pile Embedment Depth

As would be expected the lateral capacity and lateral stiffness of the model piles increased as the embedment depth increased, refer to Figure 4.2. In these tests all the piles responded as 'rigid' piles and as such the increase in lateral capacity is seen to be proportional to the embedment depth.

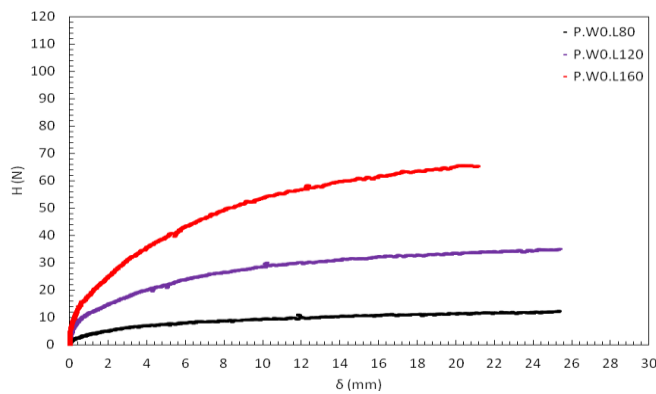


Figure 4.2 H vs. δ graph for the monopile with different embedment depths, L, of 80, 120 and 160mm.

4.3.1.3 *The Effect of the Location of the Point of Applied Lateral Load*

For this set of tests, the pile geometry was kept constant together with penetration depth of 150 mm and vertical load of 50 N. The lateral load was then applied at heights of 18 mm, 68 mm and 118 mm above the mudline. Only a single LVDT was used and the horizontal displacement is that recorded by this instrument and not the displacement at the mudline.

As would be expected the higher the point of application of the load, the greater is the moment at the mudline, and hence the lateral force required to achieve a particular displacement reduces.

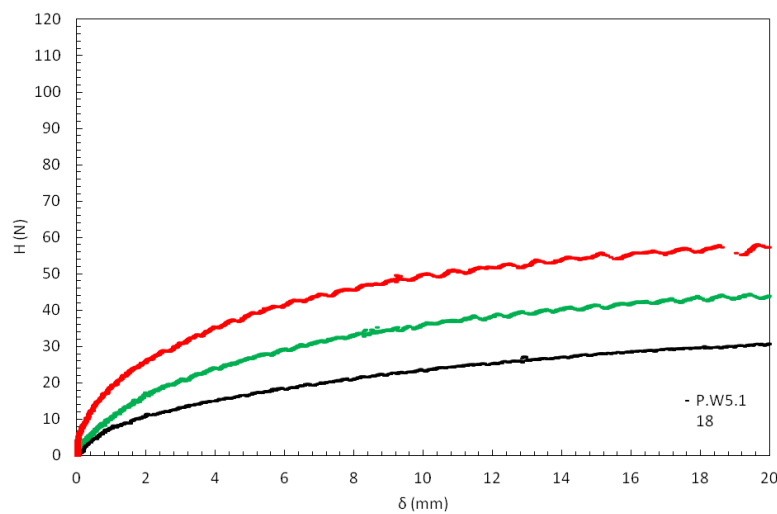


Figure 4.3. H vs. δ graph for the monopile with H applied at different heights above the soil surface.

4.3.2 *Footing Tests*

A circular footing or bearing plate is the second component of the hybrid system and as such single gravity tests were conducted to establish the behaviour of 40, 60 and 80mm footings used in the experimental tests. A typical set of centrally loaded footings are presented in Figure 4.4. A set of eccentrically loaded tests conducted on the 60mm diameter footing are shown in Figure 4.5.

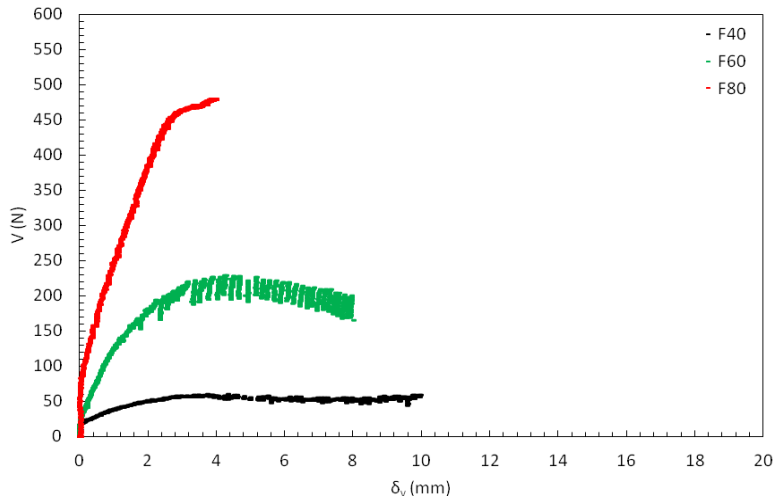


Figure 3.4 Vertical load vs. Vertical displacement (δ_v) graph for centrally loaded footings with 40, 60 and 80mm diameters.

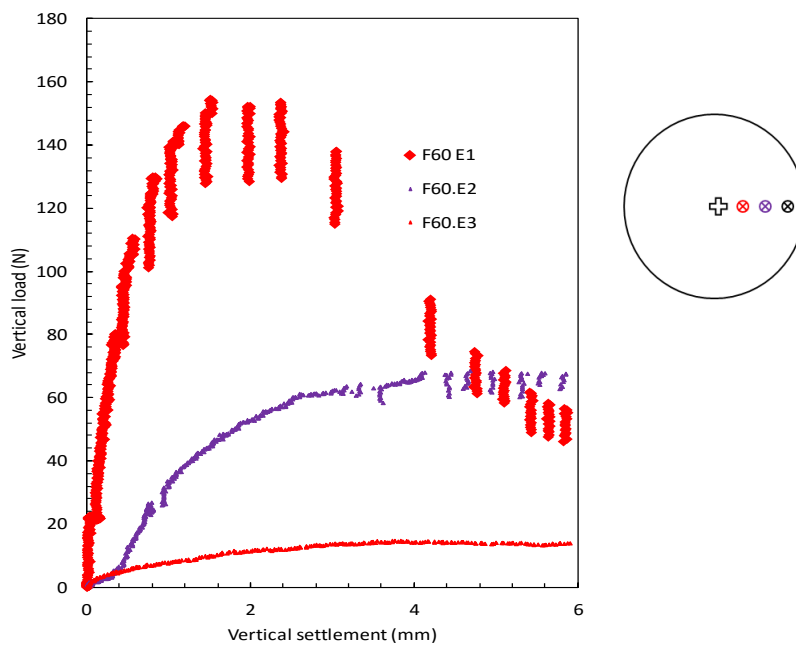


Figure 4.5. Vertical load (V) vs. δ_v for the eccentrically loaded footing 60mm diameter footing. Load eccentricities as quarter radius points shown on key

The main observations from the eccentrically loaded tests are that the footing capacity is reduced as the eccentricity increases and the overall response becomes much more strain-softening with an unstable peak strength (i.e. significant post peak capacity reduction). It is of interest to note that in the hybrid system the eccentrically loaded footing capacity would be responsible for generating the restoring moment at the pile head due to the soil pressure acting on the underside of the footing. As high footing rotations it is evident that the

restoring moment would reduce as the bearing capacity reduced. For completeness skirted footing tests were also undertaken from which the general response was similar to the unskirted tests, only the footing capacities were increased due to the shear strength mobilised on the skirt.

4.3.3 Hybrid Monopile-Footing Tests

The single gravity test programme is considered as precursor to the centrifuge study and was designed to investigate the effect of several parameters on the general response of the system. Due to the large number of permutations the majority of the tests were conducted with a single pile embedment depth (150mm) and a constant pile diameter (10mm). Footing sizes of 40 mm (F40), 60 mm (F60) and 80 mm (F80) were used with varying magnitudes of dead load (10 N and 50 N), and different pile-footing connectivity arrangements (coupled/fixed or decoupled/free). A considerable amount of test data was generated from the full programme of single gravity tests and all these data are reported in detail in Arshi (2013 -PhD Transfer report). In the following section the most significant observations are reported by way of plots of lateral load (H) versus lateral displacement at the mudline δ .

Figures 4.6a to 4.6b show a set of lateral load versus displacement plots for the three plate diameters (40, 60 and 80mm) with a vertical load of 50N for both the coupled and decoupled arrangements.

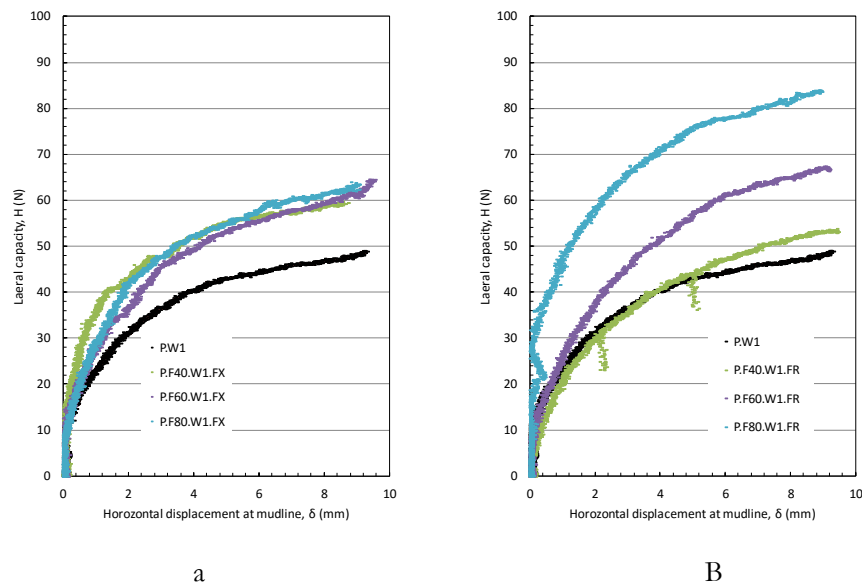


Figure 4.6 Lateral load versus displacement plots for the three plate diameters (40, 60 and 80mm) with a vertical load of 50N for (a) coupled and (b) decoupled arrangements

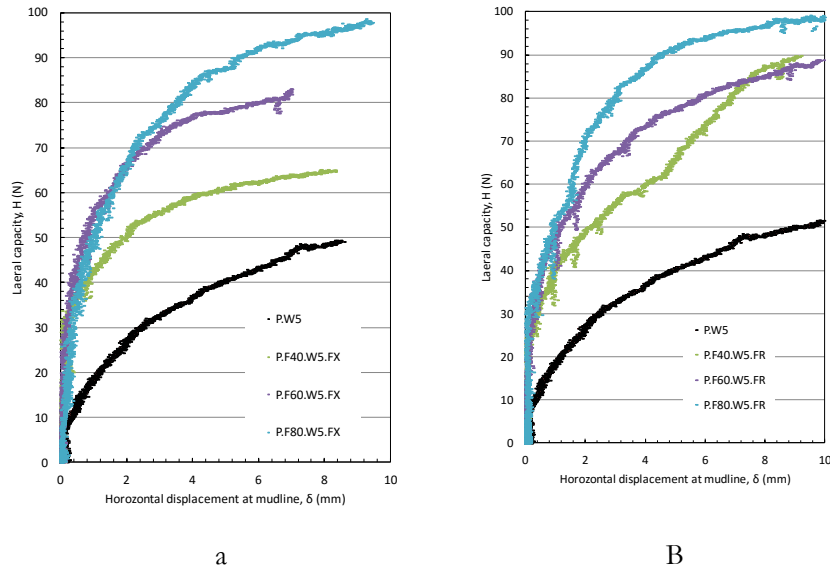


Figure 4.7 Lateral load versus displacement plots for the three plate diameters (40, 60 and 80mm) with a vertical load of 10N for (a) coupled and (b) decoupled arrangements

The behaviour of the hybrid system with the F40 footing, under 10 N vertical load and a fully fixed P-F (pile-footing) connection is shown in Figure 4.7. These data indicate that the addition of the footing seems to improve the response of the foundation as a stiffer response is exhibited by the hybrid system and the ultimate lateral capacity is significantly improved.

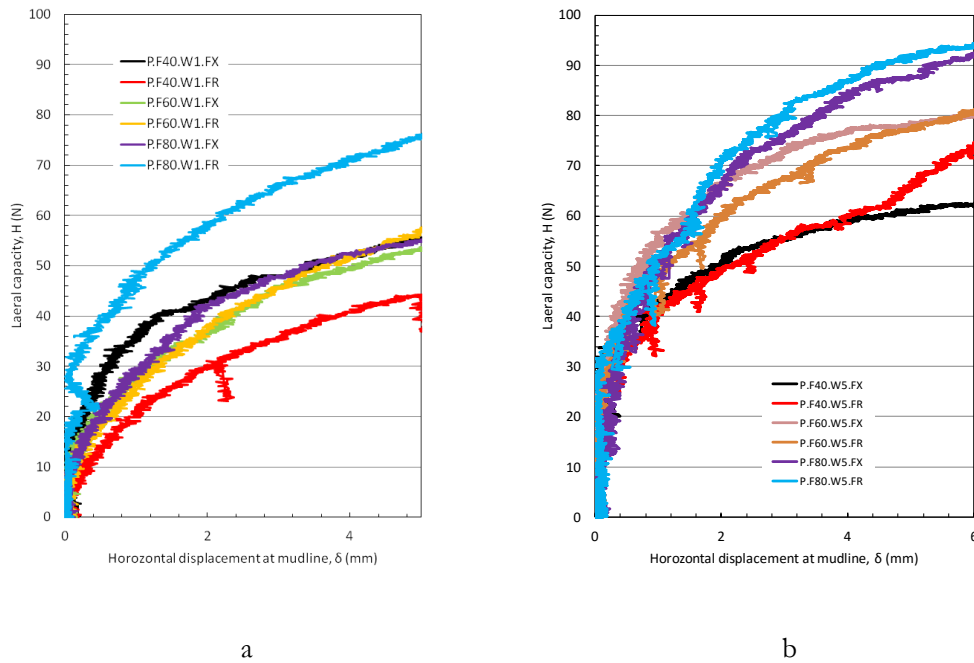


Figure 4.8 Initial lateral load versus displacement plots for the three plate diameters (40, 60 and 80mm) with a vertical load of 10N for (a) coupled and (b) decoupled arrangements

A comparison between the coupled and decoupled response is presented in Figures 4.8a and 4.8b. In general the response between the coupled and decoupled systems is similar for the 50N applied load but less so for the 10N applied load.

The pre- and post test photographs for a 10N and 50N decoupled tests for the 80mm pile and 80mm decoupled hybrid are presented below in Figure 4.9 and 4.10. For the 10N vertical load the footing does not appear to move vertically on the pile during the test. However for the 50N test it is clearly apparent that the plate has slid upwards relative to the pile shaft by some 5-6mm. This is an interesting observation and suggests that unless the plate is locked to the pile, then the bearing pressure that can be generated will be directly related to the initial contact stress created by vertical loads acting on the plate at the start of the test. This is in contrast to the coupled case where high bearing pressures can develop as the plate rotates into the soil.



a



b

Figure 4.9a. Pre- and post test (b) photos for decoupled hybrid 10N load and 80 mm plate



a



b

Figure 4.10a. Pre- and post test (b) photos for decoupled hybrid 10N load and 80 mm plate

4.3.4 Skirted Hybrid Monopile-Footing Test

The behaviour of the hybrid monopile-footing system under lateral loads was investigated in the previous section. The focus of this section is to investigate whether or not the addition of skirts improves the lateral performance of the foundation system, and if so, how does the geometry of the skirt affect this improvement. The tests were performed with skirts added to the 40, 60 and 80mm footing. Three skirt lengths of $S1=l/d=0.3$ (30% of the footing diameter), $S2=l/d=0.6$ (60% of the footing diameter), and a long skirt $S3=l/d=0.9$ (90% of the footing diameter) were used. For each footing, the hybrid system was tested with varying magnitude of dead load (set at 10 N and 50 N), and different pile-footing connectivity (coupled and decoupled).

4.3.4.1 Overview of results

As for the unskirted tests the performance of the system is illustrated through plots of the lateral load versus lateral displacement derived at the mudline. The effect of the skirts is demonstrated here with reference to the 60mm diameter footing. Figure 4.11 below shows the lateral response of the coupled (FX) and decoupled (FR) 60mm skirted footing for an applied load of 50N. Also shown on these plots are the force vs displacement plots for the unskirted hybrid system for comparison.

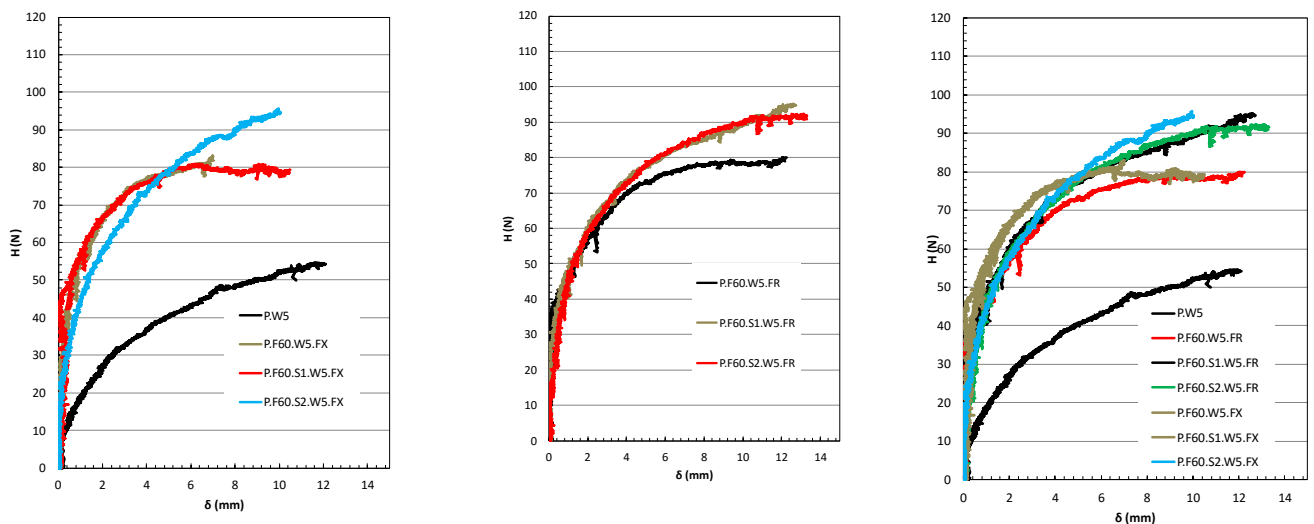


Figure 4.11, Overview of results of skirted monopiled systems and comparison to unskirted tests

It is apparent from these data that the addition of skirts has a marginal effect on both the coupled and decoupled systems, with a more marked improvement being observed for the decoupled system.

Figure 4.12 below compares the response for both a skirted and unskirted 80mm footing, coupled and decoupled system in a single plot with three skirt lengths. It is interesting to note that the response of skirted monopiled-footing systems is relatively similar, especially for the coupled system which also shows a very similar response to the unskirted coupled system. For the decoupled system there is some influence of the skirt length and the skirted systems yield a higher ultimate capacity and stiffer lateral response than the unskirted system.

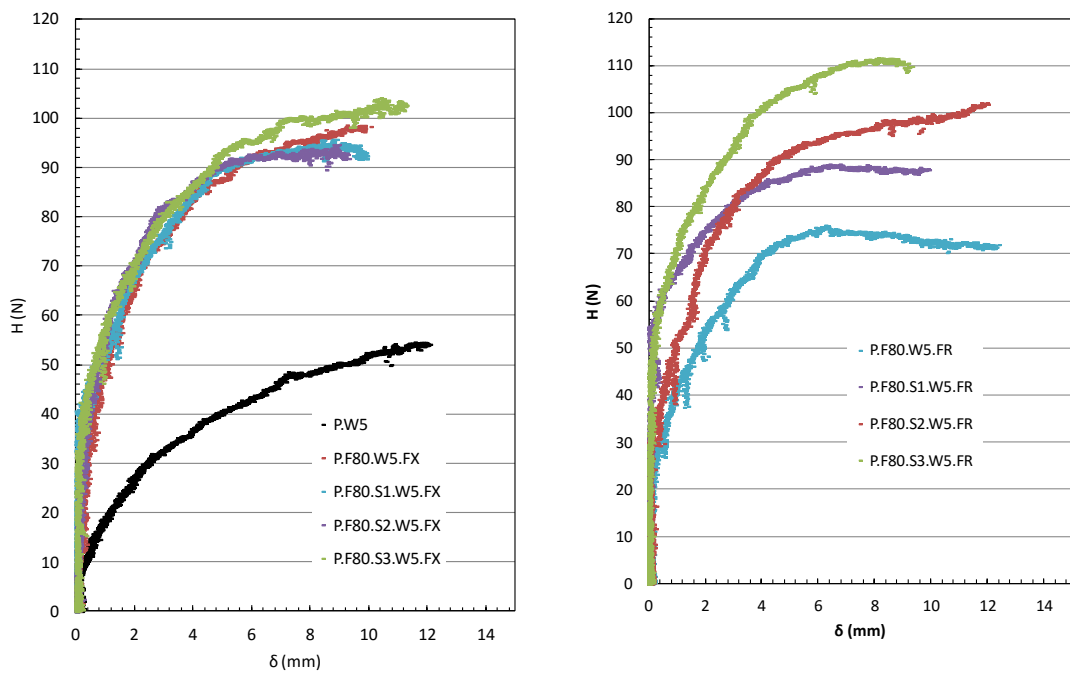


Figure 4.12. Comparison of skirt length on lateral capacity

4.4 Discussion and analysis of single gravity tests

The single gravity model study investigated the elements of the hybrid system individually and then together. Several parameters were investigated, including pile and footing geometries, vertical loading arrangements, skirted and unskirted footings and the connection between the pile and the footing. It is noted however that the vertical loads used in the tests were not selected based on a particular rationale but more for convenience of the size of the dead

weights available (1 and 5kg). It is noted that for the decoupled arrangement the dead weight would induce a bearing stress on the soil associated with the weight and plate area as follows:

	Footing diameter		
	40(mm)	60(mm)	80(mm)
Vertical Load (N)	Bering stress under footing kPa		
10	8	3.5	2
50	40	17.5	10

For the coupled arrangement where the footing and pile are rigidly connected then the pile capacity is not exceeded for either the 1kg (10N) or 5kg (50N) applied vertical loads and as a consequence the initial contact stress at the plate soil interface would be established on installation. It is thus not possible to establish what the initial contact stress is and consequently what relative proportion of the load is carried by the pile and plate. It is generally assumed that for the coupled case all the vertical load is carried by the pile.

From the results of the single gravity tests the following observations can be made.

- The results are consistent with previous single gravity modelling of a hybrid monopile-footing system in that (i) the ultimate lateral resistance is increased and (ii) the lateral stiffness is enhanced.
- The lateral capacity of the monopile increases with applied vertical load. This increase in capacity is significant for up to 10N applied load but little variation is observe for 10-50N.
- The response of the coupled system was relatively unaffected by the footing diameter for the 10N tests but for the 50N loading the ultimate capacity increased as the footing diameter increased.
- The bearing stress induced between the plate and soil in the decoupled arrangement is potentially limited by the tendency of the plate to slide up the pile.
- For the decoupled arrangement the bearing plate improved the lateral response of the system as the plate size increased, for both the coupled and uncoupled arrangements.
- The 60mm footing response was similar for both the coupled and decoupled arrangements for both the 10 and 50N loads.

- The addition of skirts has a marginal effect (slight improvement) for the decoupled monopiled-footings but a minimum effect on the coupled systems. It is noted that the presence of skirts will increase the axial capacity of the system. This may result in a lower contact stress between the footing and the soil for the decoupled system.

5. CENTRIFUGE MODEL RESULTS

5.1 Introduction

The centrifuge model test programme was essentially conducted in two main series of tests. All the tests used a 10mm diameter pile with the first series using an embedment depth of 40mm, and for the second series an embedment depth of 80mm. The footing diameters were 40, 60 and 80mm as for the single gravity tests, and both coupled and decoupled systems were tested. Importantly, axial loading for the centrifuge tests were selected to provide bearing pressures at the soil/plate interface that would be 5, 10 and 25% of the ultimate bearing capacity. It is also noted that when no load is applied, the self-weight of the plate provides some nominal bearing in the decoupled arrangement. For the 40mm footing, which was 20mm thick, the self-weight bearing pressure at a test acceleration of 50g is approximately 3% of the ultimate bearing capacity. As for the single gravity tests the individual components of the system are tested (pile and footing), as well as the hybrid system for both coupled and decoupled pile-plate connections. A summary of the centrifuge tests undertaken is presented Table 5.1 and 5.2. This latter table also presents the derived values for the plate-soil bearing pressure present at the start of each hybrid system test. It is noted that for the coupled system the initial bearing pressure is estimated by assuming that the pile is yielding and that the load carried by the plate is the difference between the total load and the ultimate axial capacity of the pile.

5.2 Vertical load response

It is of interest to investigate the vertical response of the hybrid system and the component elements (i.e. the pile and bearing plate) to establish the relative contributions of the pile and plate to the ultimate vertical capacity. In particular it is required to determine suitable values for initial vertical loading of the coupled and decoupled systems to ensure a degree of pre-stress of the underlying soil is achieved. Vertical testing of the hybrid system is only relevant for the coupled arrangement where the vertical capacity of the pile is required to be exceeded before any pre-stress can be developed between the bearing plate and the soil. In these tests the bearing plate was clamped to the pile shaft and the pile embedded such that the plate was initially clear of the soil surface at the start of loading.

Plots of vertical load versus vertical displacement for a coupled hybrid system comprising of a 40mm diameter plate and 10mm diameter pile, with an 80mm pile embedment depth, are

shown in Figures 5.1a and 5.1b for tests conducted at 20 and 40g respectively. Also shown on these plots is the vertical load response for the pile alone at the respective g-level. For both tests it is observed that for the initial portion of the plot the vertical capacity for the hybrid system is coincident with that observed for the pile. As the pile penetrates the soil the bearing plate comes into contact with the soil surface and an increase in vertical load is recorded. For the 20g test an ultimate vertical capacity of approximately 1200N is achieved. For the test conducted at 50g the capacity of the loading actuator is exceeded before the ultimate vertical capacity of the hybrid system is reached.

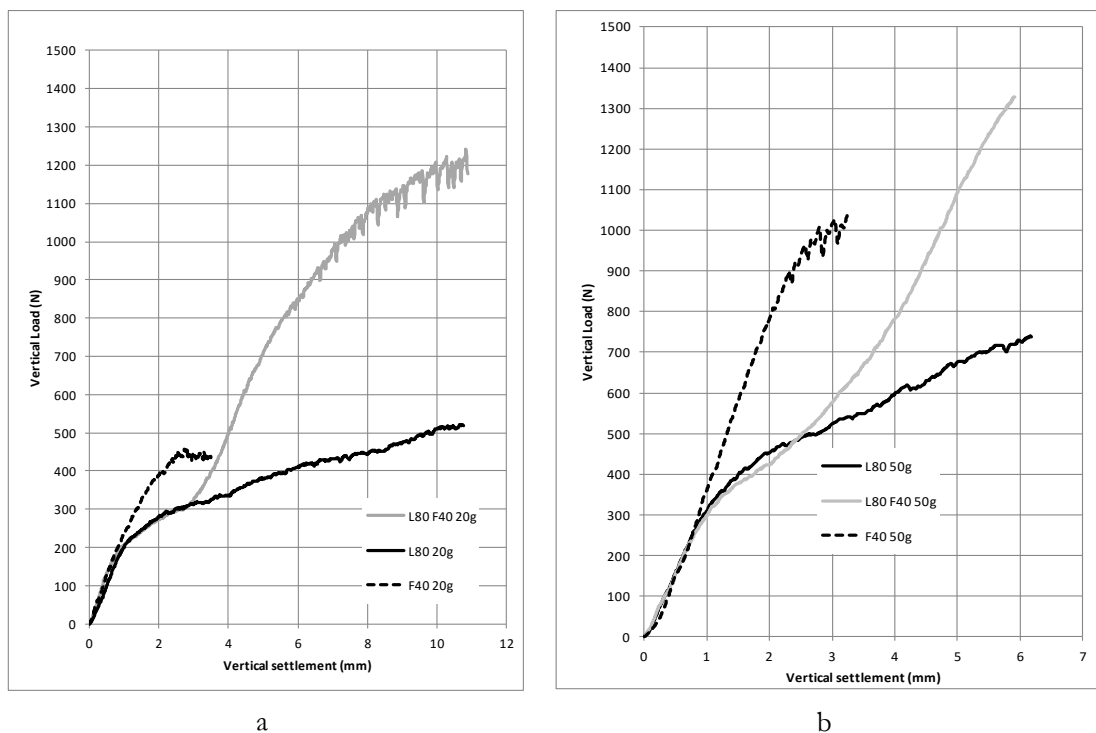


Figure 5.1a Plots vertical load versus vertical settlement for 40mm bearing plate (F40), 10mm diameter pile with 80mm penetration (L80) and coupled hybrid (L80 F40) at 20g and b) at 50g.

Vertical loading tests were also conducted to establish the ultimate bearing capacity of the footings. Figure 5.2 shows the load displacement plots for a 40mm diameter plate tested at 20 and 40g. The ultimate capacity of the footings alone is estimated at 450N and 1000N for the 20 and 50g tests respectively. It is of interest to note that for the tests conducted at 20g the ultimate capacity of the hybrid system is greater than the sum of the individual components, namely the pile and the footing. This can be attributed to (i) the increase shaft resistance generated at the pile soil interface due to the increased vertical effective stress generated by the plate bearing pressure, and (ii) the presence of the pile protruding below the footing which tends to stabilise the footing and reduce the effect of eccentric loading during the test.

It is also noted that the form of the load displacement plots for the pile and plate are significantly different. For the footing tests a relatively distinct ultimate capacity is observed, whereas for the pile tests no ultimate vertical capacity can be readily defined since the capacity continues to increase as the pile is driven into the soil.

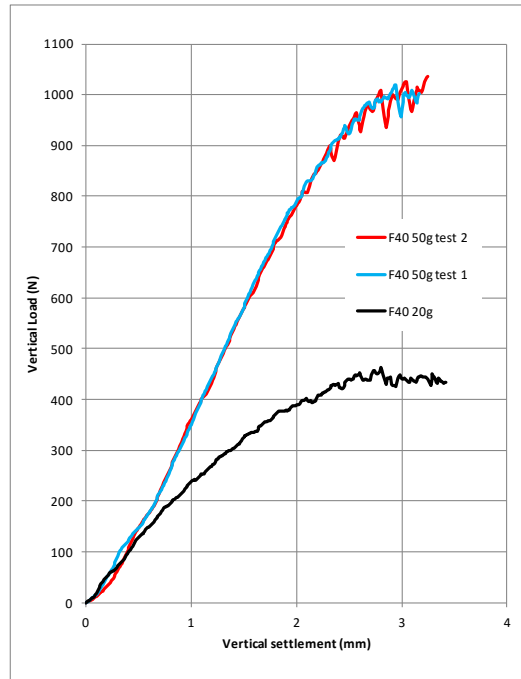
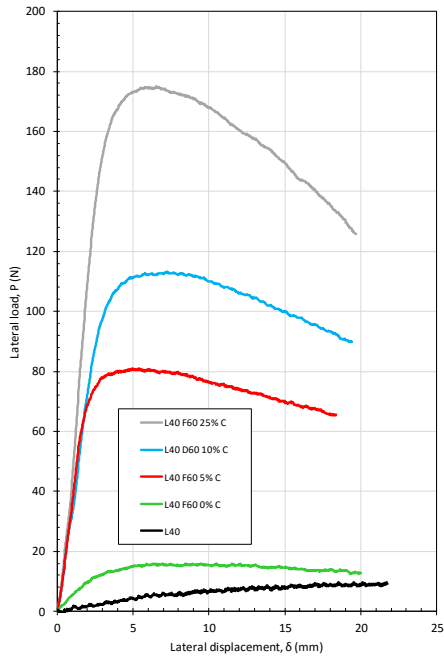


Figure 5.2. Plot of vertical load versus vertical settlement for 40mm bearing plate at 20 and 50 gravities.

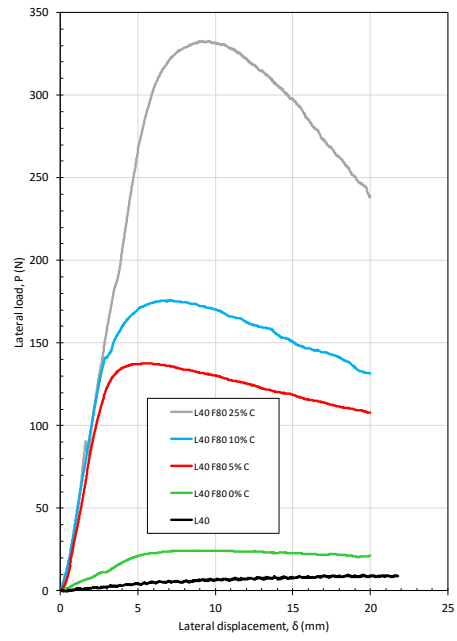
5.3 Lateral response

The results of the centrifuge tests are best presented through plots of lateral load versus lateral displacement. Two test series are reported here, in the first Series 1 tests the pile embedment depth of 40mm is used together with a 60 and 80mm bearing plate. In the second test Series 2 the pile embedment length of 80mm is used together with 40, 60 and 80 mm diameter bearing plates. In all the tests the pile diameter was 10mm and initial pre-stress loading ranged from 0% to 25% of the estimated ultimate bearing capacity of the soil.

An overview of the Series I tests is presented as follows. Figure 5.3 shows the lateral response of the coupled hybrid system with a 10mm diameter pile with 40mm embedment depth, and 60 and 80mm diameter bearing plates. Figure 5.3 shows the response for the corresponding decoupled arrangement.

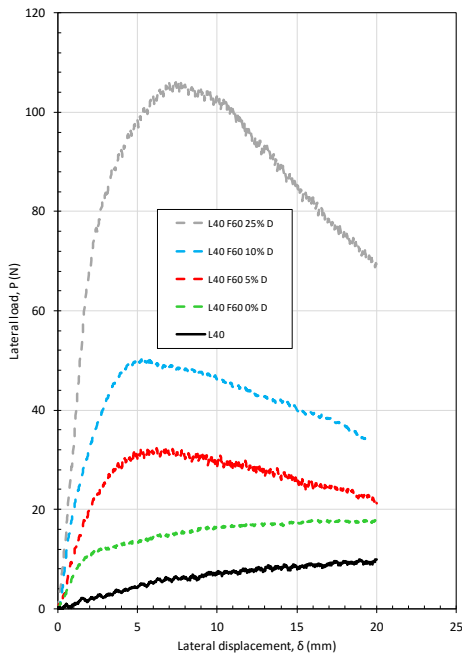


a

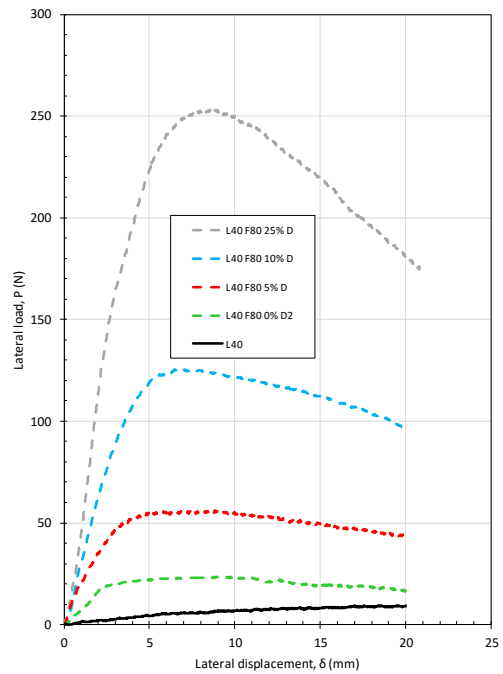


b

Figure 5.3a) Overview of coupled hybrid system; 10mm diameter pile, 40mm embedment depth (L40); 60mm bearing plate (F60) and b) 80mm diameter bearing plate (F80).



a



b

Figure 5.4a) Overview of decoupled hybrid system; 10mm diameter pile, 40mm embedment depth (L40); 60mm bearing plate (F60) and b) 80mm diameter bearing plate (F80).

The Series I tests are further presented in Figures 5.5 which plot the response of the hybrid system for each level of applied bearing stress (applied vertical load).

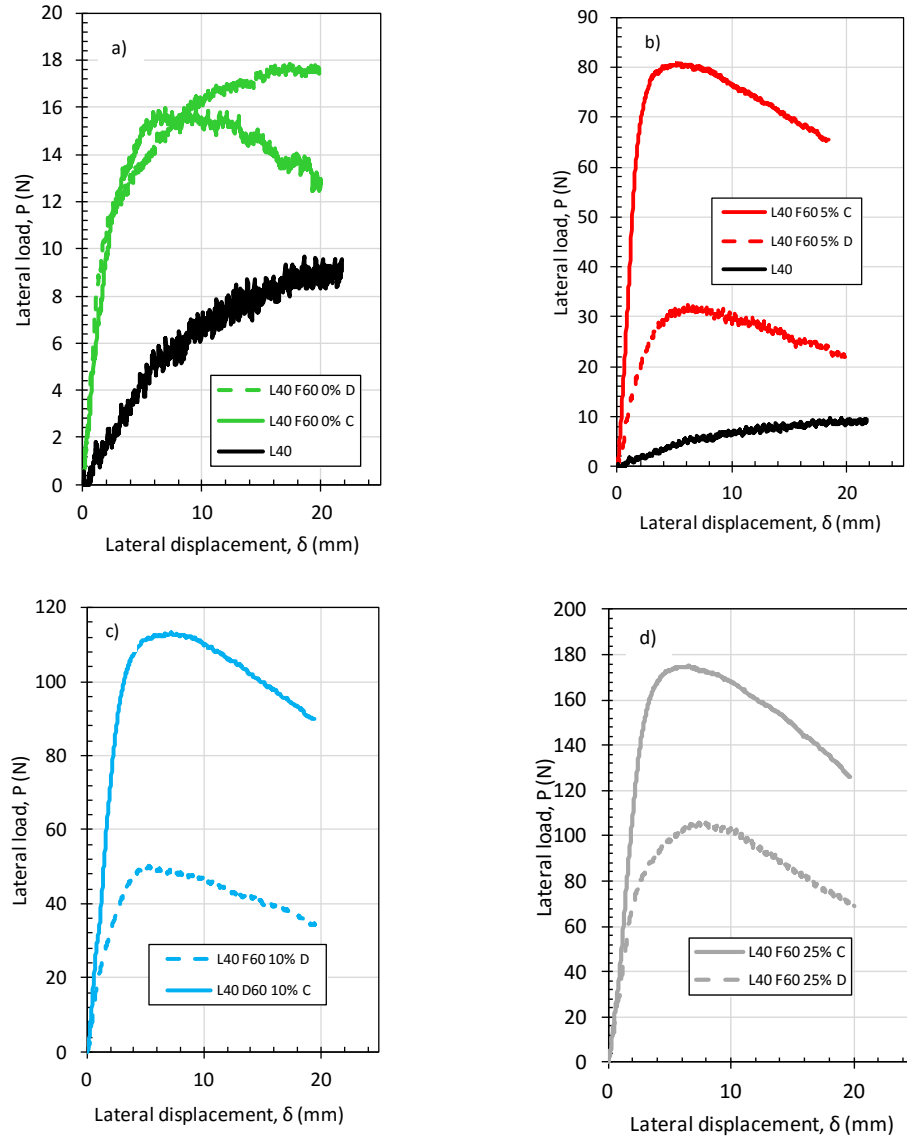


Figure 5.5. Comparison of coupled (C) and decoupled (D) lateral response for 10mm pile; 40mm embedment depth and 60mm diameter bearing plate for initial bearing stresses of a) 0%; b) 5%; c) 10% and d) 25% of estimated ultimate bearing capacity.

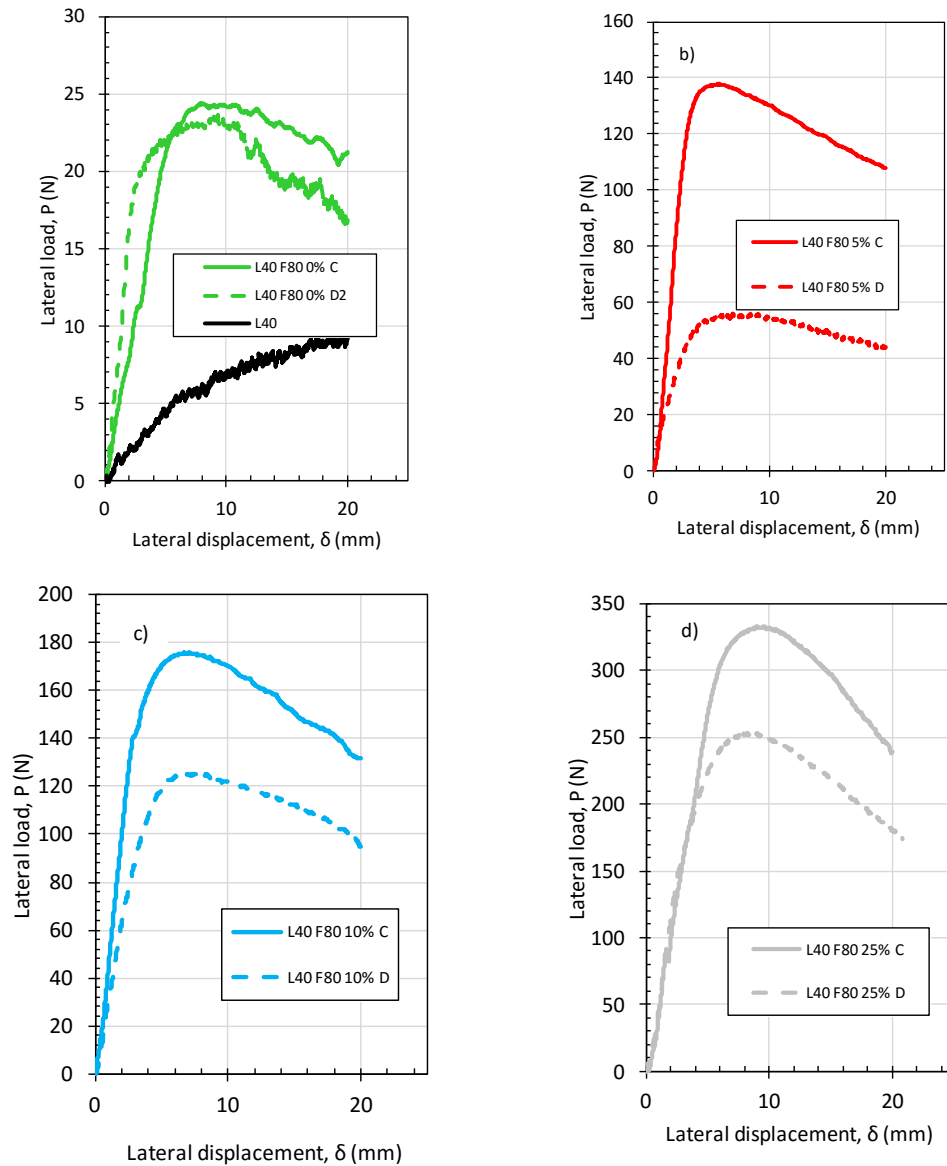


Figure 5.6. Comparison of coupled (C) and decoupled (D) lateral response for 10mm diameter pile; 40mm embedment depth and 80mm diameter bearing plate for initial bearing stresses of a) 0%; b) 5%; c) 10% and d) 25% or estimated ultimate bearing capacity.

Referring to Figures 5.5a and 5.6a for the 40mm long pile (Series 1) with 60 and 80mm diameter bearing plates, for the case where the pre-stress is derived from the self-weight of the bearing plate, it is apparent that even at this low pre-stress the bearing plate enhances the lateral capacity of the monopile with very similar response being observed for the coupled and decoupled systems. For the higher 5 and 10% pre-stress tests the results of the coupled and decoupled systems are again broadly similar, refer to Figures 5.5b, 5.5c and 5.5d, and Figures 5.6b, 5.6c and 5.6d, however it is noted that the relative increase in the lateral capacity is much more significant.

The Series 2 results, with the 80mm long pile, are presented in Figures 5.5 and 5.6. Figures 5.5a and 5.6a show the results for the 40mm bearing plate. It is interesting to note that for the coupled system (refer to 5.5a), there is an increase in lateral resistance as the result of the presence of the plate with its nominal pre-stress due to self-weight, but on further addition of load, the lateral response at the higher pre-stress levels of 5, 10 and 25% does not appear to influence the lateral capacity of the system. To a certain extent a similar trend is observed for the 60mm diameter plate (figure 5.5b). In this case there are significant increases in lateral capacity associated with the low pre-stress levels associated with the plate self-weight and 5% pre-stress case, but little variation in lateral capacity is observed for increases in pre-stress from 5 to 25 %.

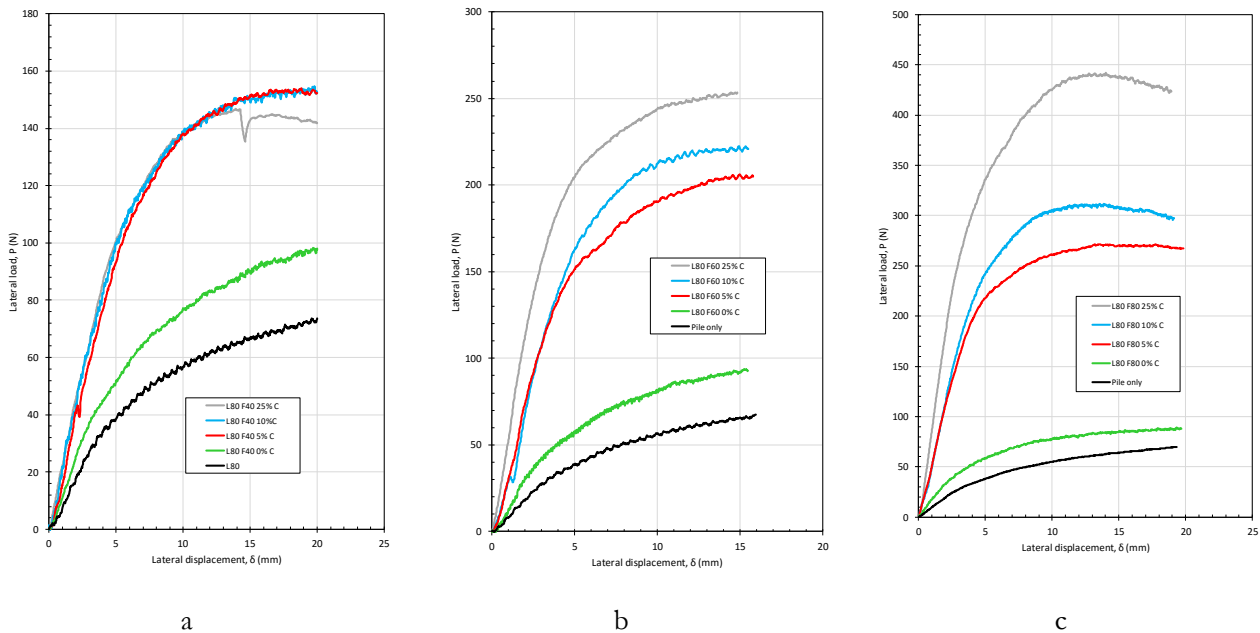


Figure 5.5a. Overview of coupled hybrid system with 10mm diameter pile, 80mm embedment depth (L80), with 40mm diameter bearing plate (F40), (b) 60mm diameter bearing plate (F60) and (c) 80mm diameter bearing plate (F80) and applied vertical stress as percentage of ultimate bearing stress.

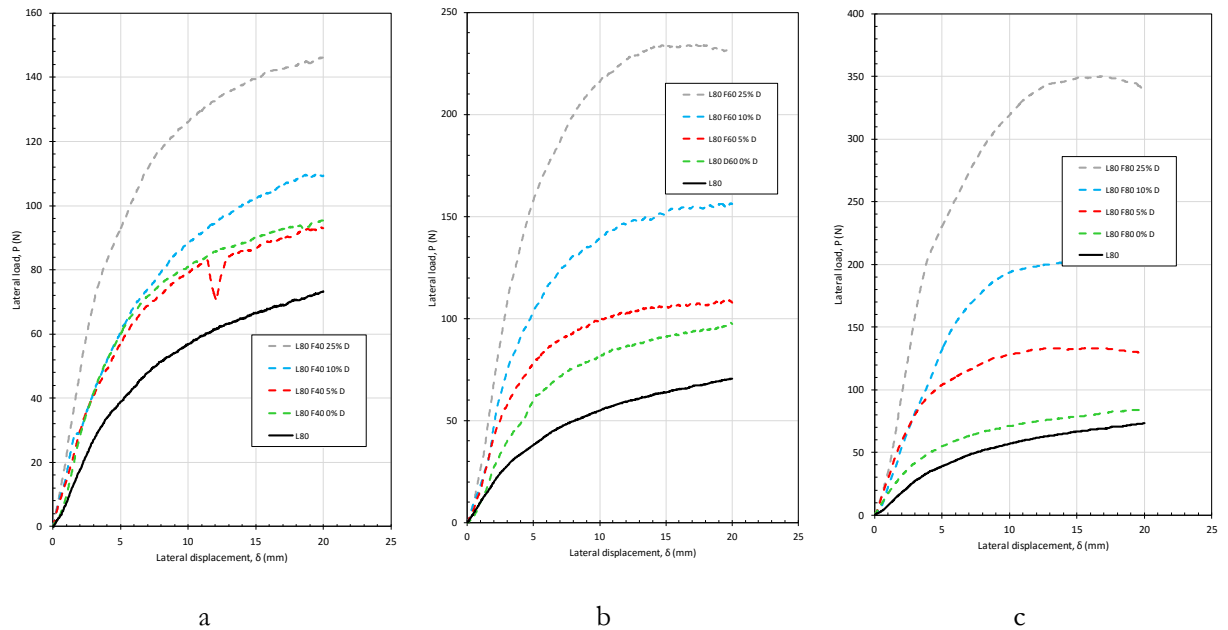


Figure 5.6 (a). Overview of decoupled hybrid system with 10mm diameter pile, 80mm embedment depth (L80), with 40mm diameter bearing plate (F40), (b) 60mm diameter bearing plate (F60) and (c) 80mm diameter bearing plate (F80) and applied vertical stress as percentage of ultimate bearing stress.

Comparison between coupled and decoupled systems is best achieved by plotting the lateral load versus displacement response for the coupled and decoupled systems together for each applied vertical load (initial bearing stress). These plots are shown in Figures 5.7, 5.8 and 5.9 for the 40, 60 and 80mm diameter footings respectively. From these figures some interesting observations are made. For example at low initial bearing stress the response of the coupled and decoupled arrangements are very similar (refer to Figures 5.7a, 5.8a and 5.9a), in fact for the 40 and 60mm bearing plates the lateral response is almost the same with only a slightly increased ultimate lateral capacity shown for the coupled 80mm footing system (over the decoupled system), refer to Figure 5.9a.

For all the 5 and 10% loadings the ultimate lateral capacity of the coupled arrangement is significantly greater than that observed for the corresponding decoupled arrangement, refer to Figures 5.7b, 5.7c, 5.8b, 5.8c, 5.9b and 5.9c. However for the 25% pre-stress loading the lateral response of the coupled and decoupled systems tend to converge, refer to Figures 5.7d, 5.8dc and 5.9d. In particular the response for the 25% loading for the 40mm plate is very similar for the coupled and decoupled arrangement (refer to Figure 5.7d). It is also noted that at the high loads required to achieve a pre-stress of 25% there would invariably be a p-delta effect due to the stack of weights placed on the foundation system, the result of this is not readily quantified by may have an impact on the quality of the load-displacement plots.

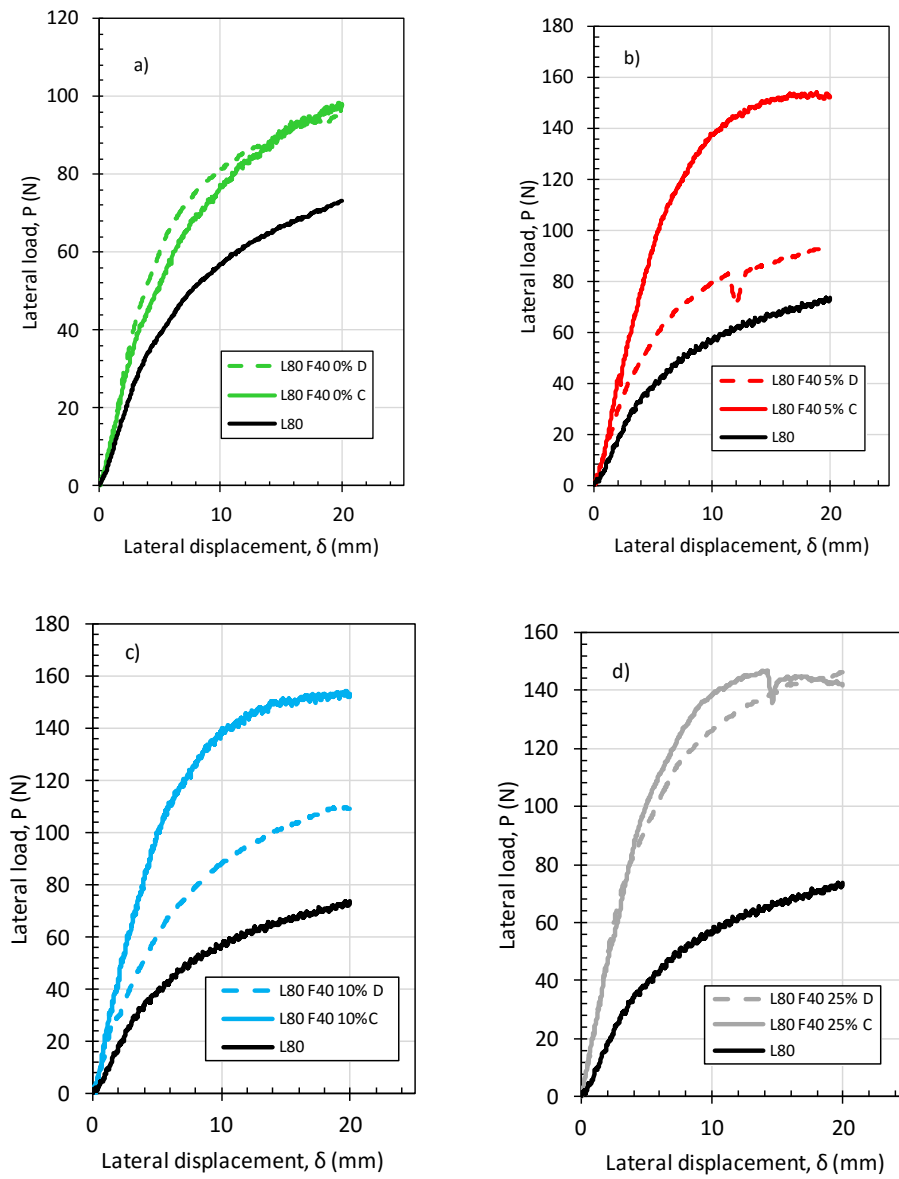


Figure 5.7. Comparison of coupled and decoupled lateral response for 10mm diameter pile with 80mm embedment depth and 40mm diameter bearing plate for initial bearing stresses of a) 0%; b) 5%; c) 10% and d) 25% or estimated ultimate bearing capacity.

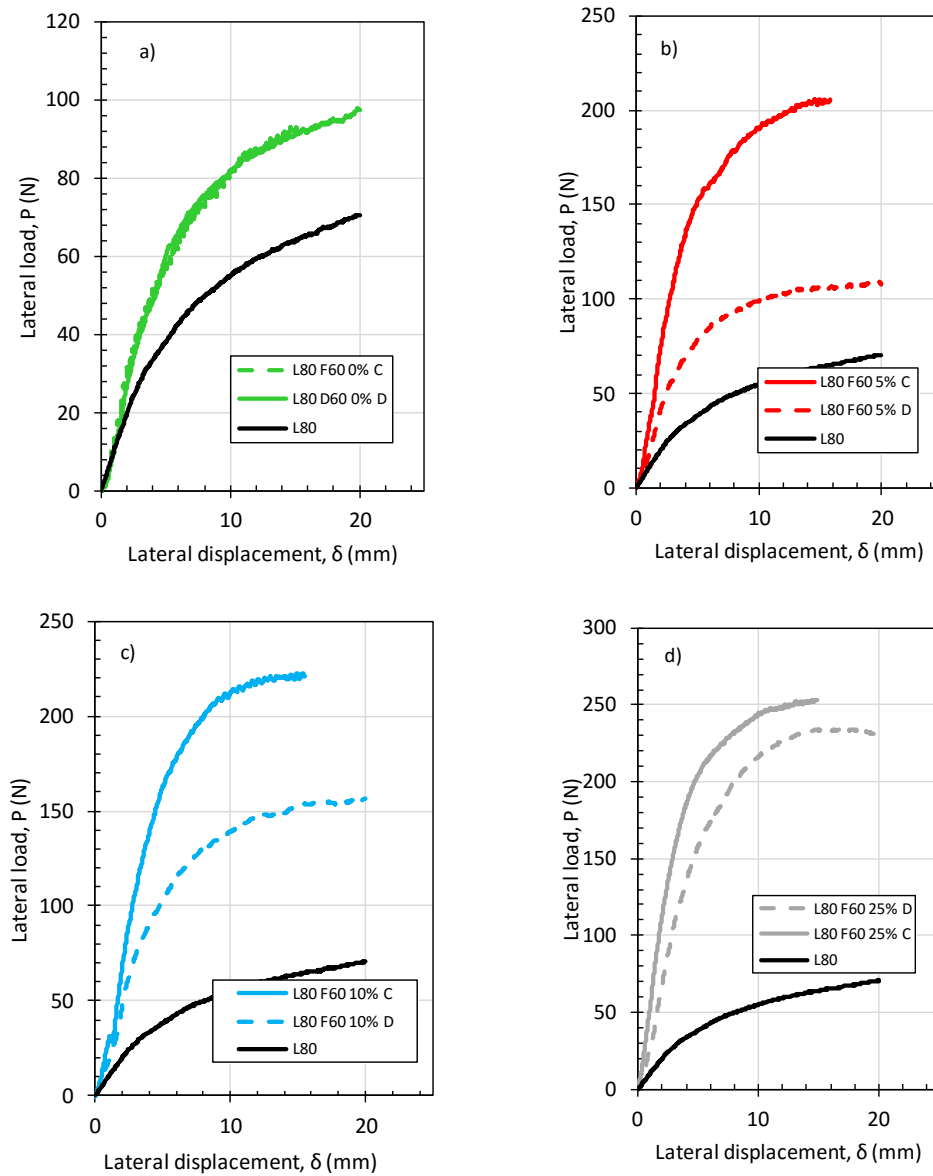


Figure 5.8. Comparison of coupled and decoupled lateral response for 10mm diameter pile with 60mm embedment depth and 80mm diameter bearing plate for initial bearing stresses of a) 0%; b) 5%; c) 10% and d) 25% or estimated ultimate bearing capacity.

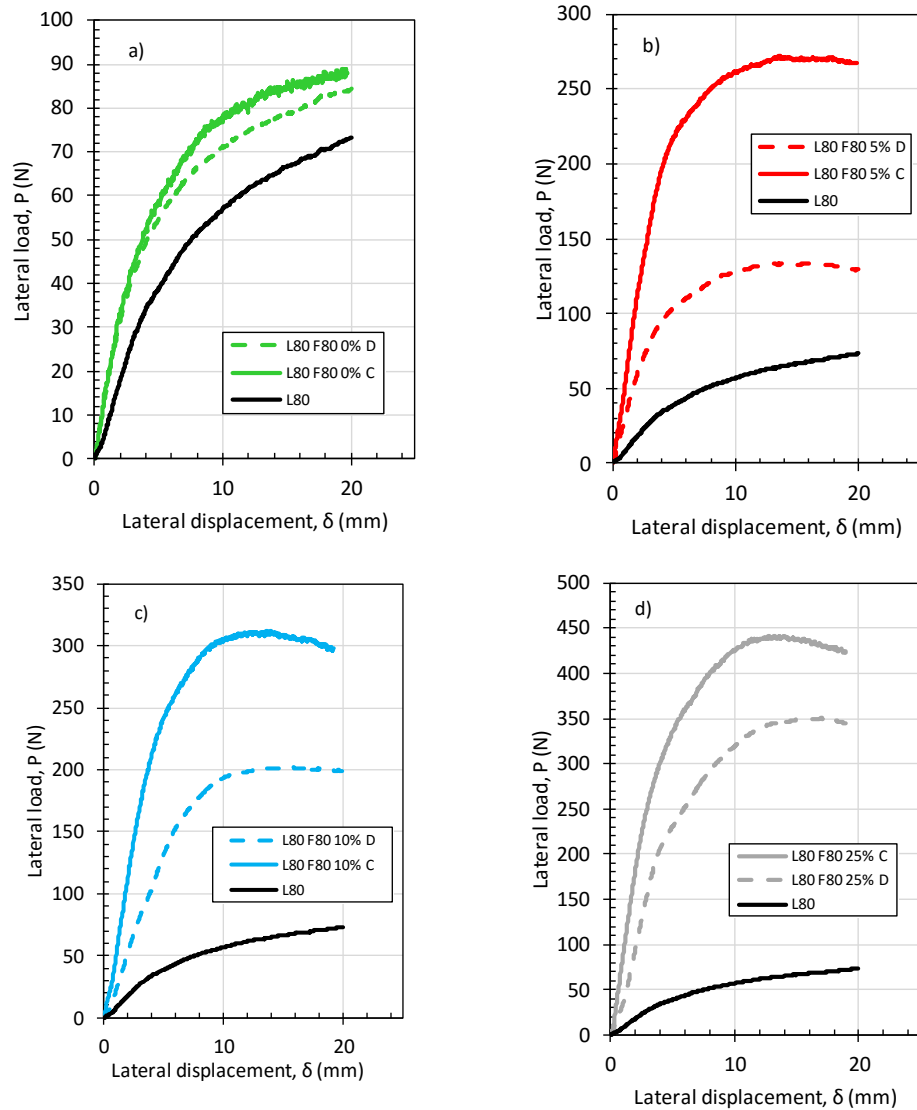


Figure 5.9. Comparison of coupled and decoupled lateral response for 10mm diameter pile with 80mm embedment depth and 80mm diameter bearing plate for initial bearing stresses of a) 0%; b) 5%; c) 10% and d) 25% or estimated ultimate bearing capacity.

5.4 Discussion of centrifuge model tests

The centrifuge model tests provide a more complete picture of the response of the hybrid monopiled-footing foundation system than that obtained from the single gravity tests. From the tests reported here the following key observations can be made.

- As for the single gravity tests the presence of a bearing plate is seen to provide a significant enhancement to the lateral capacity of the monopile.

- The effect of the initial bearing stress applied to the soil by the plate has a significant effect on the ultimate lateral resistance of the hybrid system.
- For the decoupled arrangement there appears to be a linear relationship between the applied initial bearing stress and the ultimate lateral resistance of the hybrid system.
- For the coupled hybrid system the effect of the initial bearing stress is more complex.
- At low pre-stress levels the ultimate lateral response of the coupled and decoupled hybrid systems are generally similar.

6. NUMERICAL MODELLING

6.1 Introduction

The hybrid foundation system is relatively well suited to numerical analysis since it involves a complex soil-structure interaction. This is particularly true for the coupled hybrid system which is essentially analogous to a piled-raft foundation, albeit with a single pile. The decoupled system is perhaps more readily analysed through a simple addition of the contributions of the constituent elements but is also suitable for numerical analysis. However it is noted that in order to carry out a realistic numerical analysis the programme must have as a minimum the following capabilities together with an appropriate model for the soil response.

- 3-D geometry modelling
- The ability to model separation (or zero tension) between the footing and the soil
- Interface properties between structural and soil elements
- Full decoupling between the structural elements (pile and footing) and the ability for slippage between the plate and pile

Full 3D finite element analysis that is reported in this chapter was carried out using the Imperial College Finite Element Program (ICFEP), (Potts and Zdravkovic, 1999) and was undertaken at the Geotechnics Section of Imperial College London, UK over a course of about a year. The development of ICFEP started in the 1970s by Prof. David Potts and has continued to evolve through to the present day. The program has been specifically written for analysing geotechnical problems where geometries of plane stress, plane strain, axi-symmetric and full 3-D may be analysed with linear and non-linear material constitutive models. The program also has large strain formulation allowing geometric nonlinearity to be catered for. The program utilised a sophisticated nonlinear solver to deal with rapid changes in stiffness and to solve non-symmetric stiffness matrices. Reliable failure conditions are predicted due to the ability of the program to maintain a high degree of accuracy during the solution stage of the analysis, (Potts & Zdravkovic, 1999; Ganendra (1995)). The post processor provides facilities for plotting various stress, strain and displacement parameters in tabular, graphical and contoured format.

6.2 Aims and objectives

The main aim of the 3D numerical modelling is to replicate the results of the centrifuge tests to develop numerical model which captures the response of the hybrid monopiled-plate foundation systems. Furthermore since the physical model in the centrifuge did not use strain gauges, the 3D finite element modelling will be able produce information on the soil-structure interaction through information on bending moments, shear forces, soil reactions induced in the foundation systems

6.3 The ICFEP model

The 3D finite element analyses involved scaling up the centrifuge tests and modelling the equivalent prototype. The aim was to replicate the centrifuge tests in prototype dimensions and compare the load versus deflection response of the 3D FE results with the centrifuge tests (scaled to prototype). The foundation system was modelled as a prototype installed in the middle of a 30m diameter and 30m long soil model. The construction sequence followed exactly the same steps as the centrifuge tests. Lateral loading was applied incrementally in order to produce the load versus deflection response.

The constitutive model used for modelling all soil units was the nonlinear elasto-plastic Mohr-Coulomb model (Potts & Zdravkovic, 1999). The small strain stiffness model of Jardine et al. (1986) was utilised for taking into account nonlinearity below yield. This model takes into account the variation of normalised shear and bulk stiffnesses, with deviatoric and volumetric strains, refer to Figures 6.1a and 6.1b below. The input parameters including the small strain stiffness model parameters those presented by Zdravkovic et al. (2005) for Thanet sand which was deemed to be similar in characteristics to the uniformly graded Fraction C sand used in the centrifuge tests.

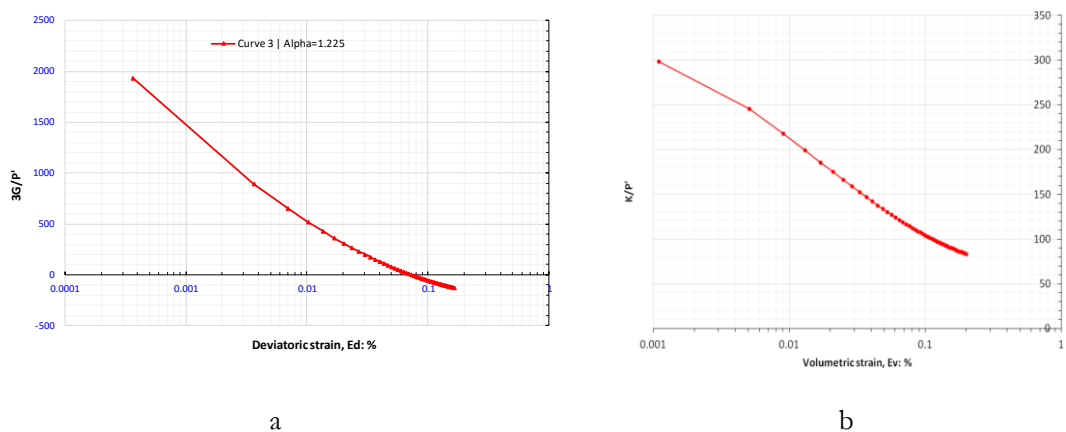


Figure 6.1a) normalised shear stiffness vs deviatoric strain and b) bulk stiffness vs volumetric strain.

A critical state friction value of 32 degrees was adopted for the soil model with a maximum dilation value of 20 degrees yielding a peak value of 52 degrees. The relatively high value of dilation is associated with the relatively low stress level and unconfined surface boundary in of the centrifuge model. Similar high dilation values have been reported by Stone (1988) and Stone and Wood (1992) and are considered a scale effect due to the relatively large particle size in relation to the model scale.

6.3.1 Constitutive Model Calibration

The result of the direct shear tests carried out on the sand used for the physical model tests showed that during normal laboratory conditions the critical state angle of friction for the sand used for the experiments is 27.5° with the soil dilating at 7° taking the peak angle of friction to 34.5°.

Investigations carried out by Bolton (1986) and Houlsby (1991) have provided in depth insight into how dilatancy effects the soil behaviour, and have related stress state and relative density of sand to it dilation. Increasing the stress levels leads to the suppression of the dilation of dense sand when it is sheared, as reported by Stone (1988) when investigating the modelling of rupture developments in soils. The relative density of above 63% has been reported to push dilation to its peak and for the sand used (David Ball Ltd, Fraction D) the recommended maximum dilation angle is 25°, as reported by White et al (2000). For the purpose of analysis the angle of dilation (recommended) is around 20°.

One of the downsides of using a centrifuge is that the g levels vary along the strongbox. This means that the stress stage of the soil along the pile length varies, however this variation was estimated to be rather small (see Taylor, 2003). Moreover, pervious research has shown that the dilation angle of sand has a partial dependency on the stress stage of the soil (Bolton 1986, Houlsby 1991, Stone 1988). This implies that the dilation angle may vary (although this variation is thought to be small). So a calibration process was undertaken whereby the single pile model was run with 3 different dilation angles to see how this variation effect the results.

6.4 ICFEP Results

The following sections present the results from the ICFEP analysis. Only selected plots are presented which illustrate the main findings of the numerical modelling and demonstrate the

response of the hybrid foundation systems. As stated earlier the results are presented at prototype scale, and where applicable the centrifuge model test data is also presented at prototype scale using the scaling relationships presented earlier in Chapter 3.

6.4.1 Displacements

Displacement profiles of the pile for the case of (i) pile only, (ii) pile with coupled bearing plate and (iii) pile and decoupled bearing plate are presented below in Figure 4.2.

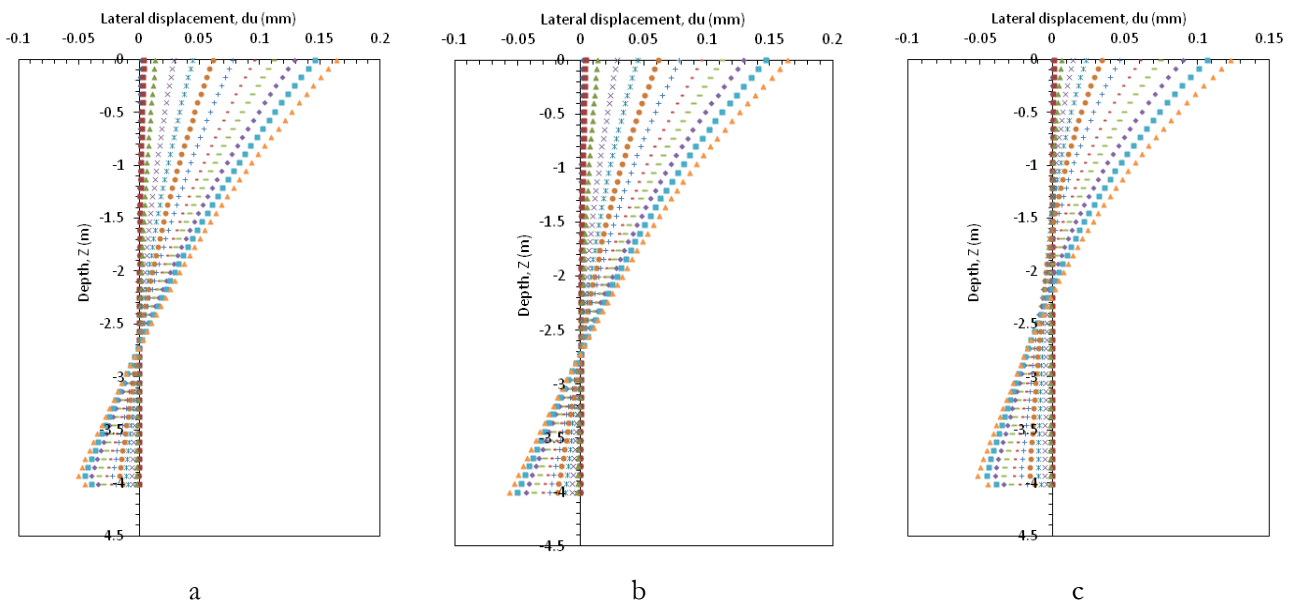


Figure 6.2. Lateral displacement profiles for (a) pile only, (b) pile and coupled bearing plate and (c) pile and decoupled bearing plate.

From Figure 6.2 it is apparent that the pile displacement profiles are very similar for the pile only and the decoupled hybrid system. The presence of the bearing plate does not appear to influence the point of rotation of the pile which appears to be at a depth of approximately 2.75m below ground level which is about 70% of the embedment depth. However for the coupled arrangement the point of rotation is seen to be at a depth of about 1.7m below ground level or at about 40-45% of the embedment depth. Figure 6.3 shows total displacement contours for the coupled and decoupled hybrid foundations. Both plots show that the soil deformation is offset in the direction of loading. For the coupled hybrid there is a definite slope to the bearing plate as evidenced by the graded contours, however this slope is not so evident for the decoupled arrangement where a more uniform settlement of the plate appears to be present.

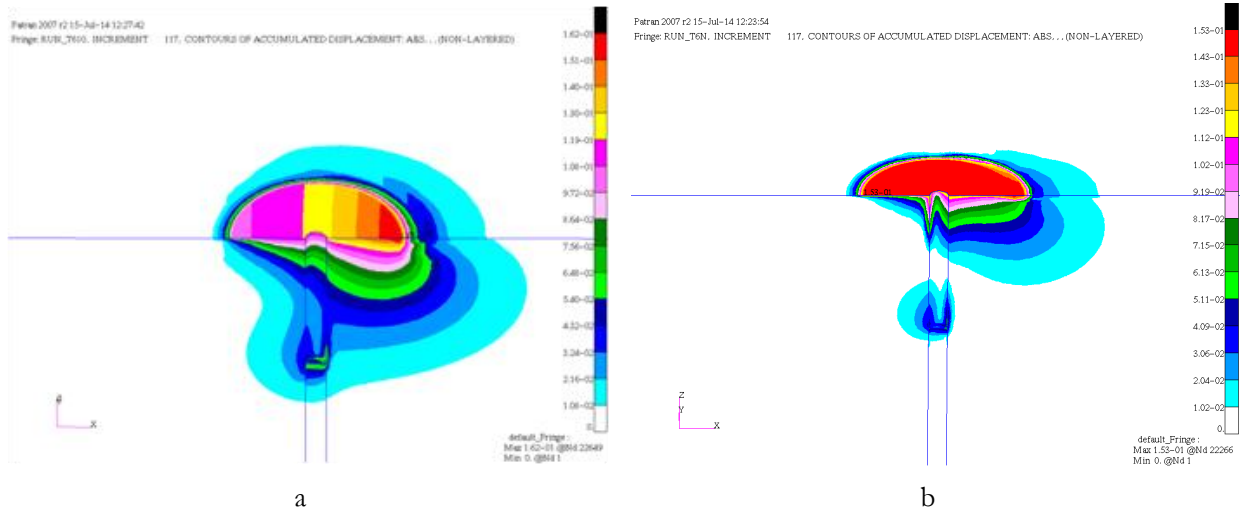


Figure 6.3. Contours of absolute total displacement for (a) coupled and (b) decoupled hybrid systems

The interaction of the plate with the underlying soil is evaluated more closely by considering the settlement profile of the plate throughout the loading process. Figures 6.4 below shows the plate rotation plotted either side of the pile for the coupled hybrid system.

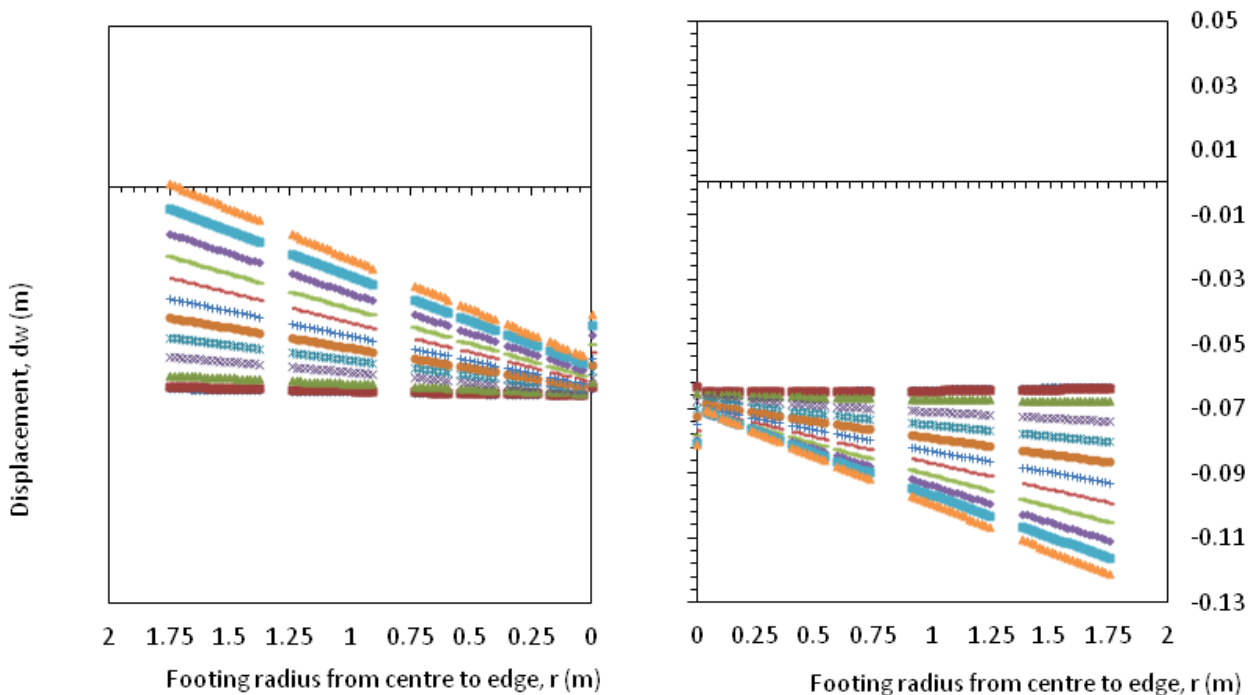


Figure 6.4. Bearing plate rotation during loading for coupled hybrid

It is evident from this plot that for the coupled system the dominant movement of the bearing plate is one of rigid body rotation with the rotation centered on the pile axis. The rotation is symmetric with the leading edge penetrating some 70mm into the soil and a

corresponding uplift to the trailing edge. Figure 6.5 shows the distribution of normal stress at the plate soil interface.

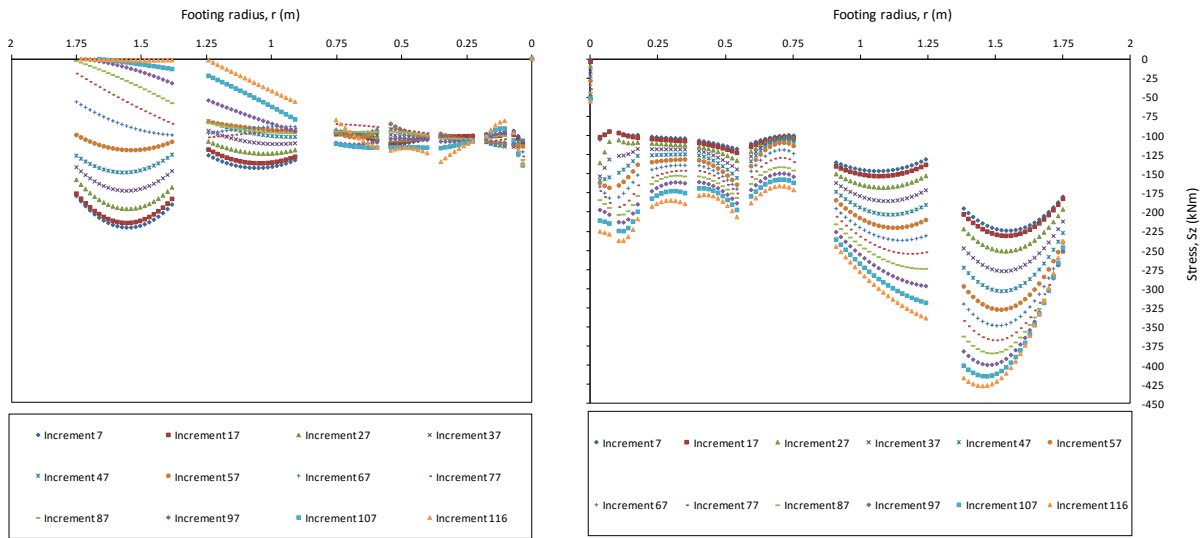


Figure 6.5 shows the distribution of normal stress at the plate soil interface for coupled hybrid system

For the decoupled system the plate rotation and the bearing stress are shown in Figures 6.6 and 6.7 respectively.

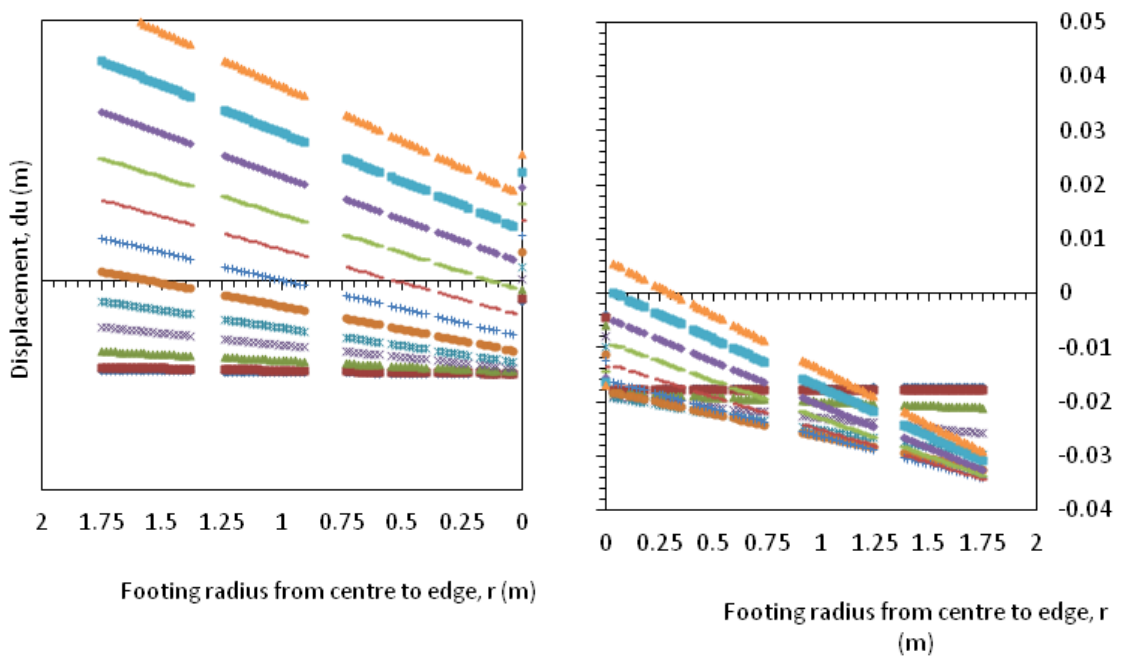


Figure 6.6. Bearing plate rotation during loading for decoupled hybrid

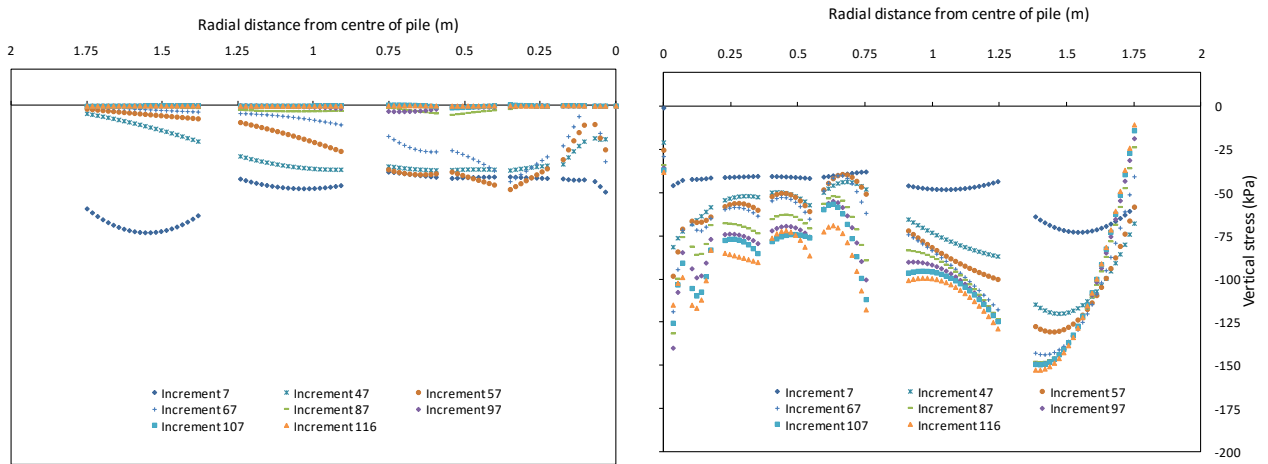


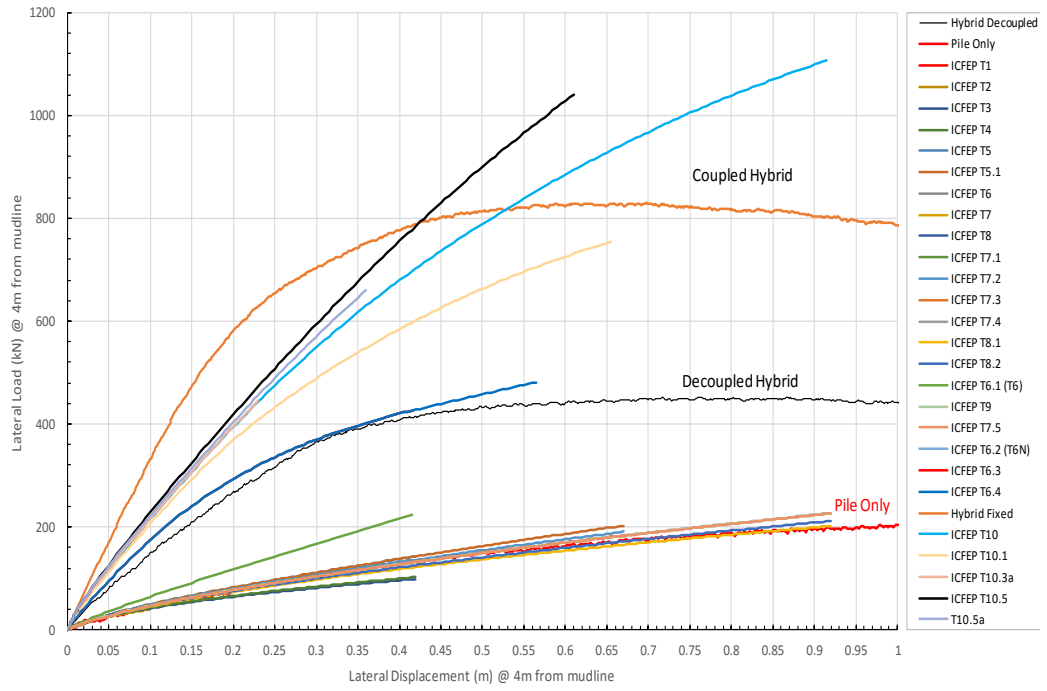
Figure 6.7 shows the distribution of normal stress at the plate soil interface for decoupled hybrid system

Comparison of Figures 6.4 and 6.5 and 6.6 and 6.7 clearly illustrate that the behaviour of the coupled and decoupled arrangements are fundamentally different through the way the plate interacts with the underlying soil. For the coupled system the rigid body plate rotation develops bearing stresses up to twice those observed for the decoupled system. But this is to be expected because the decoupled plate will tend to slide up the pile as evidenced by the plate movements shown in Figure 6.6. This observation is in agreement with experimental observations where the plate was noted to have slid up the pile during the test, refer to chapter 5.

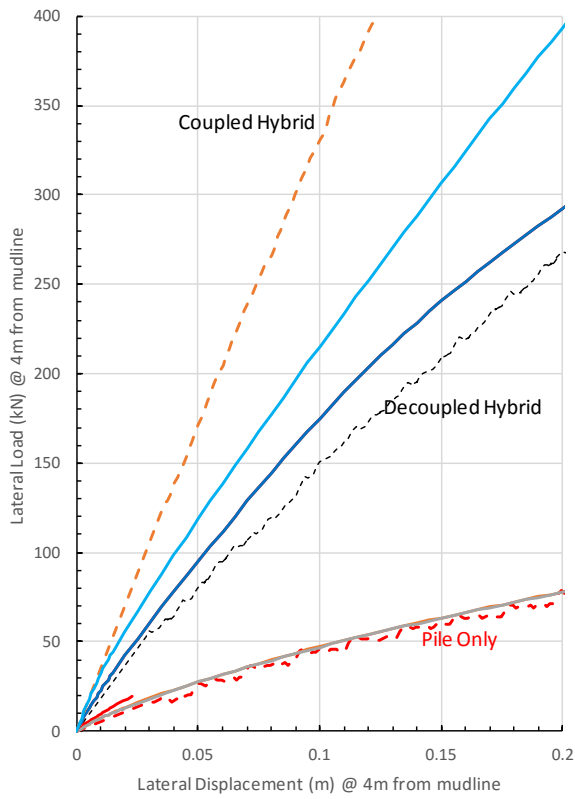
6.5 Lateral capacity

Ultimately it is of interest to develop full load-displacement curves for the hybrid systems to demonstrate an applicable method for design and further analysis. A summary of the load-displacement plots for all the ICFEP runs is shown in Figure 6.7a with a detail of the initial portion of the plot in 6.7b.

From Figure 6.7 it is apparent that, for both pile only and hybrid cases, the numerical results show a very good match between the centrifuge and 3D-FE model tests. The match is not so satisfactory for the coupled system where the experimental results are seen to present a stiffer response and an overestimate of the ultimate capacity.



a



b

Figure 6.7a Summary of ICFEP load displacement runs and b) detail at initial loading

7. DISCUSSION AND CONCLUSIONS

This section is address through a presentation of publications presenting the work undertaken to national and international audiences. Some of the publication were originally in poster format and are reproduced here at reduced scale.

(2011) BGA Annual Research Conference (poster)

(2011) European Conference on Soil Mechanics and Geotechnical Engineering

(2012) 3rd International Annual EPPM Conference

(2012) BGA Annual Research Conference (poster)

(2012) International Symposium on Offshore Site Investigation and Geotechnics

(2013) International Conference on Soil Mechanics and Geotechnical Engineering

(2015) European Conference on Soil Mechanics and Geotechnical Engineering

(2015) International Symposium on Foundation in Offshore Geotechnics

Numerical Modelling on the Degree of Rigidity at Pile Head for Offshore Hybrid Monopile-Footing Foundation Systems

Mr. Harry Arshi, Dr. Kevin Stone, Dr. Tim Newson & Dr. Friederike Gunzel

Hybrid Monopile-Footing Foundation System

The existing oil and gas industry can provide well developed technologies for the design and construction of offshore wind turbine foundations. The surface or near surface foundation solutions (Gravity base, suction caisson systems including tripods), deep foundation solutions (Large diameter piles) or through a combination of foundation elements constituting 'hybrid' systems.

For example a piled footing/bucket or piled/GBS combination

Such an arrangement consisting of a combination of foundation elements may have advantages where complex loading and/or soil conditions occur.

Here the performance of a model hybrid foundation system, which combines a monopile and circular footing or foundation plate is investigated.

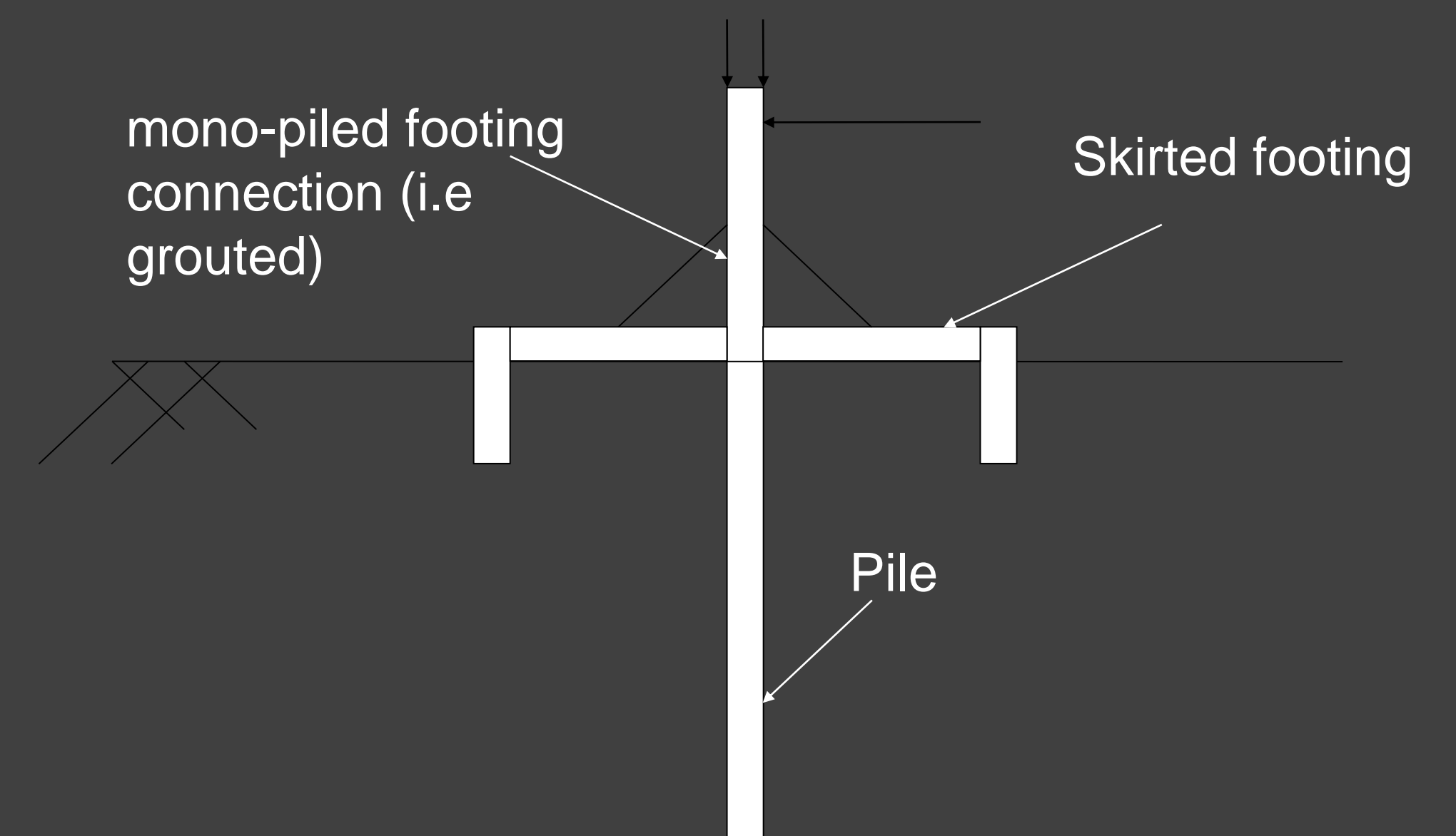


Figure 1. Structural arrangement of the hybrid monopile-footing foundation system

- The performance of such foundation systems has been under investigation and is an ongoing research project.
- So far comprehensive single gravity (1g) physical model tests have demonstrated that the lateral stability of a single monopile is significantly improved by adding a bearing plate to the monopile at the mudline.
- The single gravity tests were conducted in a loading rig (Figure 2). The model tests presented here were performed in a sand box where the vertical loads were applied via dead weights and the lateral loads via a pulley and displacement controlled loading arrangement.

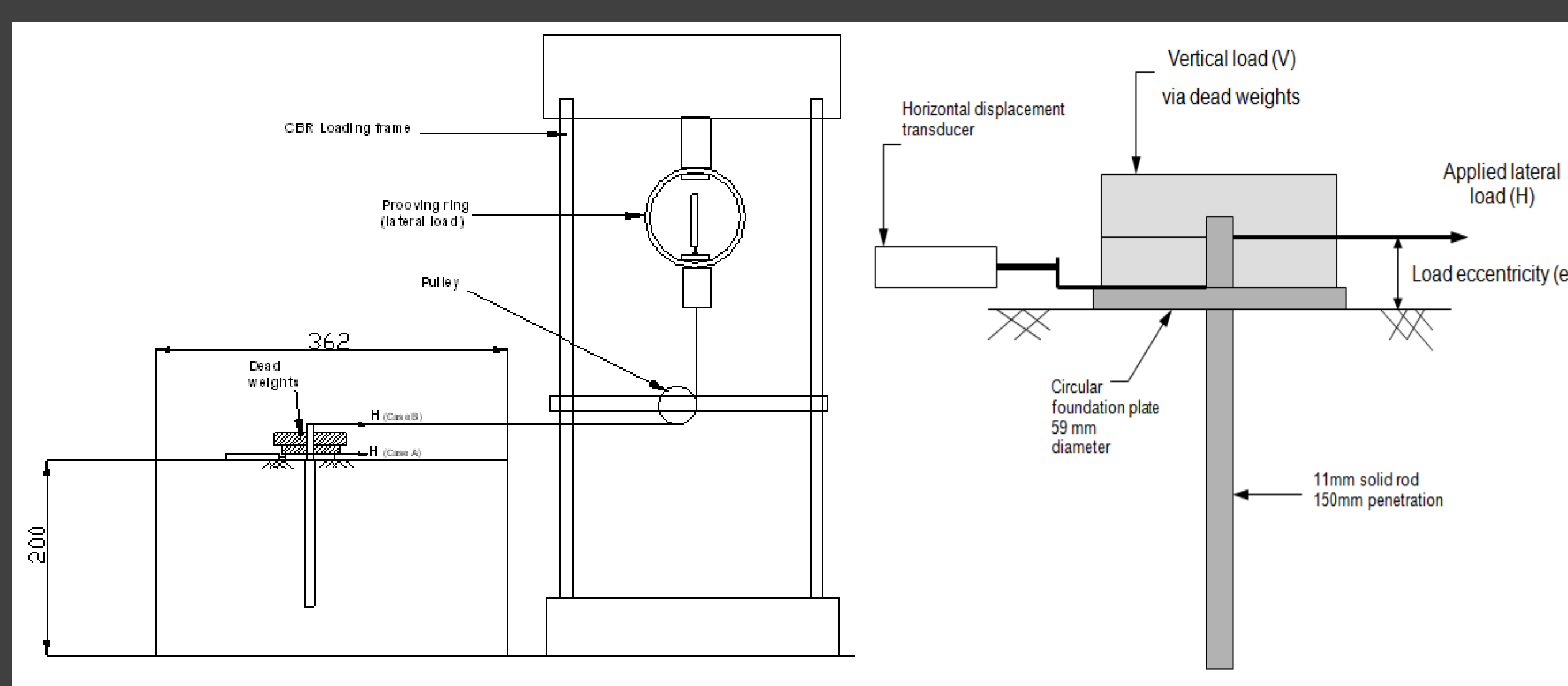


Figure 2. Single gravity (1g) test arrangement

- Assuming that the response of the hybrid system is similar to that of a fixed head pile (i.e. with moment restraint). Based on Brom's method, for an L/D (150/11) ratio of 13.6 a fixed head pile would have a lateral capacity of at least twice that obtained for the free headed case. The foundation plate provides partial moment or rotational restraint at the pile. Degree of restraint will depend on the size of plate and stiffness of the soil beneath the plate (subgrade reaction).
- Assuming that as the footing rotates, contact with the soil is lost and a reduced contact area develops (shaded region), the reduced area of the foundation plate is used to compute the total reaction force from the soil, the soil pressure is assumed uniform under the contacting plate and equal to the ultimate bearing capacity and the resultant force acts through the centroid of the reduced footing.

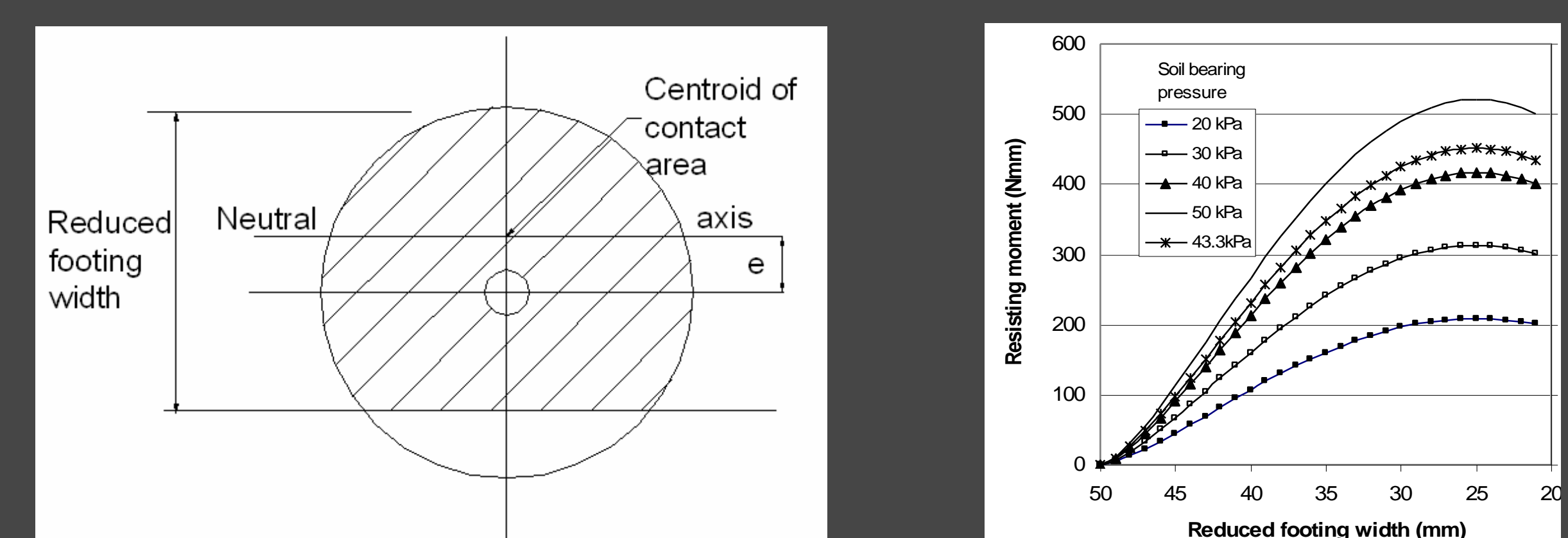


Figure 5. Demonstration of the development of resistance under the footing for sand with different bearing capacities

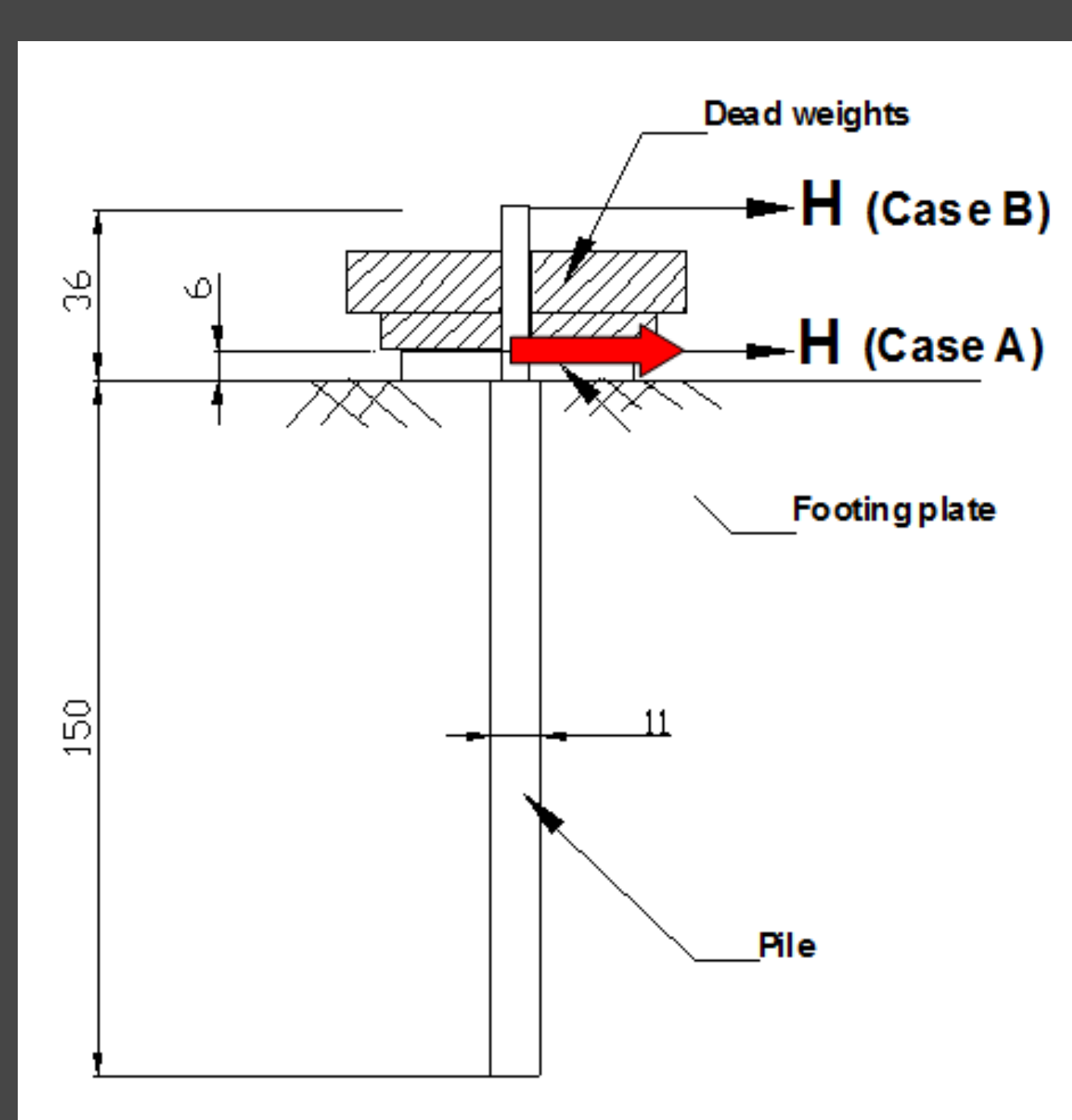


Figure 3. An example of a test setup

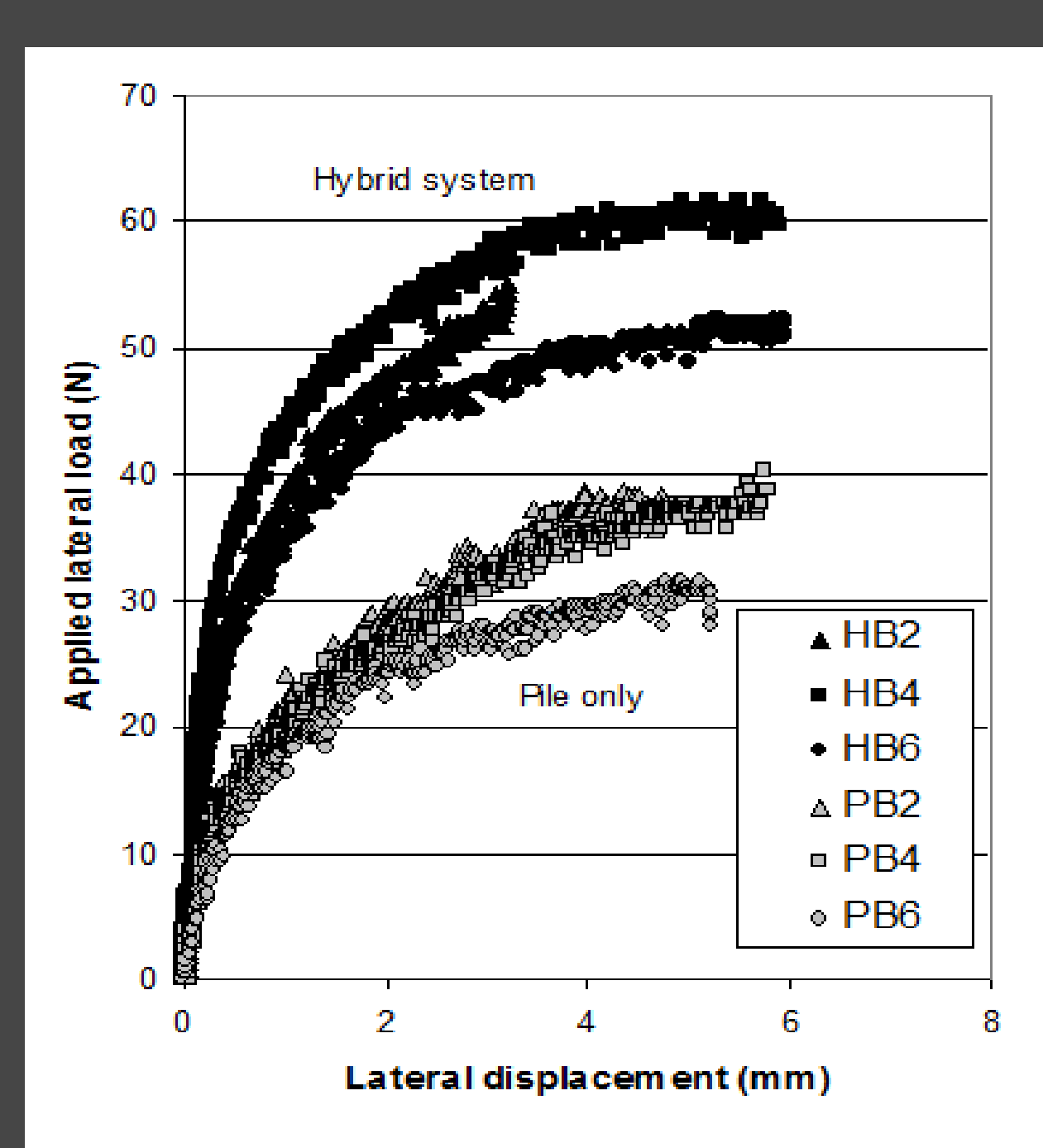


Figure 4. An example of the results of tests with monopiled footings and single piles

- The experimental data indicates that the lateral capacity of the free headed pile is increased by the presence of the foundation plate by up to 60-65%.
- For the specified pile geometry a qualitative analysis using the simplified method of Brom's can be performed to illustrate the role of the foundation plate on the lateral response of the hybrid system.
- For the hybrid system the ultimate lateral capacity measured for all the tests (Case A and B, refer to Figure 3) are tightly grouped between 60-65N with the exception of test HB6 (Case B, 6.2 kg vertical load) where P-δ effects are thought to be more apparent.
- This observation suggests that the response of the hybrid system is similar to that of a fixed head pile (i.e. with moment restraint).

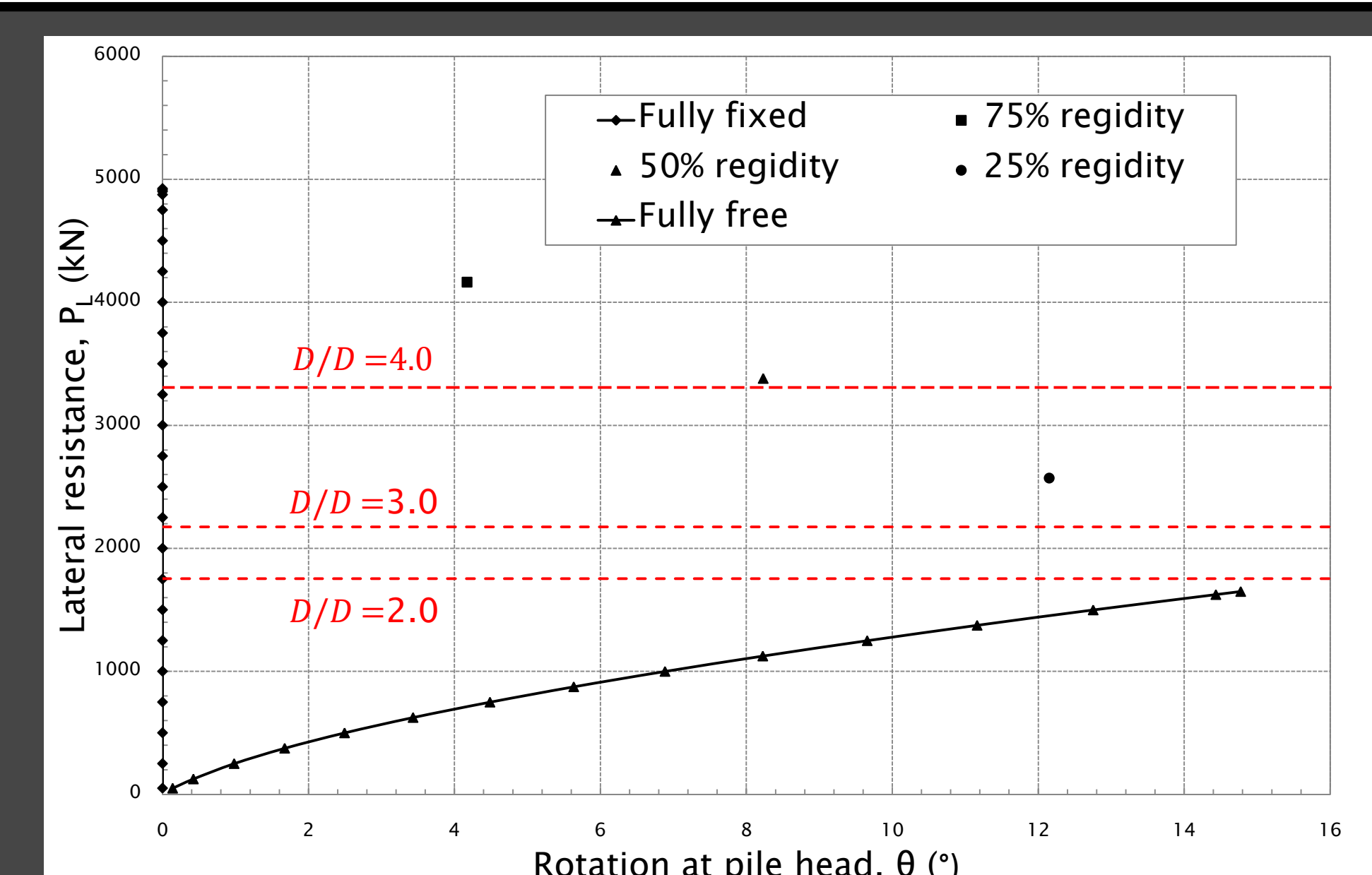


Figure 6. Lateral resistance vs. pile head rotation graph obtained numerically

- The foundation systems was modelled in LPILE for both fully free and fully fixed case.
- Since its not possible to add partial restraint at the pile head (footings) in LPILE, the effect was through bending moments acting at the pile head which develop as the bearing plate reacts against the soil.
- A series of tests were carried out for different footing sizes, and the results are illustrated in Figure 6 above.
- It is apparent that a relationship exists between the diameter of the footing and the ultimate moment of resistance of the hybrid system.
- Further numerical and physical modelling will allow the development of pile head restraint by the bearing plate or footing to be related to the development of the lateral load-displacement response of the hybrid system.

Contact Details

Mr. Harry Arshi	H.Arshi@brighton.ac.uk
Dr. Kevin Stone	Kevin.Stone@brighton.ac.uk
Dr. Tim Newson	TNewson@eng.uwo.ca
Dr. Friederike Gunzel	F.K.Gunzel@brighton.ac.uk

An investigation of a rock socketed pile with an integral bearing plate founded over weak rock

Étude d'une pile avec une plaque encastrée dans une roche molle

S. Arshi¹ & K.J.L. Stone

University of Brighton, Brighton, United Kingdom

ABSTRACT

Current offshore technology is being transferred successfully to the renewable energy sector but there is clearly scope to develop foundation systems which are more efficient, economic and satisfactory for the particular case of a wind turbine. One such approach is that foundation systems are developed which combine several foundation elements to create a 'hybrid' system. In this way it may be possible to develop a foundation system which is more efficient for the combination of vertical and lateral loads associated with wind turbines. In many of the proposed offshore European wind farms sites, it is often the case that the surficial seabed deposits are underlain by a weak rock. This paper presents the results of a series of small scale single gravity tests to investigate the performance of a monopile and combined monopiled and bearing plate foundation where the pile is socketed into a weak rock. In the model studies the weak rock layer is modelled by a weak sand and gypsum mix. The results of the study provide an insight into the effect of the various foundation elements (i.e. pile, plate and rock socket) and their contribution to the overall performance of the foundation system.

RÉSUMÉ

La technologie actuelle utilisée en offshore est réutilisée avec succès dans le secteur de l'énergie renouvelable, cependant il est possible de développer des systèmes de fondations plus efficaces, économiques et satisfaisants dans le cas des éoliennes. Une approche du problème consiste à développer un système de fondation qui combine plusieurs éléments de fondation pour créer un système hybride. De cette façon, il peut être possible de développer un système de fondation qui soit plus efficace pour des éoliennes qui subissent une charge latérale et verticale. La plupart des parcs éoliens Européens proposés se trouvent dans le cas où les dépôts des fonds marins reposent sur une roche molle. Cet article présente les résultats d'une série de tests à petite échelle et de même gravité. Ce document a pour but d'étudier la performance d'une pile et le cas d'une pile combinée avec une plaque, où la pile est encastrée dans une roche tendre. Dans cette étude, la roche molle est réalisée par le mélange de gypse et de sable faible. Les résultats donnent un aperçu de l'effet des différents éléments de fondation et leur contribution à la performance globale du système de fondation.

Keywords: Offshore turbine, weak rock, monopile, rock socket, laterally loads.

¹ Corresponding author

1 INTRODUCTION

The design of offshore foundation systems is constantly evolving. The target for this change is meeting the needs of on-going developments in the oil and energy sector. In the hydrocarbon extraction sector, exploration and development is moving in to ever deeper water resulting in ever more challenging geotechnical conditions. Similarly, the development of sites for offshore wind-farms is also extending into deeper water as the supply of shallow near shore sites is exhausted. Similarly the capacity of wind turbine generators is also increasing requiring significant development in foundation approaches to generate economic and practical solutions to the installation of these deep water wind farms.

The loadings associated with wind turbines consist of relatively low vertical loadings but high lateral loads resulting in very large overturning moments. The preferred foundation system to date has been the monopile which has been successfully employed for the majority of the offshore wind farms installed to date. The popularity of this type of foundation is due to its employability in a variety of different soil conditions.

In many of the proposed offshore wind farm locations, it is often the case that the surficial seabed deposits are underlain by rock, generally weak rocks such as mudstones and chalk. Consequently it becomes necessary to install the monopiles, generally by driving, to significant depth into the rock to achieve adequate lateral stiffness and moment resistance to carry the applied loads.

This paper presents the results of a series of small scale single gravity tests to investigate the performance of a rock socketed pile installed in a weak rock and fitted with an integral bearing plate, schematically shown in Figure 1. The objective is to investigate the effect of the bearing plate on the lateral response of the monopile. It is hoped that the results of the study will provide some insights into the effect of the various foundation elements (i.e. pile, plate and rock socket) and their contribution to the overall performance of the foundation system.

In the monopile plate foundation a circular plate is rigidly attached to the monopile at the mudline. The 2-D analogy of this system is that of a retaining wall with a stabilising base [1]. Where the plate diameter is relatively small then the system is similar to a single capped pile, for which methods have been developed for analysing the influence of the pile and pile cap under axial loading [2], and the effect of the pile cap on the lateral performance of single piles has also been investigated by others [3], [4], [5], [6].

The effect of the pile cap or bearing plate is to provide a degree of rotational restraint at the pile head, leading to an improvement in the lateral resistance of the pile. It has also been shown that the use of a relatively thick pile cap leads to an increase in the lateral resistance through the development of passive soil wedges [7], in a similar way to the behaviour of skirted foundations [8].

The lateral response of piles is well reported in the literature, and various methods of analysis have been proposed by numerous researchers, [9],[10],[11],[12],[13],[14],[15]. The bearing capacity problem has also been investigated under different loading conditions relevant to offshore foundations, see for example refs [16],[17].

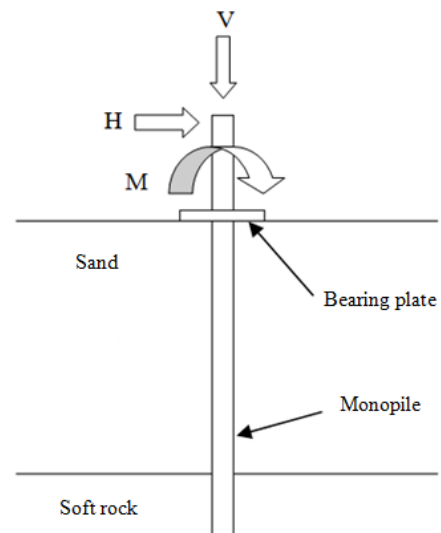


Figure 1. Schematic arrangement of monopile-footing with rock socketed pile.

Pervious investigations carried out at one gravity in ‘sand box’ tests [18], [19], [20] has shown that the lateral stiffness and ultimate capacity of the monopile is enhanced by the addition of the bearing plate. Centrifuge model tests have also indicated that for cohesionless soils the ultimate lateral capacity of a monopile is enhanced by the presence of a bearing plate [20]. However, centrifuge tests performed on clay samples did not indicate much improvement in the lateral performance of the monopile due to the presence of the bearing plate [21]. It should be noted that these centrifuge tests are not directly comparable since the relative geometries of the pile and bearing plates were significantly different in both studies.

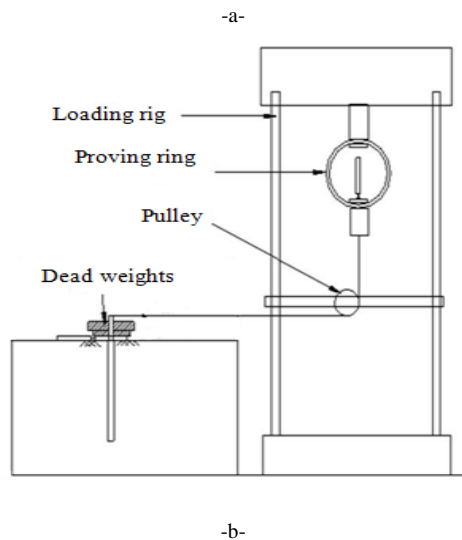
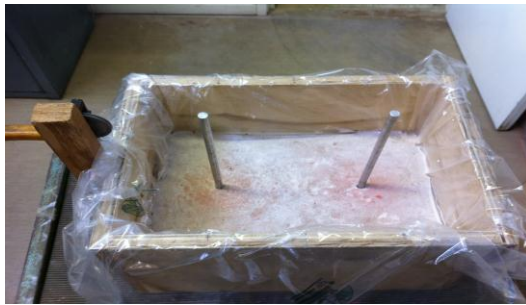


Figure 2. a) Photograph of model container showing socketed piles cast into rock prior to pluviation of overlying sand layer and b) schematic diagram of testing rig.

In the study reported here the influence of the bearing plate on the monopile response is investigated for the case of a rock socketed monopile with an overlying layer of cohesionless soil. This ground model is felt to be of particular relevance for offshore wind farm development since the potential economical benefits of reducing the pile penetration into the underlying rock layer are significant.

2 EXPERIMENTAL PREOCEDURE

2.1 Materials and model preparation

All the model tests were conducted in a ‘sand box’ of internal dimensions 363 mm x 244 mm x 203 mm deep. The stratigraphical profile consisted of a layer of cohesionless material overlying a layer of weak rock. The cohesionless material consisted of a fine grained ($d_{50}=0.25\text{mm}$) rounded to sub-rounded uniformly graded quartz sand. The maximum and minimum void ratios were 1.1 and 0.68 respectively, corresponding to dry unit weights of 12.9 and 17.0 kN/m^3 . A critical state angle of friction of 32 degrees was determined from direct shear tests.

The weak rock layer was modelled using a sand and gypsum mix. The mix proportions of 70% sand and 30% gypsum by dry weight was used. The wet mixture was poured into the model container and the piles installed to their embedment depth in the still wet mix. Once the gypsum mix had set the sand layer was placed by dry pluviation to the desired height. The bearing plate was then threaded along the pile and was clamped to the pile once it was firmly resting on the sand surface.

The model pile was fabricated from a 10 mm diameter solid aluminium rod, the bearing plate consisted of a 40 mm diameter 5 mm thick aluminium plate. The pile was threaded through the bearing plate which in turn was clamped to the pile. Thus the location of the bearing plate on the pile shaft could be adjusted.

2.2 Test setup and procedure

The completed model was placed in a loading frame and lateral loading to the pile was applied via a wire and pulley arrangement connected to a vertical actuator, refer to Figure 2b. Vertical loads were applied by dead weights (10N) placed on the bearing plate. For the pile only tests the bearing plate supporting the dead weights was raised clear of the soil surface. Two LVDT transducers were located to record the lateral displacement of the pile at two locations, one at the line of action of the lateral load, 52mm above the soil surface, and the other at a higher location.

The model test program comprised of a total of three pairs of tests. Each test pair consisted of a single monopile and a monopiled-footing foundation, and were performed in the same prepared soil model. In order to assess the influence of the rock socket, three socket depths were tested corresponding to 0%, 5%, and 20% of the total embedment length of the pile. Table 1 shows a summary of the model tests performed.

Table 1. Summary of model tests

Foundation type	Embedment depth (mm)
Monopile (P 0%)	0.0 mm (Sand only)
Monopile (P 5%)	7.5 mm (5% of pile length)
Monopile (P20%)	30 mm (20% of pile length)
Monopile-footing (H 0%)	0.0 mm (Sand only)
Monopile-footing (H 5%)	7.5 mm (5% of pile length)
Monopile-footing (H 20%)	30 mm (20% of pile length)

3 TEST RESULTS AND ANALYSIS

The results obtained from the tests are best presented through plots of the applied pile head moment against the pile head rotation. Figure 3 summarises the response of both the monopiles and the monopiled-footings for the different rock socket depths of 0%, 5% and 20% respectively.

From this figure it is apparent that the ultimate moment capacity of the monopile is enhanced by the presence of the bearing plate. For the unsocketed monopile (0%) and the 5% socketed pile ultimate capacity is approximately dou-

bled when the bearing plate is present; for the 20% socketed pile the ultimate capacity is only marginally increased. It is however apparent that for all cases the lateral stiffness of the monopile is enhanced by the presence of the bearing plate. This is particularly evident for the deep rock socketed pile (20%) where a significant improvement in the initial lateral stiffness is observed. It is also apparent that the form of the monopiled-footing response for the deep rock socket suggests that a passive failure of the soft rock occurs. This is inferred by the plastic type response of the foundation suggesting a yielding of the soft rock.

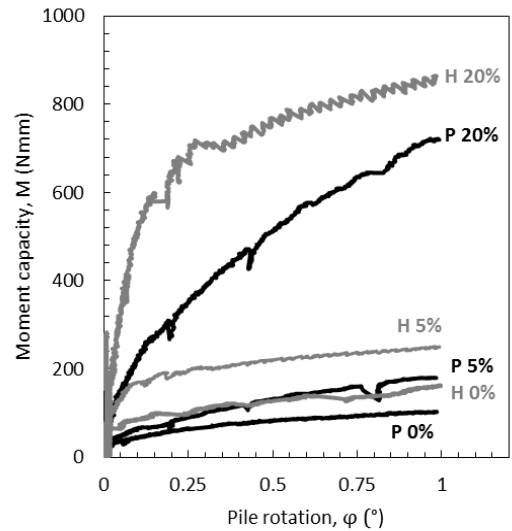


Figure 4. Moment capacity versus rotation at pile head for monopiles and monopile-footings with 0%, 5% and 20% embedment on soft rock

4 DISCUSSION AND CONCLUSIONS

From the limited study reported here it is apparent that the depth of the rock socket has an important influence on the behaviour of the foundation systems.

Figure 6 shows a schematic representation of the soil stresses developed by the rotating monopiled-footing foundation. It is apparent that the

response of the system is the result of a complex ground-structure interaction problem. For the basic one gravity tests conducted in this study the piles were extremely stiff and excavation after the tests indicated that rotation had occurred about the pile toe. Clearly the point of rotation of the piles would be influenced by the relative pile/soil stiffness and further study is required to investigate the performance of more flexible piles.

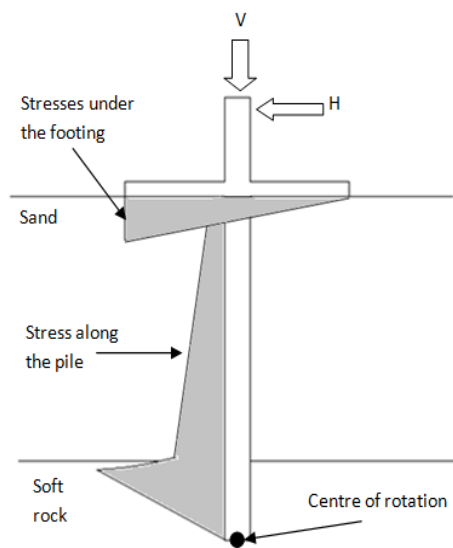


Figure 6. Schematic representation of soil stresses on a rock socketed monopile-footing foundation with rotation about the pile toe.

The study presented here is very much a feasibility study investigating the potential of enhancing the lateral performance of monopiles through the use of a bearing plate. The study has considered the case of a rock socketed monopile to supplement other studies carried out in uniform soils, both cohesionless and cohesive. The results are consistent with the previous studies undertaken in cohesionless soils, with similar pile and plate geometries, and confirm that the bearing plate appears to provide a method of enhancing the lateral capacity of monopile foundations. It is also apparent that the use of a bearing plate with a well socketed pile can considerably improve the initial lateral stiffness of the monopile.

Whilst the study reported here is limited, the results are encouraging, and it is hoped that future studies, including geotechnical centrifuge modelling, will provide a clearer picture of the complex response of rock socketed monopiled-footings.

REFERENCES

- [1] W. Powrie, and M.P. Daly, Centrifuge modeling of embedded retaining wall with stabilizing bases, *Geotechnique*, 57(6) (2007), 485-497.
- [2] H.G. Poulos, and M.F. Randolph, Pile group analysis: a study of two methods, *ASCE Journal of Geotechnical Engineering*, 109(3) (1983), 355-372.
- [3] J.B. Kim, L.P. Singh, and R.J. Brungraber, Pile cap soil interaction from full scale lateral load tests, *ASCE Journal of Geotechnical Engineering*, 105(5) (1979), 643-653.
- [4] R.L. Mokwa, and J.M. Duncan, Experimental evaluation of lateral-load resistance of pile caps, *ASCE Journal of Geotechnical and Geoenvironmental Engineering*, 127(2) (2001), 185 - 192.
- [5] R.L. Mokwa, and J.M. Duncan, Rotational restraint of pile caps during lateral loading, *ASCE Journal of Geotechnical and Geoenvironmental Engineering*, 129(9) (2003), 829 - 837.
- [6] D.K. Maharaj, Load-Deflection Response of Laterally Loaded Single Pile by Nonlinear Finite Element Analysis, *EJEG* (2003).
- [7] R.L. Mokwa, *Investigation of the Resistance of Pile Caps to Lateral Loading*, Ph.D Thesis, Virginia Polytechnic Institute, Blacksburg, Virginia, 1999.
- [8] M.F. Bransby, and M.F. Randolph, Combined loading of skirted foundations. *Geotechnique*, 48(5) (1998), 637-655.
- [9] H. Matlock, and L.C. Reese, Generalized solutions for laterally loaded piles. *ASCE Journal of Soil Mechanics and Foundations Division*, 86(SM5) (1960), 63-91.
- [10] B.B. Broms, Lateral resistance of piles in cohesionless soils, *ASCE Journal of the Soil Mechanics and Foundation Division*, 90(SM3) 1964, 123-156.
- [11] H.G. Poulos, Behaviour of laterally loaded piles: Part I-single piles, *ASCE Journal of the Soil Mechanics and Foundations Division*, 97(SM5) (1971), 711-731.
- [12] L.C. Reese, W.R. Cox, and F.D. Koop, Analysis of laterally loaded piles in sand, *Offshore Technology Conference*, Vol. II(Paper No. 2080) (1974), 473-484.
- [13] M.F. Randolph, The response of flexible piles to lateral loading, *Geotechnique*, 31(2) 91981), 247-259.
- [14] J.M. Duncan, L.T. Evans, and P.S. Ooi, Lateral load analysis of single piles and drilled shafts, *ASCE Journal of Geotechnical Engineering*, 120(6) (1994), 1018-1033.
- [15] L. Zhang, F. Silva, and R. Grismala, Ultimate Lateral Resistance to Piles in Cohesionless Soils, *Journal of*

Geotechnical and Geoenvironmental Engineering,
Vol. 131(1) (2005), 78–83.

- [16] G.T. Houlsby, and A.M. Puzrin, The bearing capacity of a strip footing on clay under combined loading, *Proc. R. Soc. London Ser. A*, 455 (1999), 893–916.
- [17] S. Gourvenec, and M. Randolph, Effect of strength non-homogeneity on the shape of failure envelopes for combined loading of strip and circular foundations on clay, *Géotechnique*, 53(6) (2003), 575–586
- [18] K.J.L. Stone, T.A. Newson, and J. Sandon, An investigation of the performance of a ‘hybrid’ monopile-footing foundation for offshore structures. *Proc. 6th Int. Offshore Site Investigation Conf.*, 11-13th Ssept 2007, London, UK, 2007.
- [19] K.J.L. Stone, T.A. Newson, and M. El Marassi, An investigation of a monopiled-footing foundation. *Int. Conf. Phys. Modelling in Geotech., ICPMG2010* (Zurich), Balkema, Rotterdam, 2010.
- [20] M. El-Marassi, T. Newson, H. El-Naggar, and K. Stone, Numerical modelling of the performance of a hybrid monopiled-footing foundation. *GeoEdmonton2008: Proceedings of the Canadian Geotechnical Conference*. (Paper No. 420, 1-8), 2008.
- [21] B.M. Lehane, W. Powrie, and L.P. Doherty, Centrifuge model tests in piled footings in clay for offshore wind turbines. *Int. Conf. Phys. Modelling in Geotech., ICPMG2010* (Zurich), Balkema, Rotterdam, 2010.

Increasing the Lateral Resistance of Offshore Monopile Foundations: Hybrid Monopile-Footing Foundation System

Harry S Arshi¹ and Kevin J L Stone²

Keywords: Offshore pile foundations, monopile-footing foundations, hybrid foundation system, laterally loaded piles, wind turbine foundations

Abstract

Due to the limitations of locations some of the recently found offshore oil and gas reservoirs, or the proposed locations for some of the offshore wind farms, there is clearly scope for developing foundations that are more efficient. One approach in increasing the lateral load bearing capacity of monopile foundations is the 'hybrid' monopile-footing foundation system with a proven record of improving the ultimate lateral resistance, particularly in cohesionless soils. This work builds on to the previous studies by investigating the behaviour of the hybrid system further. The effect of footing size, the magnitude of pre-loading and its significance in developing sufficient contact pressure beneath the footing, and the importance of the degree of rigidity is reported in this paper.

Introduction

Due to the needs of on-going developments in the oil and energy sector, the design of offshore foundations is constantly evolving. In the hydrocarbon extraction sector, exploration and development is moving in to ever deeper water resulting in ever more challenging geotechnical conditions. The development of sites for offshore wind farms (such as round 2 and 3 in the UK) is also extending into deeper water. The capacity of wind turbine generators is also increasing requiring significant development in foundation design to generate economic and practical solutions to the installation of these deep water wind farms.

The main challenge for deep-water foundations is the loading conditions. Offshore foundations are generally subject to combined loading conditions consisting of self-weight of the structure (V), relatively high horizontal loads (H) and large bending moments (M). The preferred foundation system to date has been the monopile that has been successfully employed for the majority of the offshore wind turbines installed. The advantage of the monopile is that it can be employed in a variety of different soil conditions even when loading conditions are very high. For instance in many of the proposed offshore wind farm locations it is often the case that the surficial seabed deposits are underlain by rock, generally weak rocks such as mudstones and chalk. Consequently it becomes necessary to install the monopiles, generally by driving, through the soil and into the rock, in order to achieve adequate lateral stiffness and moment resistance in order to carry the applied loads.

¹ PhD Research Student, Division of Built Environment & Civil Engineering, University of Brighton, Brighton, UK, Tel: +44-1273-642268, Email: H.Arshi@brighton.ac.uk.

² Principle Lecturer, Division of Built Environment & Civil Engineering, University of Brighton, Brighton, UK, Tel: +44-1273-642283, Email: Kevin.Stone@brighton.ac.uk.

One of the recently developed solutions for increasing the lateral resistance of deep-water monopiles is the hybrid monopile-footing system. The role of the footing is to provide a degree of rotational restraint at the pile head, leading to an improvement in the lateral resistance of the pile. It has also been shown that the use of a relatively thick pile cap leads to an increase in the lateral resistance through the development of passive soil wedges (Mokwa, 1999), in a similar way to the behaviour of skirted foundations (Bransby and Randolph, 1998).

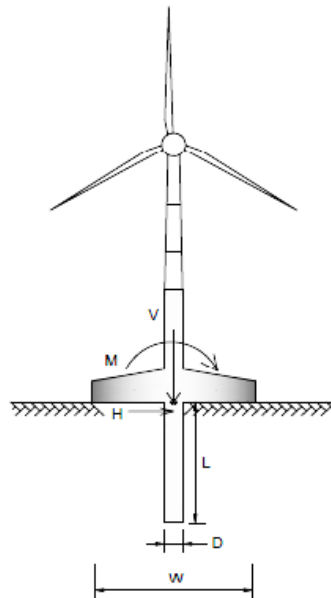


Figure 1. Schematic illustration of the prototype hybrid system

As schematically represented in Figure 1, this foundation system comprises of a circular footing is attached to the monopile at mudline. The 2D analogy of this system is that of a retaining wall with a stabilising base (Powrie and Daly, 2007). Where the plate diameter is relatively small, the system is similar to a single capped pile, for which methods have been developed for analysing the influence of the pile and pile cap under axial loading (Poulos and Randolph, 2008), and the effect of the pile cap on the lateral performance of single piles has also been investigated by others (Kim *et al* 1979), (Mokwa and Duncan, 2001; 2003), (Maharaj, 2003).

The lateral response of piles is well reported in the literature and various methods of analysis have been proposed by numerous researchers, such as Matlock and Reese (1960), Broms (1954), Poulos (1974), Reese *et al* (1974), Randolph (1981), Duncan *et al* (1994) and Zhang *et al* (2005). The bearing capacity problem has also been investigated under different loading conditions relevant to offshore foundations, see for example references Houlsby and Puzrin (1999), and Gourvenec and Randolph (2003).

Pervious investigations carried out at one gravity in ‘sand box’ tests (Stone *et al*, 2007; 2010), (Arshi 2011; 2012), (Arshi and Stone, 2011) together with 2D numerical modelling (El-Marassi, *et al* 2008), (Arshi *et al*, 2011) have shown that the lateral stiffness and ultimate capacity of the monopile is enhanced by the addition of the footing. Preliminary centrifuge model tests have also indicated that for cohesionless soils the ultimate lateral capacity of a monopile is enhanced by the presence of a footing (Stone *et al*, 2011). However, centrifuge tests performed on clay samples did not indicate much improvement in the lateral performance of the monopile (Lehane *et al*, 2010). It should be noted that

these centrifuge tests are not directly comparable since the relative geometries of the pile and bearing plates were significantly different in both studies.



Figure 2. Model foundation system

This paper focuses on analysing the load transfer mechanism within the system. It is the subject of this study to investigate how loads are transferred through different elements within the foundation system. The influence of the degree of rigidity at pile head (boundary condition in the connection between pile and footing) on the lateral resistance is also looked at. Moreover the relationship the ratio between the diameter of footing to pile and its effect on the lateral resistance of the pile is reported. This ground model is felt to be of particular relevance for offshore wind farm development due to the potential economical benefits.

Experimental Procedure

Materials and model preparation

Medium dense sand models were preprepared by pulvation sand into a box measuring 310 mm x 210 mm x 240 mm. Rounded to sub-rounded, uniformly graded quartez sand with an average particle size of 0.25 mm (Fraction D from David Ball Ltd) was used for the experiments. The maximum and minimum void ratios were 1.04 and 0.59 respectively with a correnpondant dry unit weights of 12.6 and 16.1 kN/m³. The cirritical state angle of friction was measured using direct shear box test and was found to be 32 degrees.

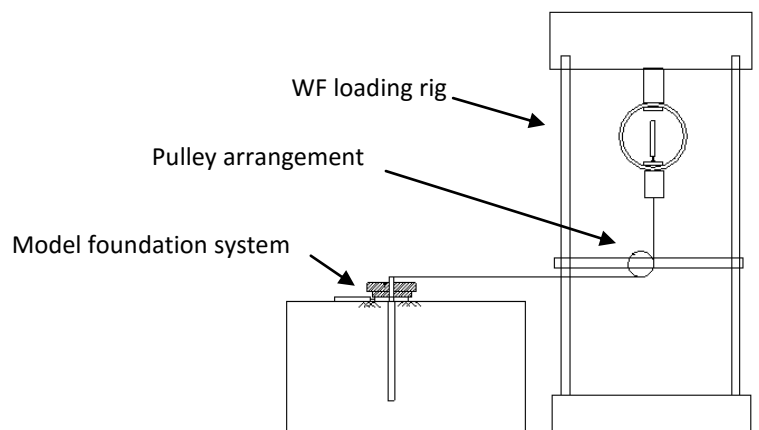


Figure 3. Test arranment for the model foundation system under lateral loading

The model foundation system comprised of a 10 mm thick 150 mm long steel rod together with 5mm thick steel plates with three different diameters of 40 mm, 60 mm and 80 mm, corresponding to pile to footing ratios of 0.4, 0.6 and 0.8 (Shown in Figure 2). The footings were fabricated in such a manner to give the option of having one directional vertical translations of the pile about the footing (i.e. translations along the y axis).

The installation of the model piles consisted of pushing the pile to about 70 % of the desired depth by hand followed by driving the rest of the pile via light tapping using a hammer until the required penetration depth was achieved.

Test procedure

All experiments took place in a single gravity Wykeham-Farrance loading rig at the University of Brighton, designed to load piles both horizontally and vertically. For tests involving only vertical loading, the load was applied directly to the top of the footings and/or piles, whereas for the tests involving lateral loading a wire and pulley arrangement was utilised (Illustrated in Figure 3).

Table 1. Summary of single gravity model tests

ID	Type	Connection	Vetr. Load* (N)
F40	Footing	-	-
F60	Footing	-	-
F80	Footing	-	-
PW1	Pile	-	10
PW2	Pile	-	50
H40W2A1	Hybrid	Rigid	50
H40W2A2	Hybrid	Free	50
H60W2A1	Hybrid	Rigid	50
H80W1A1	Hybrid	Rigid	10
H80W2A1	Hybrid	Rigid	50

* self weigh of foundation neglected

A summary of the programme is presented in Table 1. The footing only tests were carried out to determine the bearing capacity of footings with three different diameters and free from dead loads. This involved loading the footings vertically at the middle and measuring the relative vertical deflections. The deflections were measured using two LDVTs, attached to the far corners of the footings. For the pile only as well as hybrid system tests, dead loads were inserted on top of the pile, the piles were then pulled laterally and relative lateral deflections were measured using the LVDTs.

Results and Analysis

In order to be able to differentiate the contribution of different elements comprising the hybrid system, the individual performance of each element was investigated separately. Figure 4 show the plot of applied moment against relative rotation for individual footing tests. This plot shows the behaviour of footings with three diameters of 40 mm, 60 mm and 80 mm corresponding to ultimate bearing capacities of 65 Nmm, 240 Nmm and 490 Nmm

respectively. The performance of the pile-only tests, represented in terms of moment and pile head rotation, have been shown in three different graphs shown in Figure 5, 6 and 7. The performance of the pile-only tests have been used as a benchmark for analysing the behaviour of the hybrid foundation system.

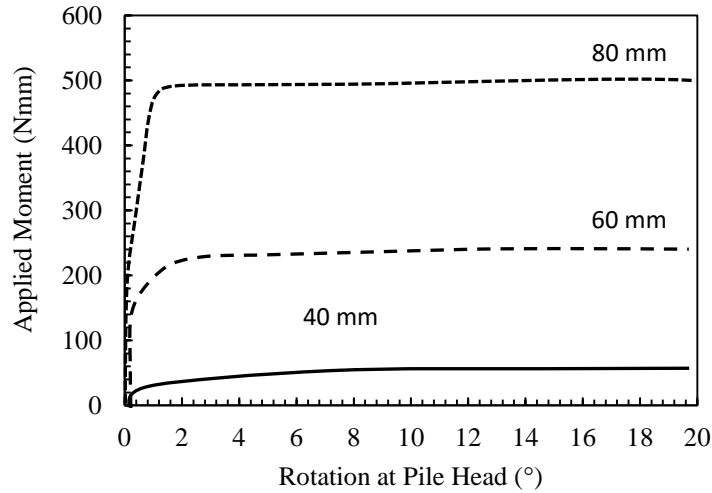


Figure 4. Moment-rotation plot for vertical footing-only tests

A total number of 5 tests were carried out on the hybrid system and the results have been presented in Figures 5, 6 and 7. All tests had a dead load of 50 N (with the exception of PF3W1A1) and the degree of rigidity between at the pile-footing connection was set at fully fixed for all tests except for PF1W2A2. All tests follow the same moment-rotation pattern with differences in the values of initial stiffness as well as the ultimate lateral resistance.

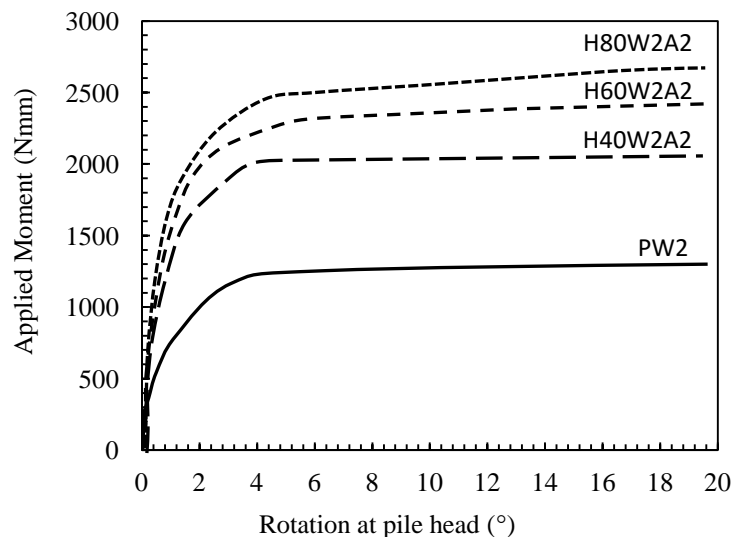


Figure 5. Moment-rotation plot for hybrid foundation system with varying footing size

Looking at the plot presented in Figure 4, it is apparent that the bearing capacity of circular footings increase with an increase in the diameter. The contribution from the addition of the footings to the pile is illustrated in Figure 5, where the initial stiffness and

the ultimate lateral resistance are significantly higher for the hybrid system. The hybrid system with the smallest footing had a 67% increase in value of the ultimate lateral resistance where the additional 50% and 100% increase in the diameter of the footings only boosted the ultimate resistance by an additional 20% and 50%.

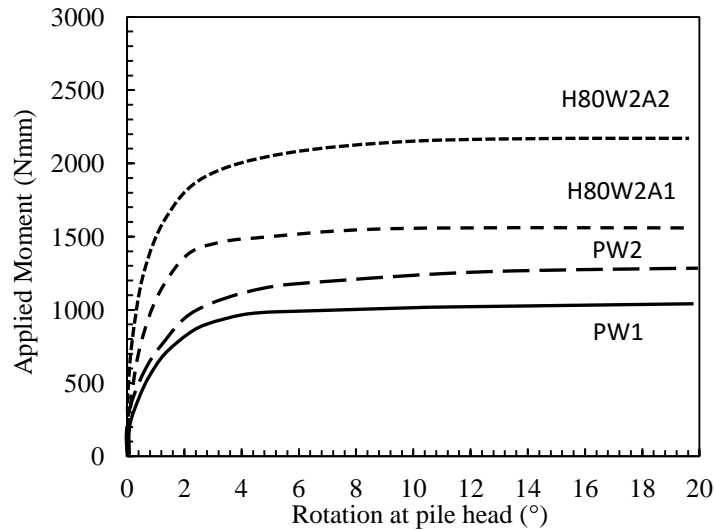


Figure 6. Moment-rotation plot for pile and hybrid foundation system test with varying dead loads

Dead loads play a major role in advancing the lateral resistance of the hybrid system. This is best illustrated in Figure 6 where pile-only as well as the hybrid system have to sustain dead loads of 10 N and 50 N. Clearly, the increase in the performance is significantly higher for the hybrid (27% increase) compared to the pile-only (12%).

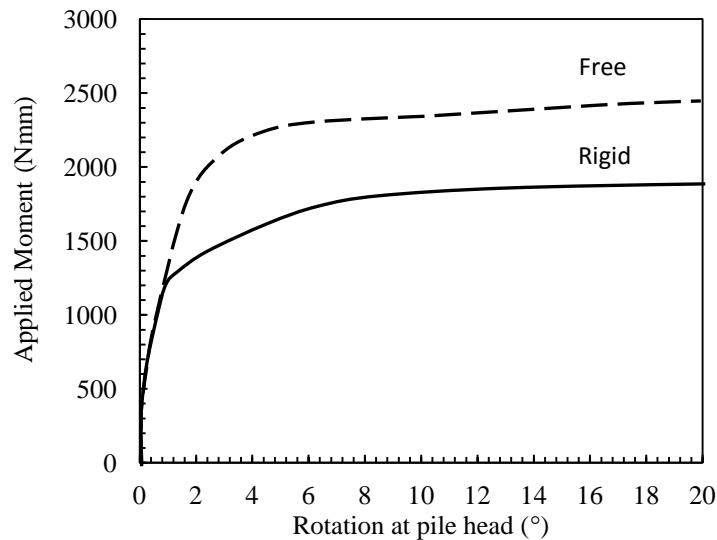


Figure 7. Moment-rotation plot for hybrid foundation system test with different degrees of rigidity at pile head

Furthermore, Figure 7 show two tests carried out in the same hybrid system but with different degrees of rigidity. For the systems under experiment, it was observed that having the pile free (in translation along the y axis) from the footing seem to have an advantage in

improving the performance of the system, where the ultimate lateral resistance was about 40% higher when the pile was free. In a free system, dead loads are carried fully but the footings where magnitude of dead load is directly proportional to the bearing capacity of the footings.

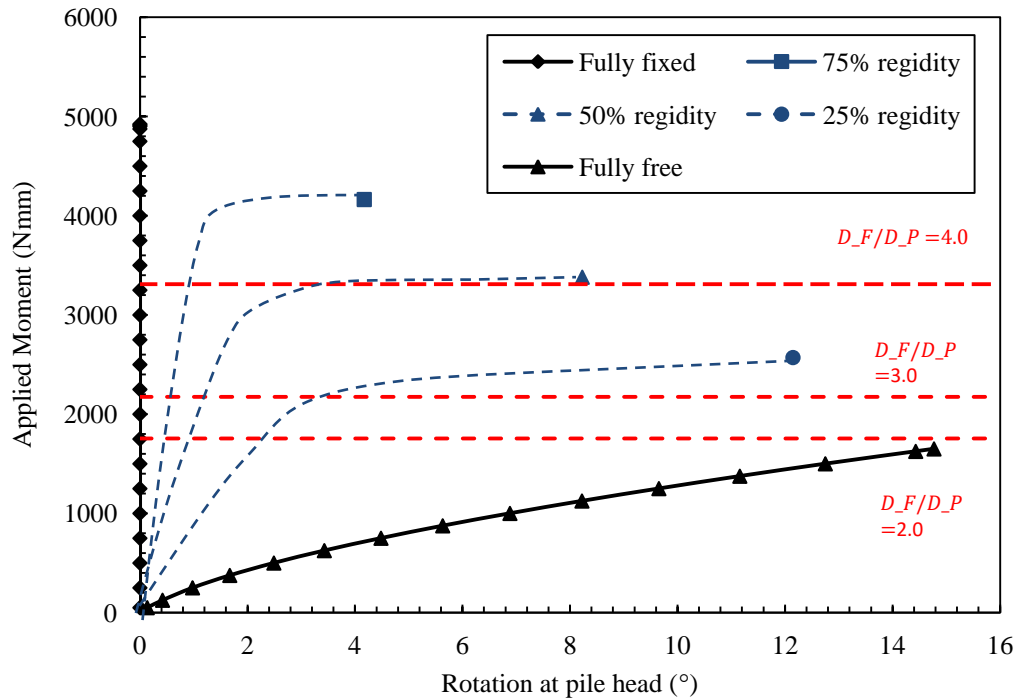


Figure 8. Moment-rotation plot for hybrid foundation system obtained using LPILE

The behaviour of the hybrid system was numerically analysed using the computer program LPILE and the results are illustrated in Figure 8. This program does not have an option for adding the footing to the pile and creating a hybrid system, however it does allow the user to introduce bending moments to the pile head in all directions. In order to illustrate the behaviour of the system, the resistance of the footings was calculated analytically and was added to the ultimate resistance of the fully free pile. This is shown as dashed red lines in Figure 8 for different pile to footing diameter ratios. Furthermore it is shown how the resistance of the hybrid system compares to piles with different degrees of rigidity.

Discussion and Conclusion

It was demonstrated that the addition of the footing to the pile, which creates the ‘hybrid’ system, increases the initial stiffness as well as the ultimate lateral resistance of individual monopiles. Individual tests were carried out to establish the ultimate bearing capacity that would be mobilised on the underside of the footings of the hybrid system. Clearly, the actual degree of rigidity provided at the pile head depends on several factors such as (i) size of the footing (ii) the initial contact of bedding with soil surface (iii) the stiffness of the soil beneath the footing.

If the actual capacity of the pile is very high, it is difficult to get a good positive contact between the footing and the soil until the system starts to rotate and that means that the stiffness does not increase significantly. It is apparent that a more efficient system would require a good contact between the footing and the soil and that the contact remains

present during the loading cycle. In a fully rigid system, the drawback is that the pile needs to be rather short in order to let the working loads generate the contact pressure underneath the footing. However, the results here show that it is possible to overcome this by designing the system with a sliding connection where vertical translations of the pile is permitted.

The results of this investigation is limited to 1g tests. A comprehensive series of centrifuge tests are currently undertaking. The results of the tests together with a series of 3D numerical model study will be reported in the near future.

References

- Arshi HS. (2011). Structural behavior and performance of skirted hybrid monopile-footing foundations for offshore oil and gas facilities. *Proceedings of the Institution of Structural Engineers: Young Researchers Conference '11*. London: IStructE Publications, 8.
- Arshi HS, Stone KJL and Newson TA. (2011). Numerical modelling on the degree of rigidity at pile head for offshore monopile-footing foundation systems. *9th British Geotechnical Association Annual Conference, London*.
- Arshi HS and Stone KJL. (2011). An investigation of a rock socketed pile with an integral bearing plate founded over weak rock. *Proceedings of the 15th European Conference of Soil Mechanics and Geotechnical Engineering*. Amsterdam: Ios Pr Inc, 705 – 711.
- Arshi HS. (2012). A new design solution for increasing the lateral resistance of offshore pile foundations for wind turbines located in deep-water. *Proceedings of the Institution of Structural Engineers: Young Researchers Conference '12*. London: IStructE Publications, 10.
- Bransby MF and Randolph MF. (1998). Combined loading of skirted foundations. *Géotechnique*. 48(5), 637–655.
- Broms BB. (1964). Lateral resistance of piles in cohesionless soils. *ASCE Journal of the Soil Mechanics and Foundation Division*. 90(SM3), 123-156.
- Duncan JM, Evans LT and Ooi PS. (1994). Lateral load analysis of single piles and drilled shafts. *ASCE Journal of Geotechnical Engineering*. 120(6), 1018-1033.
- El-Marassi M, Newson T, El-Naggar H and Stone KJL. (2008). Numerical modelling of the performance of a hybrid monopiled-footing foundation. *Proceedings of the 61st Canadian Geotechnical Conference, GeoEdmonton 2008*. Edmonton, (Paper No. 480), 97 – 104.
- Gourvenec S and Randolph M. (2003). Effect of strength non-homogeneity on the shape of failure envelopes for combined loading of strip and circular foundations on clay. *Géotechnique*. 53(6), 575–586.
- Houlsby GT and Puzrin AM. (1999). The bearing capacity of a strip footing on clay under combined loading. *Proc. R. Soc. London Ser. A*. 455, 893–916.
- Kim JB, Singh LP and Brungraber RJ. (1979). Pile cap soil interaction from full scale lateral load tests. *ASCE Journal of Geotechnical Engineering*. 105(5), 643-653.
- Lehane BM, Powrie W and Doherty LP. (2010). *Centrifuge model tests in piled footings in clay for offshore wind turbines*. Proceedings of *International Conference in Physical Modelling in Geotechnics, ICPMG2010*. Rotterdam: Balkema.
- Maharaj DK. (2003). Load-deflection response of laterally loaded single pile by nonlinear finite element analysis. *EJEG*.
- Matlock H and Reese LC. (1960). Generalized solutions for laterally loaded piles. *ASCE Journal of Soil Mechanics and Foundations Division*. 86(SM5), 63-91.

- Mokwa RL. (1999). Investigation of the Resistance of Pile Caps to Lateral Loading. *Ph.D Thesis*. Virginia Polytechnic Institute, Blacksburg, Virginia.
- Mokwa RL and Duncan JM. (2001). Experimental evaluation of lateral-load resistance of pile caps. *ASCE Journal of Geotechnical and Geoenvironmental Engineering*. 127(2), 185 - 192.
- Mokwa RL and Duncan JM. (2003). Rotational restraint of pile caps during lateral loading. *ASCE Journal of Geotechnical and Geoenvironmental Engineering*. 129(9), 829 - 837.
- Poulos HG. (1971). Behaviour of laterally loaded piles: Part I-single piles. *ASCE Journal of the Soil Mechanics and Foundations Division*. 97(SM5), 711-731.
- Poulos HG and Randolph MF. (1983). Pile group analysis: a study of two methods. *ASCE Journal of Geotechnical Engineering*. 109(3), 355-372.
- Powrie W, and Daly MP. (2007). Centrifuge modelling of embedded retaining wall with stabilising bases. *Geotechnique*. 57(6), 485-497.
- Randolph MF. (1981). The response of flexible piles to lateral loading. *Géotechnique*. 31(2), 247-259.
- Reese LC, Cox WR and Koop FD. (1974). Analysis of laterally loaded piles in sand. *Offshore Technology Conference*. Vol. II (Paper No. 2080), 473-484.
- Stone KJL, Newson TA and Sandon J. (2007). An investigation of the performance of a 'hybrid' monopole-footing foundation for offshore structures. *Proceedings of 6th International on Offshore Site Investigation and Geotechnics*. London: SUT, 391-396.
- Stone KJL, Newson T and El Marassi, M. (2010). An investigation of a monopiled-footing foundation. *International Conference on Physical Modelling in Geotechnics, ICPMG2010*. Rotterdam: Balkema, 829-833.
- Zhang L, Silva F and Grismala R. (2005) Ultimate lateral resistance to piles in cohesionless soils. *Journal of Geotechnical and Geoenvironmental Engineering*. Vol. 131(1), 78-83.

10th Annual British Geotechnical Association Conference, 2012
Decoupled Hybrid Monopile-Footing Foundation System

Harry Arshi, Kevin Stone (University of Brighton) & Mohsen Vaziri (Ramboll UK Ltd)

Fixed or Decoupled Pile-Footing Connection?

Pervious research has shown a promising increase of the lateral resistance of offshore monopiles by adding a circular footing to the pile at mudline. However an obvious disadvantage of this system is that when the footing is rigidly fixed to the pile, the magnitude of vertical load required to provide sufficient positive contact between the footing and the pile is impractically large.

Researchers at the University of Brighton (together with associates from industry) have come up with a novel solution to make the hybrid system more efficient where the magnitude of vertical load could be reduced while sufficient contact between the footing and pile is maintained.

In this design, denote as the 'decoupled' hybrid system, the connection between footing and pile is decoupled. This means that the pile is free to move in the vertical direction but still provides the lateral support to the pile through its collar's tight connection (the blue section in Figure 1).

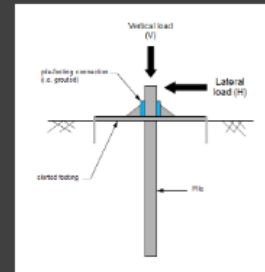


Figure 1. Structural arrangement of the decoupled hybrid monopile-footing foundation system

Description of the Decoupled Hybrid System

- The decoupled hybrid system comprises of a monopile and a footing.
- The pile is free to move in the vertical direction but any lateral movement will naturally be restrained by the present of the footing and its collar section (see Figure 2).
- The decoupled system will allow the footing to reposition itself when soil undergoes settlement over time and so the positive contact between the footing and soil is constantly maintained.
- The footing is circular and is flat at its base.
- The footing is fabricated from steel and is typically 0.4m-0.65m thick at its base. This value is not fixed and could be adjusted depending on how stiff the footing is required to be (based on loading criteria). The simplicity of this footing design itself is an advantage for reducing material and fabrication costs.
- The footing comprises of two sections, namely the base and the collar (collar refers to the side wall/ring/bore/throat section shown in Figure 2).
- The length of the collar section could be adjusted based on the lateral resistance requirements and piles rotational limitations. This could sometimes extend till above the water surface, if that length provides sufficient lateral support while allowing sufficient free vertical pile movement.
- The structure will then be connected to/mounted on the top of the collar section of the footing, which will transfer all the vertical load directly to the footing. This way there is no need for providing other materials to maintain vertical load on the footing and the required surcharge or effective maintenance of positive contact pressure between the footing base and seabed will be coming directly from the self weight of the structure.
- The gap between the pile and collar section of the footing is adjustable, but this is typically small enough to allow vertical translations of the pile while preventing the pile from large rotations/lateral displacements (large within the means of design's rotational restrictions).
- A specific type of rubber with low frictional properties will be placed at the small gap between the pile and the footing collar. This type of rubber is currently being used in marine structures, specifically in floating pontoon technology. This rubber has proven to be very efficient in maintaining a tight fit between piles and dampers while allowing the vertical movement and providing effective lateral support.
- There is a gap provided between the top of the pile and the top section of the collar. This will permit the vertical movement of the pile without touching the top section of the collar. This is done to avoid the pile from taking vertical load and the sole duty of the pile is to provide lateral support while interacting with the footing laterally.
- The pile does not take any vertical load and is free to move in the vertical direction along the footing.
- The pile could be of any cross sectional shape, but hollow steel section/tubes are the most common type used.
- The recommended footing shape is circular steel plate but the aim here is to provide a rigid/stiff plate to support the pile without bending and so other footing configurations that provide this rigidity could also be used.

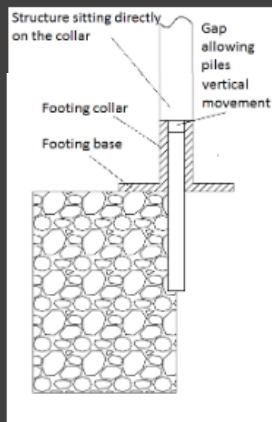


Figure 2. Comprising elements of the decoupled hybrid system

Installation of the Decoupled Hybrid System

- The first step is lowering the pile, positioning and hammering the pile until desired penetration depth is achieved.
- The soil around the pile often gets disturbed following the installation of the pile. It is vital to make sure the soil around the pile is in as good a condition as possible. Using underwater vehicles the soil around the pile is then smoothed, tamped and prepared until a smooth and straight surface for the installation of the footing is achieved.
- The footing (both the base and the collar section which are once piece) is then lowered by sliding the pile through its central hole. Once the footing is sitting on the soil, using underwater monitoring technology, it will be ensured that the footing is in the right place and the footing base is in sufficient and satisfactory contact with the soil underneath.
- Once the footing is in place, the gap between the pile and the collar section of the footing is placed with damper rubber and the top section (gap above the pile see Figure 2) is then sealed to avoid other marine presence from inhabiting in the gap.
- The lower part of the structure is then positioned and mounted on top of the collar section and then secured/fixed in place.

Performance of the Decoupled Hybrid System

- The difference between a fixed (footing is rigidly fixed to the pile) and decoupled pile-footing connection is shown in the Figure 3. For the same pile and footing geometry and loading condition, the decoupled system shows a 40% increase compared to the fixed system. Note that the surcharge/vertical load applied is only 50 kPa, so rather lightly loaded.
- Based on the experimental data and for the given geometry under study, the lateral capacity of the free headed pile is increased by the addition of the decoupled foundation plate by up to an outstanding 280%. The magnitude of this increase depends on the diameter of the footing as well as the magnitude of the applied vertical load on the footing. An example of this is shown in Figure 4.
- For the specified pile geometry a qualitative analysis using the simplified method of Brom's can be performed to illustrate the role of the foundation plate on the lateral response of the hybrid system.
- Refer to Arshi & Stone 2012(a) and 2012(b) for more information regarding the performance of the DECOUPLED hybrid system.
- This poster only describes/introduces the decoupled system with a very brief look at the preliminary results. A comprehensive report on the details and behaviour of the decoupled hybrid system which analyses the results of 1g and centrifuge tests together with 3D finite element analysis in preparation and will be published in a specialist journal soon.

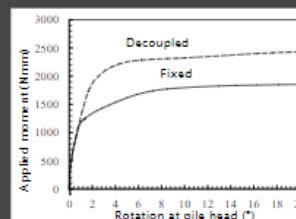


Figure 3. Load vs. deflection behaviour for fixed and decoupled hybrid systems

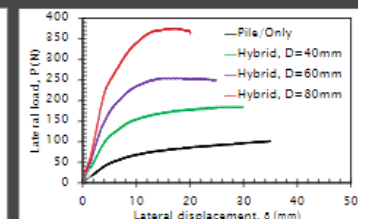


Figure 4. Load vs. deflection behaviour for decoupled hybrid system with varying footing diameter

Contact Details

Harry Arshi	H.Arshi@brighton.ac.uk
Kevin Stone	Kevin.Stone@brighton.ac.uk
Mohsen Vaziri	M.Vaziri@ramboll.co.uk

LATERAL RESISTANCE OF HYBRID MONOPILE-FOOTING FOUNDATIONS IN COHESIONLESS SOILS FOR OFFSHORE WIND TURBINES

HS Arshi and KJL Stone

University of Brighton, Brighton, UK

Abstract

Current offshore foundation technology is being transferred successfully to the renewable energy sector, but there is clearly scope for developing foundations that are more tuned to the needs of the renewable power systems such as wind turbines. One such approach is the 'hybrid' monopile-footing system with a proven record of improving the ultimate lateral resistance, particularly in cohesionless soils. This work builds on to the previous studies by investigating the behaviour of the hybrid system further. The effect of footing size, the magnitude of pre-loading and its significance in developing sufficient contact pressure beneath the footing, and the importance of the degree of rigidity is reported in this paper.

1. Introduction

Due to the needs of on-going developments in the oil and energy sector, the design of offshore foundations is constantly evolving. In the hydrocarbon extraction sector, exploration and development is moving in to ever deeper water resulting in ever more challenging geotechnical conditions. The development of sites for offshore wind farms (such as round 2 and 3 in the UK) is also extending into deeper water. The capacity of wind turbine generators is also increasing requiring significant development in foundation design to generate economic and practical solutions to the installation of these deep water wind farms.

The main challenge for deep-water foundations is the loading conditions. Offshore foundations are generally subject to combined loading conditions consisting of self-weight of the structure (V), relatively high horizontal loads (H) and large bending moments (M). The preferred foundation system to date has been the monopile that has been successfully employed for the majority of the offshore wind turbines installed. The advantage of the monopile is that it can be employed in a variety of different soil conditions even when loading conditions are very high. For instance in many of the proposed offshore wind farm locations it is often the case that the surficial seabed deposits are underlain by rock, generally weak rocks such as mudstones and chalk. Consequently it becomes necessary to install the monopiles, generally by driving, through the soil and into

the rock, in order to achieve adequate lateral stiffness and moment resistance in order to carry the applied loads.

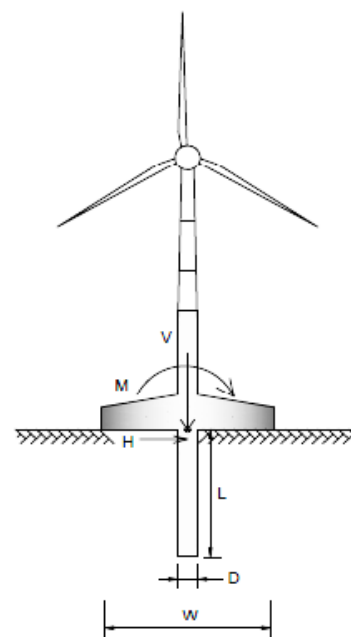


Figure 1: Schematic illustration of the prototype hybrid system

One of the recently developed solutions for increasing the lateral resistance of deep-water monopiles is the hybrid monopile-footing system. The role of the footing is to provide a degree of rotational restraint at the pile head, leading to an improvement in the lateral resistance of the pile. It has also been shown that the use of a relatively thick pile cap leads to an increase in the lateral resistance through the development of passive soil wedges (Mokwa, 1999), in a

similar way to the behaviour of skirted foundations (Bransby and Randolph, 1998).

As schematically represented in Figure 1, this foundation system comprises of a circular footing is attached to the monopile at mudline. The 2D analogy of this system is that of a retaining wall with a stabilising base (Powrie and Daly, 2007). Where the plate diameter is relatively small, the system is similar to a single capped pile, for which methods have been developed for analysing the influence of the pile and pile cap under axial loading (Poulos and Randolph, 2008), and the effect of the pile cap on the lateral performance of single piles has also been investigated by others (Kim *et al* 1979), (Mokwa and Duncan, 2001; 2003), (Maharaj, 2003).

The lateral response of piles is well reported in the literature and various methods of analysis have been proposed by numerous researchers, such as Matlock and Reese (1960), Broms (1954), Poulos (1974), Reese *et al* (1974), Randolph (1981), Duncan *et al* (1994) and Zhang *et al* (2005). The bearing capacity problem has also been investigated under different loading conditions relevant to offshore foundations, see for example references Houlsby and Puzrin (1999), and Gourvenec and Randolph (2003).



Figure 2: Model foundation system

Pervious investigations carried out at one gravity in 'sand box' tests (Stone *et al*, 2007; 2010), (Arshi 2011; 2012), (Arshi and Stone, 2011) together with 2D numerical modelling (El-Marassi, *et al* 2008), (Arshi *et al*, 2011) have shown that the lateral stiffness and ultimate capacity of the monopile is enhanced by the addition of the footing. Preliminary centrifuge model tests have also indicated that for cohesionless soils the ultimate lateral capacity of a monopile is enhanced by the presence of a footing (Stone *et al*, 2011). However, centrifuge tests performed on clay samples did not indicate much improvement in the lateral performance of the monopile (Lehane *et al*, 2010). It should be noted

that these centrifuge tests are not directly comparable since the relative geometries of the pile and bearing plates were significantly different in both studies.

This paper focuses on analysing the load transfer mechanism within the system. It is the subject of this study to investigate how loads are transferred through different elements within the foundation system. The influence of the degree of rigidity at pile head (boundary condition in the connection between pile and footing) on the lateral resistance is also looked at. Moreover the relationship the ratio between the diameter of footing to pile and its effect on the lateral resistance of the pile is reported. This ground model is felt to be of particular relevance for offshore wind farm development duo to the potential economical benefits.

2. Experimental Procedure

2.1 Materials and model preparation

Medium dense sand models were preprepared by pulvation sand into a box measuring 310 mm x 210 mm x 240 mm. Rounded to sub-rounded, uniformly graded quartz sand with an average particle size of 0.25 mm (Fraction D from David Ball Ltd) was used for the experiments. The maximum and minimum void ratios were 1.04 and 0.59 respectively with a correspondant dry unit weights of 12.6 and 16.1 kN/m³. The critical state angle of friction was measured using direct shear box test and was found to be 32 degrees.

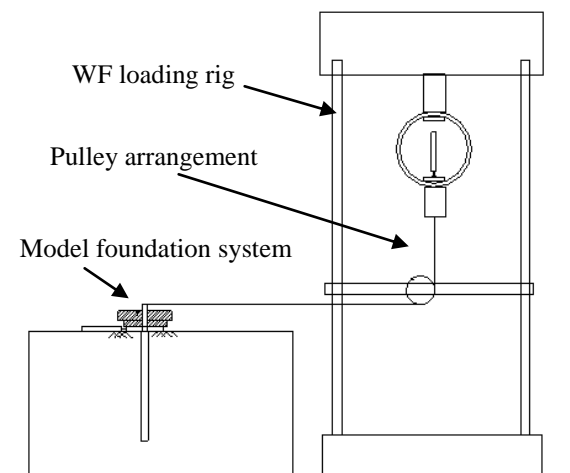


Figure 3: Test arrangement for the model foundation system under lateral loading

The model foundation system comprised of a 10 mm thick 150 mm long steel rod together with 5mm thick steel plates with three different diameters of 40 mm, 60 mm and 80 mm, corresponding to pile to footing ratios of 0.4, 0.6 and 0.8 (Shown in Figure 2). The footings were fabricated in such a manner to

give the option of having one directional vertical translations of the pile about the footing (i.e. translations along the y axis).

The installation of the model piles consisted of pushing the pile to about 70 % of the desired depth by hand followed by driving the rest of the pile via light tapping using a hammer until the required penetration depth was achieved.

2.2 Test procedure

All experiments took place in a single gravity Wykeham-Farrance loading rig at the University of Brighton, designed to load piles both horizontally and vertically. For tests involving only vertical loading, the load was applied directly to the top of the footings and/or piles, whereas for the tests involving lateral loading a wire and pulley arrangement was utilised (Illustrated in Figure 3).

Table 1: Summary of single gravity model tests

ID	Type	Connection	Vetr. Load* (N)
F40	Footing	-	-
F60	Footing	-	-
F80	Footing	-	-
PW1	Pile	-	10
PW2	Pile	-	50
PF1W2A1	Hybrid	Rigid	50
PF1W2A2	Hybrid	Free	50
PF2W2A1	Hybrid	Rigid	50
PF3W1A1	Hybrid	Rigid	10
PF3W2A1	Hybrid	Rigid	50

* self weigh of foundation neglected

A summary of the programme is presented in Table 1. The footing only tests were carried out to determine the bearing capacity of footings with three different diameters and free from dead loads. This involved loading the footings vertically at the middle and measuring the relative vertical deflections. The deflections were measured using two LDVTs, attached to the far corners of the footings. For the pile only as well as hybrid system tests, dead loads were inserted on top of the pile, the piles were then pulled laterally and relative lateral deflections were measured using the LVDTs.

3. Results and Analysis

In order to be able to differentiate the contribution of different elements comprising the hybrid system, the individual performance of each element was investigated separately. Figure 4 show the plot of applied moment against relative rotation for individual footing tests. This plot shows the behaviour of footings with three diameters of 40

mm, 60 mm and 80 mm corresponding to ultimate bearing capacities of 65 Nmm, 240 Nmm and 490 Nmm respectively. The performance of the pile-only tests, represented in terms of moment and pile head rotation, have been shown in three different graphs shown in Figure 5, 6 and 7. The performance of the pil-only tests have been used as a benchmark for analysing the behaviour of the hybrid foundation system.

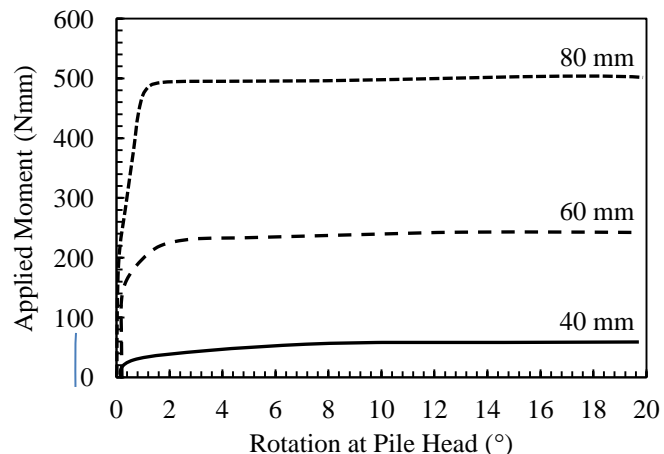


Figure 4: Moment-rotation plot for vertical footing-only tests

A total number of 5 tests were carried out on the hybrid system and the results have been presented in Figures 5, 6 and 7. All tests had a dead load of 50 N (with the exception of PF3W1A1) and the degree of rigidity between at the pile-footing connection was set at fully fixed for all tests except for PF1W2A2. All tests follow the same moment-rotation pattern with differences in the values of initial stiffness as well as the ultimate lateral resistance.

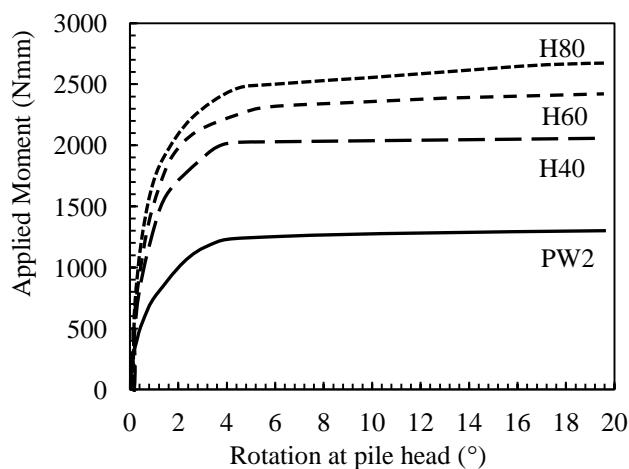


Figure 5: Moment-rotation plot for hybrid foundation system with varying footing size

Looking at the plot presented in Figure 4, it is apparent that the bearing capacity of circular footings increase with an increase in the diameter. The contribution from the addition of the footings to

the pile is illustrated in Figure 5, where the initial stiffness and the ultimate lateral resistance are significantly higher for the hybrid system. The hybrid system with the smallest footing had a 67% increase in value of the ultimate lateral resistance where the additional 50% and 100% increase in the diameter of the footings only boosted the ultimate resistance by an additional 20% and 50%.

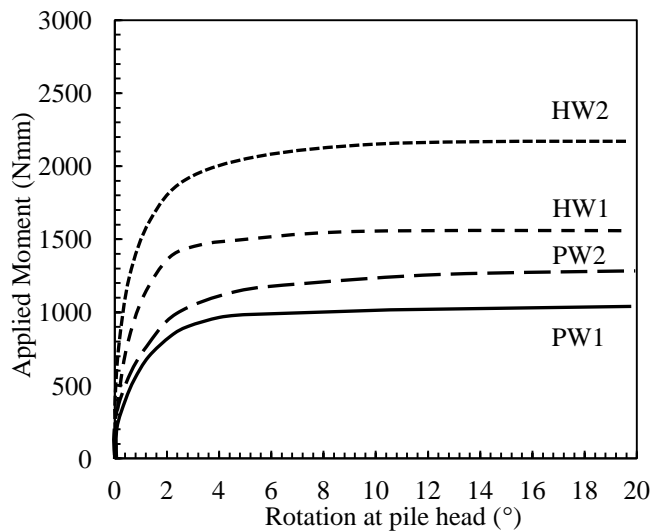


Figure 6: Moment-rotation plot for pile and hybrid foundation system test with varying dead loads

Dead loads play a major role in advancing the lateral resistance of the hybrid system. This is best illustrated in Figure 6 where pile-only as well as the hybrid system have to sustain dead loads of 10 N and 50 N. Clearly, the increase in the performance is significantly higher for the hybrid (27% increase) compared to the pile-only (12%).

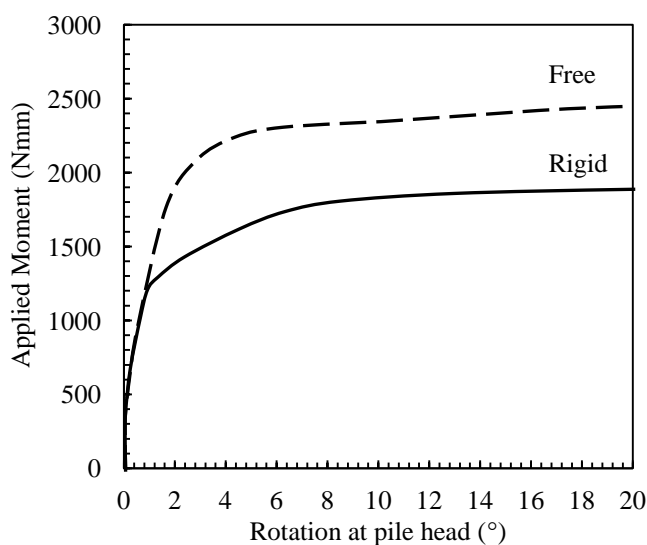


Figure 7: Moment-rotation plot for hybrid foundation system test with different degrees of rigidity at pile head

Furthermore, Figure 7 show two tests carried out in the same hybrid system but with different degrees of

rigidity. For the systems under experiment, it was observed that having the pile free (in translation along the y axis) from the footing seem to have an advantage in improving the performance of the system, where the ultimate lateral resistance was about 40% higher when the pile was free. In a free system, dead loads are carried fully but the footings where magnitude of dead load is directly proportional to the bearing capacity of the footings.

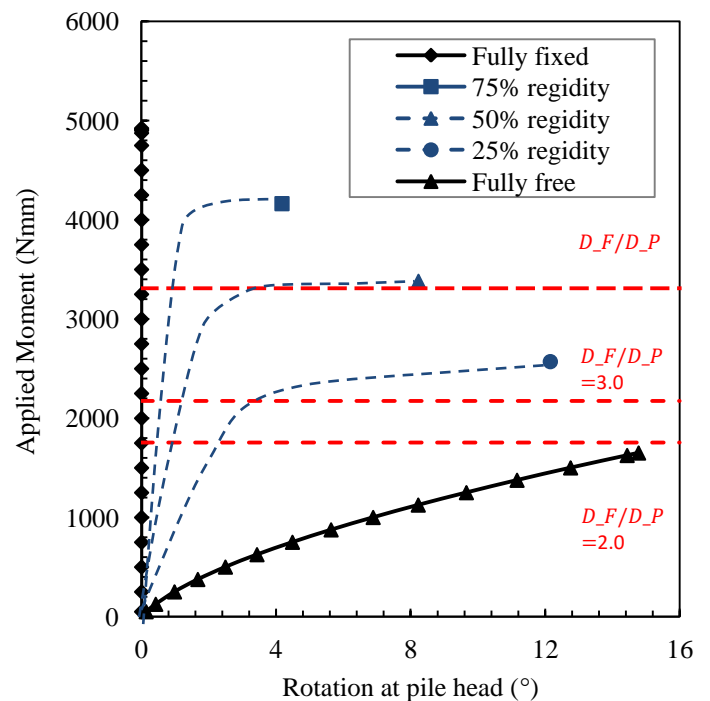


Figure 8: Moment-rotation plot for hybrid foundation system obtained using LPILE

The behaviour of the hybrid system was numerically analysed using the computer program LPILE and the results are illustrated in Figure 8. This program does not have an option for adding the footing to the pile and creating a hybrid system, however it does allow the user to introduce bending moments to the pile head in all directions. In order to illustrate the behaviour of the system, the resistance of the footings was calculated analytically and was added to the ultimate resistance of the fully free pile. This is shown as dashed red lines in Figure 8 for different pile to footing diameter ratios. Furthermore it is shown how the resistance of the hybrid system compares to piles with different degrees of rigidity.

5. Discussion and Conclusion

It was demonstrated that the addition of the footing to the pile, which creates the 'hybrid' system, increases the initial stiffness as well as the ultimate lateral resistance of individual monopiles. Individual tests were carried out to establish the ultimate bearing capacity that would be mobilised on the underside of the footings of the hybrid system. Clearly, the actual

degree of rigidity provided at the pile head depends on several factors such as (i) size of the footing (ii) the initial contact of bedding with soil surface (iii) the stiffness of the soil beneath the footing.

If the actual capacity of the pile is very high, it is difficult to get a good positive contact between the footing and the soil until the system starts to rotate and that means that the stiffness does not increase significantly. It is apparent that a more efficient system would require a good contact between the footing and the soil and that the contact remains present during the loading cycle. In a fully rigid system, the drawback is that the pile needs to be rather short in order to let the working loads generate the contact pressure underneath the footing. However, the results here show that it is possible to overcome this by designing the system with a sliding connection where vertical translations of the pile is permitted.

The results of this investigation is limited to 1g tests. A comprehensive series of centrifuge tests are currently undertaking. The results of the tests together with a series of 3D numerical model study will be reported in the near future.

References

- Arshi HS. (2011). Structural behavior and performance of skirted hybrid monopile-footing foundations for offshore oil and gas facilities. *Proceedings of the Institution of Structural Engineers: Young Researchers Conference '11*. London: IStructE Publications, 8.
- Arshi HS, Stone KJL and Newson TA. (2011). Numerical modelling on the degree of rigidity at pile head for offshore monopile-footing foundation systems. *9th British Geotechnical Association Annual Conference, London*.
- Arshi HS and Stone KJL. (2011). An investigation of a rock socketed pile with an integral bearing plate founded over weak rock. *Proceedings of the 15th European Conference of Soil Mechanics and Geotechnical Engineering*. Amsterdam: Ios Pr Inc, 705 – 711.
- Arshi HS. (2012). A new design solution for increasing the lateral resistance of offshore pile foundations for wind turbines located in deep-water. *Proceedings of the Institution of Structural Engineers: Young Researchers Conference '12*. London: IStructE Publications, 10.
- Bransby MF and Randolph MF. (1998). Combined loading of skirted foundations. *Géotechnique*. 48(5), 637–655.
- Broms BB. (1964). Lateral resistance of piles in cohesionless soils. *ASCE Journal of the Soil Mechanics and Foundation Division*. 90(SM3), 123-156.
- Duncan JM, Evans LT and Ooi PS. (1994). Lateral load analysis of single piles and drilled shafts. *ASCE Journal of Geotechnical Engineering*. 120(6), 1018-1033.
- El-Marassi M, Newson T, El-Naggar H and Stone KJL. (2008). Numerical modelling of the performance of a hybrid monopiled-footing foundation. *Proceedings of the 61st Canadian Geotechnical Conference, GeoEdmonton 2008*. Edmonton, (Paper No. 480), 97 – 104.
- Gourvenec S and Randolph M. (2003). Effect of strength non-homogeneity on the shape of failure envelopes for combined loading of strip and circular foundations on clay. *Géotechnique*. 53(6), 575–586.
- Houlsby GT and Puzrin AM. (1999). The bearing capacity of a strip footing on clay under combined loading. *Proc. R. Soc. London Ser. A*. 455, 893–916.
- Kim JB, Singh LP and Brungraber RJ. (1979). Pile cap soil interaction from full scale lateral load tests. *ASCE Journal of Geotechnical Engineering*. 105(5), 643-653.
- Lehane BM, Powrie W and Doherty LP. (2010). *Centrifuge model tests in piled footings in clay for offshore wind turbines*. Proceedings of *International Conference in Physical Modelling in Geotechnics, ICPMG2010*. Rotterdam: Balkema.
- Maharaj DK. (2003). Load-deflection response of laterally loaded single pile by nonlinear finite element analysis. *EJEG*.
- Matlock H and Reese LC. (1960). Generalized solutions for laterally loaded piles. *ASCE Journal of Soil Mechanics and Foundations Division*. 86(SM5), 63-91.
- Mokwa RL. (1999). Investigation of the Resistance of Pile Caps to Lateral Loading. *Ph.D Thesis*. Virginia Polytechnic Institute, Blacksburg, Virginia.
- Mokwa RL and Duncan JM. (2001). Experimental evaluation of lateral-load resistance of pile caps. *ASCE Journal of Geotechnical and Geoenvironmental Engineering*. 127(2), 185 - 192.
- Mokwa RL and Duncan JM. (2003). Rotational restraint of pile caps during lateral loading. *ASCE Journal of Geotechnical and Geoenvironmental Engineering*. 129(9), 829 - 837.
- Poulos HG. (1971). Behaviour of laterally loaded piles: Part I-single piles. *ASCE Journal of the Soil Mechanics and Foundations Division*. 97(SM5), 711-731.
- Poulos HG and Randolph MF. (1983). Pile group analysis: a study of two methods. *ASCE Journal of Geotechnical Engineering*. 109(3), 355-372.
- Powrie W, and Daly MP. (2007). Centrifuge modelling of embedded retaining wall with stabilising bases. *Geotechnique*. 57(6), 485-497.
- Randolph MF. (1981). The response of flexible piles to lateral loading. *Géotechnique*. 31(2), 247-259.

- Reese LC, Cox WR and Koop FD. (1974). Analysis of laterally loaded piles in sand. *Offshore Technology Conference*. Vol. II (Paper No. 2080), 473-484.
- Stone KJL, Newson TA and Sandon J. (2007). An investigation of the performance of a 'hybrid' monopole-footing foundation for offshore structures. *Proceedings of 6th International on Offshore Site Investigation and Geotechnics*. London: SUT, 391-396.
- Stone KJL, Newson T and El Marassi, M. (2010). An investigation of a monopiled-footing foundation. *International Conference on Physical Modelling in Geotechnics, ICPMG2010*. Rotterdam: Balkema, 829-833.
- Zhang L, Silva F and Grismala R. (2005) Ultimate lateral resistance to piles in cohesionless soils. *Journal of Geotechnical and Geoenvironmental Engineering*. Vol. 131(1), 78-83.

Modelling of Monopile-Footing Foundation System for Offshore Structures in Cohesionless Soils

Modélisation du système de semelle de fondation monopile sur les structures extracôtières dans les sols pulvérulents

H.S. Arshi & K.J.L. Stone
University of Brighton, UK

M. Vaziri
Ramboll UK Limited, UK

T.A. Newson & M. El-Marassi
University of Western Ontario, Canada

R.N. Taylor & R.J. Goodey
City University London, UK

ABSTRACT: While monopiles have proven to be an economically sound foundation solution for wind turbines, especially in relatively shallow water, their installation in deeper water and in hard ground may require a more complex foundation design in order to satisfy the loading conditions. One approach is that foundation systems are developed which combine several foundation elements to create a 'hybrid' system. In this way it is possible to develop a foundation system which is more efficient for the combination of vertical and lateral loads associated with wind turbines while maintaining the efficiency and simplicity of the design. Previous studies have reported the results of single gravity tests of the hybrid system where the benefits of adding the footing to the pile are illustrated. This paper presents experimental results on the performance of skirted and unskirted monopile-footings. A simplified design approach based on conventional lateral pile analysis is presented.

RÉSUMÉ : Alors que monopiles se sont révélés être une solution économiquement viable pour les fondations des éoliennes, en particulier dans les eaux relativement peu profondes, leur installation dans des eaux plus profondes et dans un sol dur peut exiger une conception des fondations plus complexes afin de satisfaire les conditions de chargement. Une approche possible est que les systèmes de base sont développées qui combinent plusieurs éléments de fondation pour créer un système hybride. De cette manière, il est possible de développer un système de fondation qui est plus efficace pour la combinaison de charges verticales et latérales associées aux éoliennes, tout en maintenant l'efficacité et la simplicité de la conception. Des études antérieures ont rapporté les résultats d'essais simples de gravité du système hybride où les avantages de l'ajout du pied à la pile sont illustrés. Cet article présente des résultats expérimentaux sur la performance des jupes et non jupée semelles monopile. Une approche de conception simplifiée basée sur l'analyse pile latéral classique est présentée.

KEYWORDS: Hybrid monopile footing, offshore piles, laterally loaded piles, wind turbine foundations

1 INTRODUCTION

Due to the needs of on-going developments in the oil and energy sector, the design of offshore foundations is constantly evolving. In the hydrocarbon extraction sector, exploration and development is moving in to ever deeper water resulting in ever more challenging geotechnical conditions. Similarly the expansion of the offshore wind sector involves the development of deepwater sites, together with requirements for heavier high capacity turbines. Conventional offshore foundations are not always economical or practical for this new generation of turbines, and there remains a requirement to develop foundation solutions which can better satisfy future developments in the offshore wind sector.

The foundations of a typical offshore wind turbine are subjected to combined loading conditions consisting of the self-weight of the structure (V), relatively high horizontal loads (H) and large bending moments (M). The preferred foundation system to date has been the monopile, which has the advantage that it can be employed in a variety of different soil conditions. However, a disadvantage in the use of monopiles in deep water sites is that the system can be overly compliant. For sites with intermediate water depths, it may be possible to stiffen the lateral response of the monopile at the mudline.

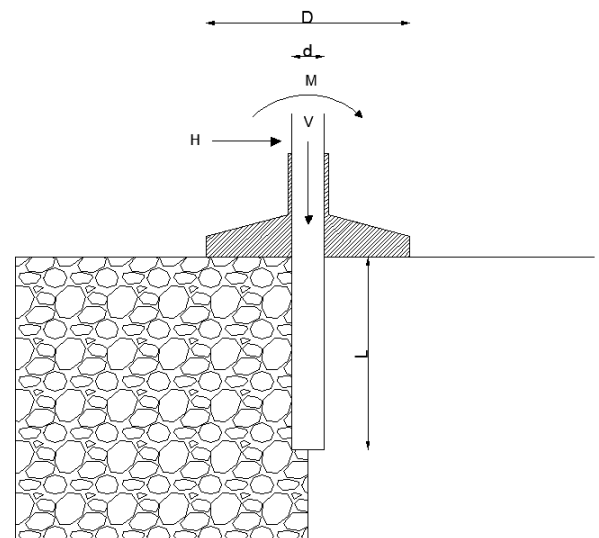


Figure 1. Schematic illustration of the prototype hybrid system

One such approach to increase the lateral resistance of a monopile is the 'hybrid' monopile-footing system. As schematically represented in Figure 1, this foundation system

comprises of a circular footing attached to the monopile at the mudline. A 2-D analogy of this system is that of a retaining wall with a stabilising base (Powrie and Daly, 2007). The role of the footing is to provide a degree of rotational restraint at the pile head, leading to an improvement in the lateral resistance of the pile. It has also been shown that the use of a relatively thick pile cap leads to an increase in the lateral resistance through the development of passive soil wedges (Mokwa, 1999), in a similar way to the behaviour of skirted foundations (Bransby and Randolph, 1998).

Analysis of the hybrid system would involve both lateral pile analysis and bearing capacity analysis. The lateral response of piles is well reported in the literature and various methods of analysis have been proposed by numerous researchers, such as Matlock and Reese (1960), Broms (1954), Poulos (1971), Reese *et al.* (1974), Randolph (1981), Duncan *et al.* (1994) and Zhang *et al.* (2005). Where the plate diameter is relatively small, the system is similar to a single capped pile, for which methods have been developed for analysing the influence of the pile and pile cap under axial loading (Poulos and Randolph, 1983), and the effect of the pile cap on the lateral performance of single piles has also been investigated by others (Kim *et al.*, 1979), (Mokwa and Duncan, 2001: 2003), (Maharaj, 2003).

The bearing capacity problem has also been investigated under different loading conditions relevant to offshore foundations, see for example references Houslyby and Puzrin (1999), and Gourvenec and Randolph (2003).

2. EXPERIMENTAL INVESTIGATIONS

The potential performance of the hybrid system was investigated in single gravity studies (Stone *et al.* (2007)) and is illustrated in Figure 2. These studies suggested that the additional rotation restraint provided by the footing can result in a stiffer lateral response of the pile and greater ultimate lateral load. The degree of restraint at the pile head was dependent on the size of the footing, the initial contact between the soil and the footing and the stiffness of the soil beneath the footing. Observations of heaved and displaced soil in front of the edge of the footing also suggested that a degree of passive soil resistance is likely to be generated under the lateral movement and rotation of the footing.

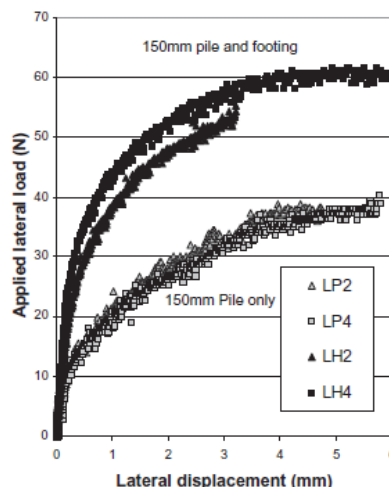


Figure 2. Lateral load response of the hybrid system (after Stone *et al.* 2007)

Arshi (2011), and Arshi and Stone (2012) reported the results of a comprehensive series of single gravity testes carried out on the foundation system where the elements affecting the overall performance of the foundation system was investigated

in depth. It was reported that the size for the footing has a direct effect on the overall lateral load bearing capacity of the foundation system. Furthermore it was reported that the ratio between the vertical and horizontal load has a significant effect on the lateral performance of the foundation system where larger vertical loads tend to improve the lateral load bearing capacity of the hybrid system. The connection between the footing and the pile was also investigated where it was suggested that the hybrid foundation system tends to be more effective if vertical movements are allowed at the pile-footing connection. This movement allows the footing to act independently from the pile where the positive contact between the footing and the soil underneath is solely controlled by the vertical load acting on the footing.

Table 1. Notations for skirted hybrid foundations system

ID	Footing size (mm)	Skirt length (mm)	Dead load (N)	Footing to pile connection
P.W0	-	-	0	-
P.F80.W1.FR	80	-	10	Slipping
P.F80.S1.W1.FR	80	-	10	Slipping
P.F80.S2.W1.FR	80	-	10	Slipping
P.F80.S3.W1.FR	80	-	10	Slipping

More recent single gravity tests are presented in Figure 3 where skirts with different lengths have been added to the footing. The tests were conducted in sand and the results indicate that the presence of the skirts has a relatively significant contribution on the lateral load capacity of the system. The results show that adding the skirts to the footing and increasing the skirt length tends to increase the lateral load bearing capacity of the foundation system by about 50% in comparison to a non-skirted hybrid system. It is also apparent that footings with very short skirts do not tend to show any 'apparent' additional advantage to that without the skirt. This could be due to the fact that the stresses around the skirt induced by the soil are very small at 1g. Further studies in the centrifuge are in the taking place to investigate the effect of the skirts and the results will be reported soon.

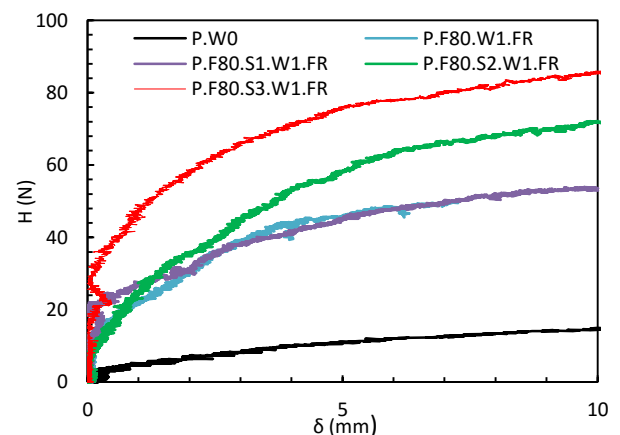


Figure 3. Load vs. deflection plot for the hybrid system with skirts

Stone *et al.* (2011) reported the results of a series of centrifuge tests in sand. The results of the combined vertical and lateral loading tests are best represented through plots of lateral load versus lateral displacement. Figure 4 shows a plot of the lateral load versus lateral displacement for the monopile-footing (HL 1) and single pile (PL 1) with a vertical load of 600N at 50 g. It is apparent from this plot that the initial lateral stiffness of the monopile-footing and pile are similar for the first 1–1.5mm of lateral displacement. However the monopile-

footing continues to exhibit a stiffer response than the single pile as the lateral displacement increases. Further analyses of these data provided information on the redistribution of bending moment in the pile due to the plate.

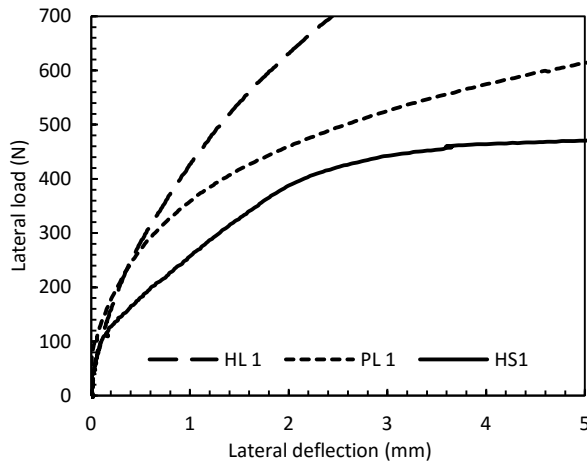


Figure 4. Load deflection graph for centrifuge tests carried out on the hybrid system (after Stone *et al.* 2011)

In Figure 5, the bold lines represent the bending moments at 5% and 20% of the maximum deflection for the pile only case and the dashed lines show the behaviour of the hybrid system. The results show that adding the footing to the pile reduces the bending moment at any given deflection, and as a result increases the moment capacity of the system at any given applied lateral load. The results indicate about 25% improvement in the bending moment for at both deflections.

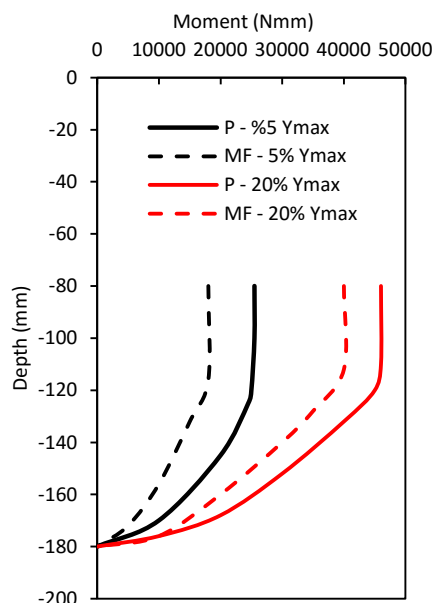


Figure 5. Bending moment distribution along the pile length for the hybrid system

3. ANALYSIS

Whilst some advanced numerical modelling of monopiled footings has been undertaken (El-Marassi *et al.* 2008; Stone *et al.* 2010; Arshi *et al.* 2011; Arshi and Stone 2012), the method presented here utilises conventional lateral pile analysis methodology where the hybrid system is idealised to a lateral pile with a resisting moment applied at the mudline. The

resisting moment capacity provided by the footings were estimated analytically using conventional bearing capacity theory and applied at the mudline acting in the opposite direction to the loading. This approach only considers the ultimate condition of the system and does not allow the moment developed by the footing to be generated as a function of the footing rotation.

The results generated by this approach are illustrated in Figure 6 where it is shown how different pile to footing diameter increases the moment capacity of the piles, where this variation lies between a fully free and a fully fixed pile.

The dashed lines in Figure 6 show the ultimate moment capacities of the hybrid system. Although this method successfully leads to obtaining the ultimate load bearing capacity of the hybrid system (D.O.R 75%, 50% and 25% showing the ultimate capacity of the system when 75%, 50% and 25% of the ultimate moment at pile head is applied to the free headed pile) of the system are shown as a benchmark for comparing how different pile to footing diameters relate to the fully fixed moment. As apparent in Figure 6, increasing the size of the footing tends to increase the lateral load bearing capacity. As the footing size increases, it gets close to the fully fixed head condition. This also indicates that there for a given pile diameter and length, there ought to be a footing size after which increasing the footing size further will not enhance the lateral load bearing capacity of the foundation system.

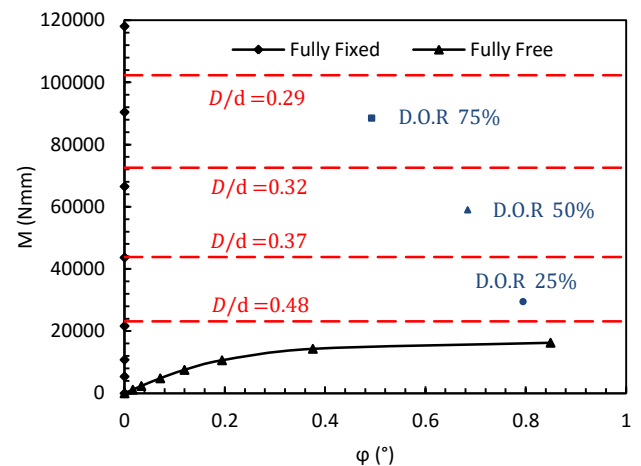


Figure 6. Moment vs. rotation plot for the hybrid system with different pile to footing ratios

In addition to this, design charts have been developed which relate the pile embedment length to pile and footing diameters. Numerous design charts have been developed covering a wide range of pile diameters, pile lengths, footing diameters and normalized moment capacities an example of which is shown in Figure 8 where the L/D ratios vary from 1 to 10 and the footing to pile diameter ratios varies from 0 to 1. The moment capacity of the hybrid system has been normalised and is shown against footing to pile diameter ratio. The lines in between represent different pile embedment depth where for a given moment capacity the designer could utilise this graph to choose the appropriate pile length as well as pile and footing diameters. It is also notable that for any given value of normalized moment capacity the designer has the option of choosing a short pile relatively large footing diameter, or long pile with relatively small footing diameter. The flexibility in this design approach is beneficial in particular designing the hybrid system in difficult soil conditions.

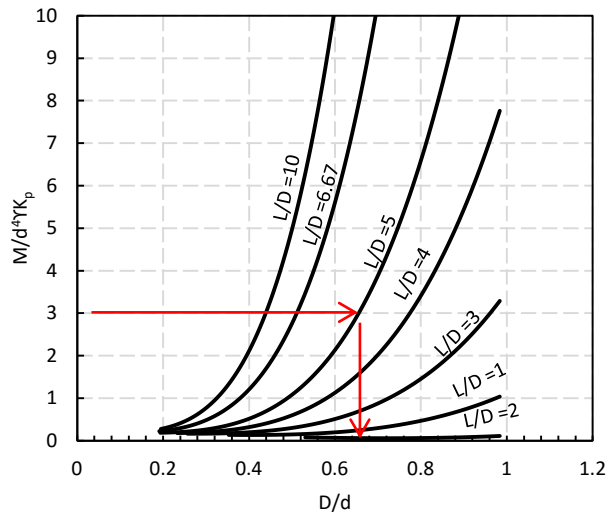


Figure 7. Example of a design chart for the hybrid system developed using analytical and numerical methods

4. DISCUSSION & CONCLUSION

It is apparent that the ultimate lateral response of a single monopile foundation can be enhanced by the presence of a footing resulting in a greater ultimate lateral capacity. This improvement was observed at both load versus deflection as well as the bending moment versus depth plots. Whilst the effect on the initial lateral stiffness may not be significant, the lateral stiffness beyond this initial movement was significantly enhanced through the presence of the footing.

The effect of adding skirts to the hybrid system has been shown to further increase the lateral performance of the hybrid system, and centrifuge tests are planned to investigate the skirted system in more detail.

A simple analytical approach using conventional lateral pile analysis methods is presented from which preliminary design charts can be generated. This approach can be developed to generate realistic design charts where the lateral capacity of the hybrid system is related to the development of bearing capacity coupled to the lateral resistance of the pile shaft.

5. REFERENCES

- Arshi HS. (2011). Structural behavior and performance of skirted hybrid monopile-footing foundations for offshore oil and gas facilities. *Proceedings of the Institution of Structural Engineers: Young Researchers Conference '11*. London: IStructE Publications, 8.
- Arshi HS, Stone KJL and Newson TA. (2011). Numerical modelling on the degree of rigidity at pile head for offshore monopile-footing foundation systems. *9th British Geotechnical Association Annual Conference, London*.
- Arshi HS and Stone KJL. (2011). An investigation of a rock socketed pile with an integral bearing plate founded over weak rock. *Proceedings of the 15th European Conference of Soil Mechanics and Geotechnical Engineering*. Amsterdam: Ios Pr Inc, 705 – 711.
- Arshi HS. (2012). A new design solution for increasing the lateral resistance of offshore pile foundations for wind turbines located in deep-water. *Proceedings of the Institution of Structural Engineers: Young Researchers Conference '12*. London: IStructE Publications, 10.
- Arshi HS and Stone KJL. (2012). Lateral resistance of hybrid monopile-footing foundations in cohesionless soils for offshore wind turbines. *Proceedings of the 7th International Conference on*

- Offshore Site Investigation and Geotechnics*. London: Society for Underwater Technology, 519 – 526.
- Bransby MF and Randolph MF. (1998). Combined loading of skirted foundations. *Géotechnique*. 48(5), 637–655.
- Broms BB. (1964). Lateral resistance of piles in cohesionless soils. *ASCE Journal of the Soil Mechanics and Foundation Division*. 90(SM3), 123-156.
- Duncan JM, Evans LT and Ooi PS. (1994). Lateral load analysis of single piles and drilled shafts. *ASCE Journal of Geotechnical Engineering*. 120(6), 1018-1033.
- El-Marassi M, Newson T, El-Naggar H and Stone KJL. (2008). Numerical modelling of the performance of a hybrid monopiled-footing foundation. *Proceedings of the 61st Canadian Geotechnical Conference, GeoEdmonton 2008*. Edmonton, (Paper No. 480), 97 – 104.
- Gourvenec S and Randolph M. (2003). Effect of strength non-homogeneity on the shape of failure envelopes for combined loading of strip and circular foundations on clay. *Géotechnique*. 53(6), 575–586.
- Houlsby GT and Puzrin AM. (1999). The bearing capacity of a strip footing on clay under combined loading. *Proc. R. Soc. London Ser. A*. 455, 893–916.
- Kim JB, Singh LP and Brungraber RJ. (1979). Pile cap soil interaction from full scale lateral load tests. *ASCE Journal of Geotechnical Engineering*. 105(5), 643-653.
- Maharaj DK. (2003). Load-deflection response of laterally loaded single pile by nonlinear finite element analysis. *EJEG*.
- Matlock H and Reese LC. (1960). Generalized solutions for laterally loaded piles. *ASCE Journal of Soil Mechanics and Foundations Division*. 86(SM5), 63-91.
- Mokwa RL. (1999). Investigation of the Resistance of Pile Caps to Lateral Loading. *Ph.D Thesis*. Virginia Polytechnic Institute, Blacksburg, Virginia.
- Mokwa RL and Duncan JM. (2001). Experimental evaluation of lateral-load resistance of pile caps. *ASCE Journal of Geotechnical and Geoenvironmental Engineering*. 127(2), 185 - 192.
- Mokwa RL and Duncan JM. (2003). Rotational restraint of pile caps during lateral loading. *ASCE Journal of Geotechnical and Geoenvironmental Engineering*. 129(9), 829 - 837.
- Poulos HG. (1971). Behaviour of laterally loaded piles: Part I-single piles. *ASCE Journal of the Soil Mechanics and Foundations Division*. 97(SM5), 711-731.
- Poulos HG and Randolph MF. (1983). Pile group analysis: a study of two methods. *ASCE Journal of Geotechnical Engineering*. 109(3), 355-372.
- Powrie W, and Daly MP. (2007). Centrifuge modelling of embedded retaining wall with stabilising bases. *Geotechnique*. 57(6), 485-497.
- Randolph MF. (1981). The response of flexible piles to lateral loading. *Géotechnique*. 31(2), 247-259.
- Reese LC, Cox WR and Koop FD. (1974). Analysis of laterally loaded piles in sand. *Offshore Technology Conference*. Vol. II (Paper No. 2080), 473-484.
- Stone KJL, Newson TA and Sandon J. (2007). An investigation of the performance of a 'hybrid' monopile-footing foundation for offshore structures. *Proceedings of 6th International on Offshore Site Investigation and Geotechnics*. London: SUT, 391-396.
- Stone KJL, Newson TA and El Marassi, M. (2010). An investigation of a monopiled-footing foundation. *International Conference on Physical Modelling in Geotechnics, ICPMG2010*. Rotterdam: Balkema, 829-833.
- Stone KJL, Newson TA, El Marassi M, El Naggar H, Taylor RN, and Goodey RA (2011). An investigation of the use of bearing plate to enhance the bearing capacity of monopile foundations. *International Conference on Frontiers in Offshore Geotechnics II - ISFOG*. London: Taylor and Francis Group, 623-628.
- Zhang L, Silva F and Grismala R. (2005) Ultimate lateral resistance to piles in cohesionless soils. *Journal of Geotechnical and Geoenvironmental Engineering*. Vol. 131(1), 78–83.

Laterally loaded piles with integral bearing plate for offshore structures

Pieux chargés latéralement avec plaque de roulement pour les structures offshore

H.S. Arshi^{*1}, K.J.L. Stone¹, F.K. Gunzel¹ and T.A. Newson²

¹ *University of Brighton, Brighton, UK*

² *University of Western Ontario, London, Canada*

** Corresponding Author*

ABSTRACT In the case of laterally loaded piles offshore, the addition of a circular bearing plate to the monopile at mudline, known as the hybrid monopile-footing foundation system, has proven to increase the lateral load bearing capacity of the foundation system significantly. Previously this was studied in single gravity conditions and some preliminary tests were carried out in the centrifuge. This paper extends this investigation by studying the performance of the foundation system at 50g and reports how different foundation and geometric components affect this increase.

RÉSUMÉ Dans le cas des pieux chargés latéralement au large des côtes, l'ajout d'une plaque d'appui circulaire pour la monopile au fond de la mer, appelé système de base monopile - footing hybride, s'est révélé augmenter la capacité latérale d'appui de charge du système de base. Précédemment a été étudiée dans cette unique condition de gravité et de quelques tests préliminaires ont été effectués dans la centrifugeuse. Cet article étend cette enquête par l'étude de la performance du système de fondation à 50g de rapports et comment les différents fondations et effet géométrique de cette augmentation.

1 INTRODUCTION

Offshore foundations are constantly evolving in terms of capability and design which is due to the needs of on-going developments in the oil and energy sector. In the oil and gas sector, the geotechnical design has become ever more challenging which is mainly to do with exploration and development that is moving in to ever deeper water. In the offshore wind sector the development has moved into deep-water sites ever reached, together with requirements for heavier high capacity turbines. A good example of this is the round 2 and 3 of the UK offshore wind turbine program. The work done in the offshore wind sector in the UK has shown that the conventional off-

shore foundations are not always economical or practical for this new generation of turbines, and there remains a requirement to develop foundation solutions which can better satisfy future developments in the offshore wind sector.

For the particular case of typical offshore wind turbines, the foundation(s) are subjected to combined loading conditions consisting of the self-weight of the structure (V), relatively high horizontal loads (H) and resultant large bending moments (M). The preferred foundation system to date has been the monopile, which has the advantage that it can be employed in a variety of different soil conditions. A disadvantage in the use of monopiles in deep water sites is that the system can be overly compliant, mainly due

to their required diameter and penetration depth. However, it may be possible to stiffen the lateral response of the monopile at the mudline.

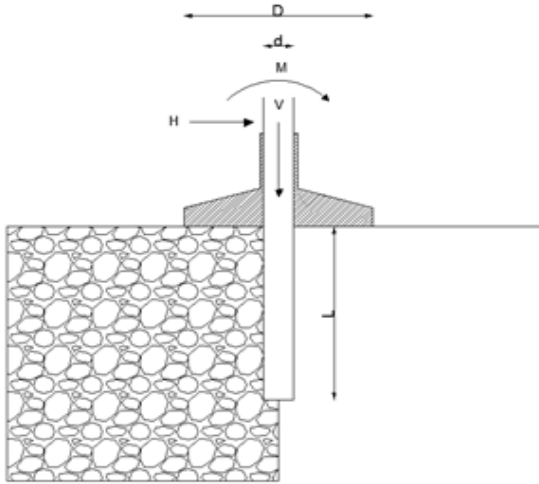


Figure 1. Illustration of the hybrid system

One approach for increase the lateral resistance of a monopile is the ‘hybrid’ monopile-footing system. As schematically represented in Figure 1, this foundation system comprises of a circular footing attached to the monopile at the mudline. A 2D analogy of this system is that of a retaining wall with a stabilising base (Powrie and Daly, 2007). The role of the footing is to provide a degree of rotational restraint at the pile head, leading to an improvement in the lateral resistance of the pile. It has also been shown that the use of a relatively thick pile cap leads to an increase in the lateral resistance through the development of passive soil wedges (Mokwa, 1999), in a similar way to the behaviour of skirted foundations (Bransby and Randolph, 1998).

Both lateral pile analysis and bearing capacity analysis is required for analyzing the hybrid system as an individual foundation unit. The lateral response of piles is well reported in the literature and various methods of analysis have been proposed by numerous researchers, such as Matlock and Reese (1960), Broms (1954), Poulos (1971), Reese *et al.* (1974), Randolph (1981), Duncan *et al.* (1994) and Zhang *et al.* (2005). Where the plate diameter is relatively small, the system is similar to a single capped pile,

for which methods have been developed for analysing the influence of the pile and pile cap under axial loading (Poulos and Randolph, 1983), and the effect of the pile cap on the lateral performance of single piles has also been investigated by others (Kim *et al.*, 1979), (Mokwa and Duncan, 2001: 2003), (Maharaj, 2003).

Also, the bearing capacity problem has been thoroughly investigated under different loading conditions relevant to offshore foundations, see for example references Hously and Puzrin (1999), and Gourvenec and Randolph (2003).

2 RECENT RESEARCH

A single gravity study carried out on the hybrid system (Stone *et al.*, 2007) suggested that the additional rotation restraint provided by the footing can result in a stiffer lateral response of the pile and greater ultimate lateral load. The degree of restraint at the pile head was dependent on the size of the footing, the initial contact between the soil and the footing and the stiffness of the soil beneath the footing. Observations of heaved and displaced soil in front of the edge of the footing also suggested that a degree of passive soil resistance is likely to be generated under the lateral movement and rotation of the footing.

A comprehensive series of single gravity testes carried out on the hybrid system where the elements affecting the overall performance of the foundation system was investigated in depth was reported by Arshi (2011), and Arshi and Stone (2011, 2012a, 2012b). It was reported that the size for the footing has a direct effect on the overall lateral load bearing capacity of the foundation system. Furthermore it was reported that the ratio between the vertical and horizontal load has a significant effect on the lateral performance of the foundation system where larger vertical loads tend to improve the lateral load bearing capacity of the hybrid system. The connection between the footing and the pile was also investigated where it was suggested that the hybrid foundation system tends to be more effective if vertical movements are allowed at the pile-footing connection. This movement allows the footing to act independently from the pile where the positive contact between the footing and the soil underneath is solely controlled by the vertical load acting on the footing.

The results of a series of more comprehensive single gravity tests together with preliminary centrifuge tests were carried out and the results were reported by Arshi *et al.* (2013). In the case of single gravity tests, skirts with different lengths were added to the footing. The tests were conducted in sand and the results indicated that the presence of the skirts has a relatively significant contribution on the lateral load capacity of the system. The results show that adding the skirts to the footing and increasing the skirt length tends to increase the lateral load bearing capacity of the foundation system by about 50% in comparison to a non-skirted hybrid system. It is also apparent that footings with very short skirts do not tend to show any ‘apparent’ additional advantage to that without the skirt. Furthermore, bending moment versus depth plots were extracted from instrumented piles tested in centrifuge at 50g, for piles with and without the footings (see Figure 2) and indicated the additional capacity enhanced by the addition of the footing.

3 CENTRIFUGE TESTS & ANALYSIS

A series of preliminary centrifuge tests were carried out at the Centre for Geotechnical Modelling, City University, London. The model foundation (see Figure 2) was fabricated from a 150mm long and 19mm diameter hollow steel tube with 0.5mm wall thickness together with 4 strain gauges at equal intervals along the pile. The aluminum bearing plate used was 100mm in diameter and 5mm thick with a clamping arrangement for adjusting the locations of the plate.



Figure 2. Model hybrid monopile foundation

The centrifuge tests were carried out at 50g which represents the prototype foundation dimensions of 0.95m diameter 9m long pile with 5m diameter bearing plate. The lateral load versus lateral deflection tests together with bending moment versus depth profiles are shown in Figures 3 and 4 respectively.

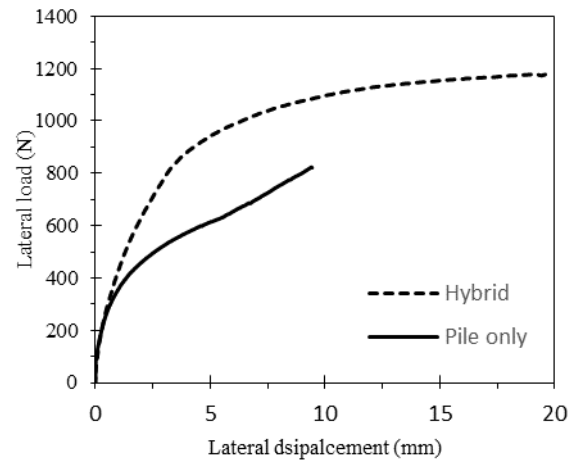


Figure 3. Lateral load vs. lateral displacement test at 50g

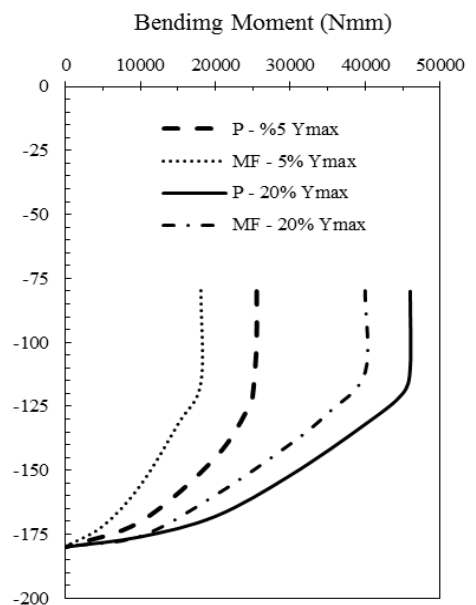


Figure 4. Bending moment versus depth profiles at 50g

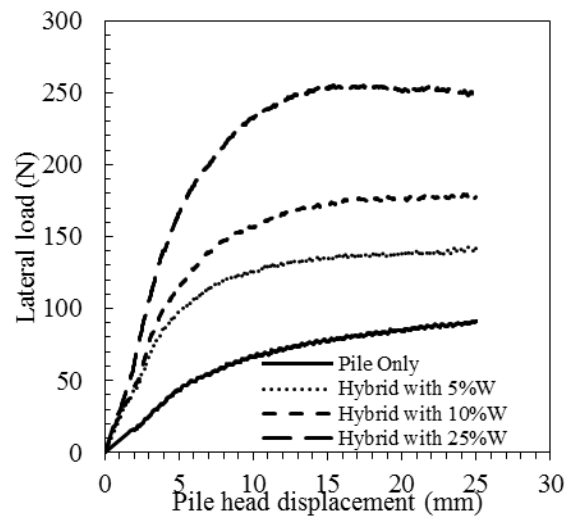
Furthermore, a comprehensive series of detailed centrifuge tests were carried at the University of Brighton, Brighton Geotechnical Centrifuge. The results of a selected series of tests are represented in this paper. The soil used for the tests was a rounded to sub-rounded fine grained, uniformly graded, quartz sand with an average particle size of 0.25mm (Fraction D from David Ball Ltd.). The maximum and minimum void ratios were determined to be 1.06 and 0.61 respectively. These correspond to dry unit weights of 12.6 and 16.5 kN/m³. The critical state friction angle, determined from direct shear testing, was 32 degrees. The sample were prepared by dry pluviation of sand into a 320mm diameter 180mm deep circular tub, and the tub was then placed mounted into a square strongbox.

The model foundation system was fabricated from a 10mm diameter thin-walled, open-ended steel tube ($t=0.5$ mm). The bearing plate was 80mm diameter and formed from a 5mm thick aluminium plate with a clamping arrangement allowing the location of the plate to be varied in relation to the pile, i.e. the length of pile protruding below the plate can be adjusted.

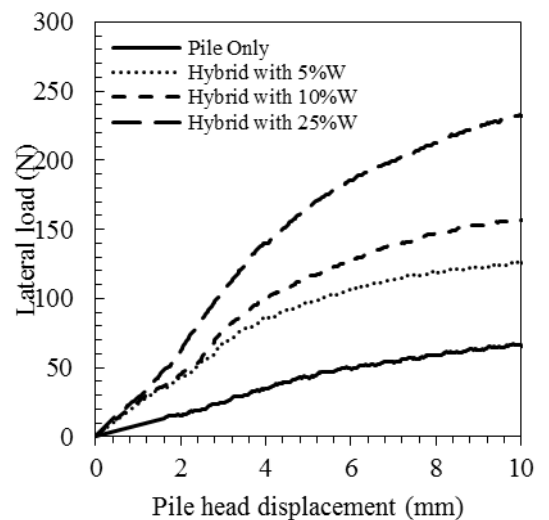
The samples were prepared by air pulvation of sand with a unit weight of 16.5 kN/m³, void ratio of 0.89 and a relative density of 94%. On completion of pouring the sand bed, the strongbox was mounted on to the centrifuge platform.

The installation method consisted of pushing the pile by hand to about 40% of its desired penetration depth and then final driving of the pile by light tapping with a hammer to the desired depth of installation. The footing was then slid along the pile down to the soil surface, care was taken to ensure that the bearing plate was in firm contact with the soil surface on completion of installation. For tests when only the vertical capacity of the hybrid system was required, the bearing plate was fixed to the pile shaft some 5-10mm clear of the soil surface.

Vertical load of the model foundation was provided via placing weights right on top of the footing. Lateral loading was provided using a steel wire looped around the pile at 80mm from the mudline in order to create rather high bending moments, and was connected to a load actuator. A linear variable differential transformer (LVDT) was used to record the lateral displacement at the pile head. All the centrifuge tests were conducted at 50 gravities.



(a)



(b)

Figure 5. Load vs. deflection test results at 50g (a) ultimate load (b) working load

The results of the centrifuge tests showing the lateral load deflection response of the pile against hybrid system are presented in Figure 4. Here all tests are carried out with a constant pile length (80mm) and the results here show the obvious advantage of the addition of the plate. It is worthwhile noting that the lateral response of the single piles is almost line-

arly increasing with deflection, and deciding the value of the ultimate load is often down to interpretation and deflection based in practice. However, the addition of the footing to the pile converts this behaviour at higher loads to the way eccentrically loaded circular footings response, hence choosing the value of the ultimate load more obvious.

Comparing the results of the preliminary tests (Figure 3) with main tests (Figure 5) shows a difference in the capacity of improvement where the improvements in the main tests are significantly higher. This difference is directly related to the magnitude of bearing or vertical load provided where this variable is known to be controlling the provision of positive contact between the plate and the soil.

Also, the ultimate bearing capacity of the footing was first estimated experimentally, then 5%, 10% and 25% of that was applied as a pre loading to the footing prior to the application the lateral load. The benefits of the perennial presence as well as the magnitude of pre loading is well illustrated in Figures 5(a) and (b) where the ultimate lateral loads increase by 136%, 175% and 252% and under working loads this increase is 92%, 140% and 357%, respectively for 5%, 10% and 25% bearing loads. This is indicative of the importance of the presence and magnitude of bearing load

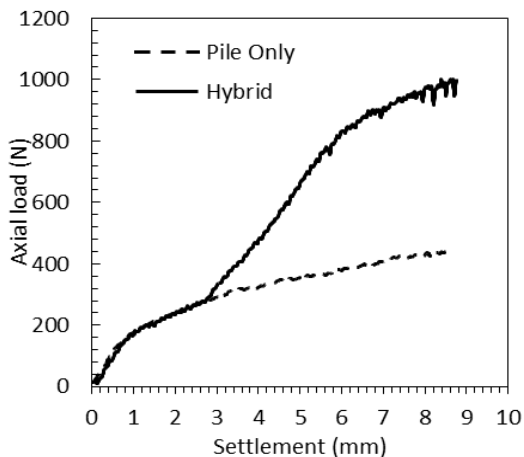


Figure 6. Axial load tests at 50g

The bending moment profiles presented at 5% and 25% of the maximum deflection is shown in Figure 4

which shown another advantage of the presence of the footing where the addition of the footing tends to increase the bending capacity for the foundation system by 10 kNm. The magnitude of this increase was found to be directly proportional to the size of the footing.

Another significant advantage of the hybrid system, as apparent from Figures 5(a) and (b), is the increase in stiffness. This becomes particularly important under working load conditions where the stiffness increases by 100% when the footing is added to the pile. The results show that this increase is independent of the magnitude of bearing load under working load condition (in particular 10% pile diameter deflection) and minimum bearing load is required in order to maintain this stiffness.

In order to examine the relationship between load-deflection stiffness and the contribution that the addition of footing makes in terms of stiffness, the hybrid system was tested under purely axial load and was compared against the monopile. For the case of the hybrid test, the footing was set 5mm from mudline in order to see how the gradient of the settlement graph changes when the footing starts to have contact with soil and the results are presented in Figure 4. This gradient is almost identical up until 0.5mm settlement for both the pile only and hybrid however, after about 1mm the advantage of the addition of plate is apparent. This suggests that stiffness here is mainly dominated by the footing component.

4 CONCLUSION

The benefits of adding a circular bearing plate or a footing to a monopile for offshore loading conditions was illustrated. This was done in a series of centrifuge tests and the advantages was shown in terms of load deflection and depth bending moment profiles. A number of variables were examined and their importance and the role they play were highlighted in this paper.

It is notable that this paper solely focuses on the results of a selected number of centrifuge tests. There are two very detailed papers in preparation and will be published in relevant journals soon which will present design methods and charts for the hybrid monopile-footing foundation system.

REFERENCES

- Arshi HS. (2011). Structural behavior and performance of skirted hybrid monopile-footing foundations for offshore oil and gas facilities. *Proceedings of the Institution of Structural Engineers: Young Researchers Conference '11*. London: IStructE Publications, 8.
- Arshi HS and Stone KJL. (2011). An investigation of a rock socketed pile with an integral bearing plate founded over weak rock. *Proceedings of the 15th European Conference of Soil Mechanics and Geotechnical Engineering*. Amsterdam: Ios Pr Inc, 705 – 711. ISBN 1607508001
- Arshi HS and Stone KJL. (2012). Lateral resistance of hybrid monopile-footing foundations in cohesionless soils for offshore wind turbines. *Proceedings of the 7th International Conference on Offshore Site Investigation and Geotechnics*. London: Society for Underwater Technology, 519 – 526. ISBN 0906940532
- Arshi HS and Stone KJL. (2012) Increasing the lateral resistance of offshore monopole foundations: hybrid monopole-footing foundation system. In: *Proceedings of the 3rd International Conference on Engineering, project and production management, Brighton, September 10th – 11th 2012*. Brighton: University of Brighton, pp. 217-226. ISBN 9781905593866
- Arshi HS, Stone KJL, Vaziri M, Newson T, El-Marasi M, Taylor RN and Goody R. (2013). Physical model testing of hybrid monopile-footing foundation system in sand for offshore structures. In: *Proceeding of the 19th International Conference on Soil Mechanics and Geotechnical Engineering*, Paris, Sep 2nd 2013. Pp. 2307-2310. ISBN 9782859784744
- Bransby MF and Randolph MF. (1998). Combined loading of skirted foundations. *Géotechnique*. 48(5), 637–655.
- Broms BB. (1964). Lateral resistance of piles in cohesionless soils. *ASCE Journal of the Soil Mechanics and Foundation Division*. 90(SM3), 123-156.
- Duncan JM, Evans LT and Ooi PS. (1994). Lateral load analysis of single piles and drilled shafts. *ASCE Journal of Geotechnical Engineering*. 120(6), 1018-1033.
- El-Marassi M, Newson T, El-Naggar H and Stone KJL. (2008). Numerical modelling of the performance of a hybrid monopile-footing foundation. *Proceedings of the 61st Canadian Geotechnical Conference, GeoEdmonton 2008*. Edmonton, (Paper No. 480), 97 – 104.
- Gourvenec S and Randolph M. (2003). Effect of strength non-homogeneity on the shape of failure envelopes for combined loading of strip and circular foundations on clay. *Géotechnique*. 53(6), 575–586.
- Houlsby GT and Puzrin AM. (1999). The bearing capacity of a strip footing on clay under combined loading. *Proc. R. Soc. London Ser. A*. 455, 893–916.
- Jardine RJ, Potts DM and Fourie AB. (1986). Studies of the influence of non-linear stress-strain characteristics in soil-structure interaction. *Geotechnique*. 36(3). 377-396.
- Kim JB, Singh LP and Brungraber RJ. (1979). Pile cap soil interaction from full scale lateral load tests. *ASCE Journal of Geotechnical Engineering*. 105(5), 643-653.
- Maharaj DK. (2003). Load-deflection response of laterally loaded single pile by nonlinear finite element analysis. *EJEG*.
- Matlock H and Reese LC. (1960). Generalized solutions for laterally loaded piles. *ASCE Journal of Soil Mechanics and Foundations Division*. 86(SM5), 63-91.
- Mokwa RL. (1999). Investigation of the Resistance of Pile Caps to Lateral Loading. *Ph.D Thesis*. Virginia Polytechnic Institute, Blacksburg, Virginia.
- Mokwa RL and Duncan JM. (2001). Experimental evaluation of lateral-load resistance of pile caps. *ASCE Journal of Geotechnical and Geoenvironmental Engineering*. 127(2), 185 - 192.
- Mokwa RL and Duncan JM. (2003). Rotational restraint of pile caps during lateral loading. *ASCE Journal of Geotechnical and Geoenvironmental Engineering*. 129(9), 829 - 837. London, Thomas Telford.
- Poulos HG. (1971). Behaviour of laterally loaded piles: Part I-single piles. *ASCE Journal of the Soil Mechanics and Foundations Division*. 97(SM5), 711-731.
- Poulos HG and Randolph MF. (1983). Pile group analysis: a study of two methods. *ASCE Journal of Geotechnical Engineering*. 109(3), 355-372.
- Powrie W, and Daly MP. (2007). Centrifuge modelling of embedded retaining wall with stabilising bases. *Geotechnique*. 57(6), 485-497.
- Randolph MF. (1981). The response of flexible piles to lateral loading. *Géotechnique*. 31(2), 247-259.
- Reese LC, Cox WR and Koop FD. (1974). Analysis of laterally loaded piles in sand. *Offshore Technology Conference*. Vol. II (Paper No. 2080), 473-484.
- Stone KJL, Newson TA and Sandon J. (2007). An investigation of the performance of a ‘hybrid’ monopile-footing foundation for offshore structures. *Proceedings of 6th International on Offshore Site Investigation and Geotechnics*. London: SUT, 391-396.
- Stone KJL, Newson TA and El Marassi, M. (2010). An investigation of a monopiled-footing foundation. *International Conference on Physical Modelling in Geotechnics, ICPMG2010*. Rotterdam: Balkema, 829-833.
- Stone KJL, Newson TA, El Marassi M, El Naggar H, Taylor RN, and Goodey RA (2011). An investigation of the use of bearing plate to enhance the bearing capacity of monopile foundations. *International Conference on Frontiers in Offshore Geotechnics II - ISFOG*. London: Taylor and Francis Group, 623-628.
- Zhang L, Silva F and Grismala R. (2005) Ultimate lateral resistance to piles in cohesionless soils. *Journal of Geotechnical and Geoenvironmental Engineering*. Vol. 131(1), 78–83.

Improving the lateral resistance of offshore pile foundations for deepwater application

H.S. Arshi & K.J.L. Stone

University of Brighton, Brighton, UK

ABSTRACT: The monopile has proven to be the preferred foundation solution for offshore wind turbines in shallow water and this is mainly due to its simplicity of design, fabrication and installation which leads to it being an economically sound foundation solution. The rounds 2 and 3 of the UK offshore wind farms are located at ever deeper water, some at the deepest waters wind turbines have ever been set to be installed. During the past 5 years several foundation solutions have been proposed for deepwater application and they mainly comprise of a number of foundation elements such as tripod system and the hybrid monopile-footing foundation system. The hybrid system, which comprises of a monopile and a bearing plate attached to the pile at mudline, has proven to significantly enhance the lateral capacity of the monopile. This paper reports the results of a series of centrifuge tests (to recreate prototype stress and load conditions) carried out to investigate the behavior of the hybrid system in Sand. Furthermore, the results of a series of 3D finite element analyses (using ICFEP) have been reported.

1 INTRODUCTION

The design of offshore foundations is constantly evolving which is due to the needs of on-going developments in the oil and energy sector. In the hydrocarbon extraction sector, the geotechnical design of foundations are ever more challenging, which is mainly to do with exploration and development that is moving into ever deeper water. Similarly, in the offshore wind sector the requirement for having heavier high capacity turbines has resulted in the development of sites located in deepwater. A good example of this is the round 2 and 3 of the UK offshore wind turbine program. The work done in the offshore wind sector in the UK has shown that the conventional offshore foundations are not always economical or practical for this new generation of turbines, and there remains a requirement to develop foundation solutions which can better satisfy future developments in the offshore wind sector.

For the particular case of typical offshore wind turbines, foundation(s) are subjected to combined loading conditions consisting of the self-weight of the structure (V), relatively high horizontal loads (H) and resultant large bending moments (M). The preferred foundation system to date has been the monopile, which has the advantage that it can be employed in a variety of different soil conditions. A

disadvantage in the use of monopiles in deepwater sites is that the system can be overly compliant, mainly due to their required diameter and penetration depth. However, it may be possible to stiffen the lateral response of the monopile at the mudline.

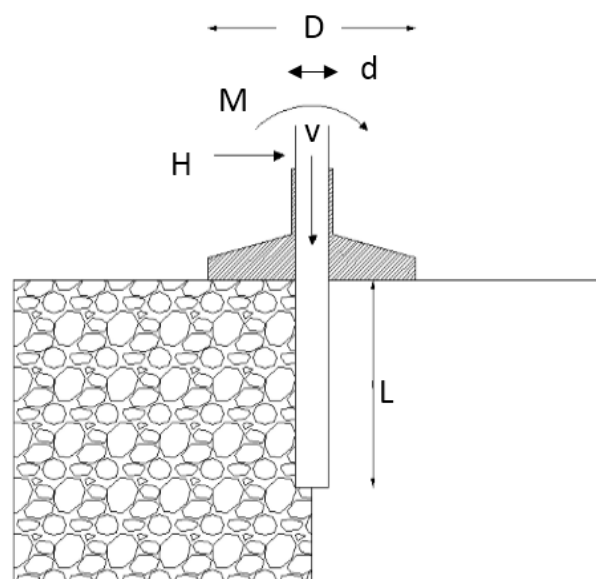


Figure 1. Schematic illustration of the foundation system

One design that helps increase the lateral resistance of a monopile is the use of 'hybrid' monopile-footing foundation system. As schematically represented in Figure 1, this foundation system comprises of a circular footing attached to the monopile

at the mudline. A 2D analogy of this system is that of a retaining wall with a stabilising base (Powrie and Daly, 2007). The role of the footing is to provide a degree of rotational restraint at the pile head, leading to an improvement in the lateral resistance of the pile. It has also been shown that the use of a relatively thick pile cap leads to an increase in the lateral resistance through the development of passive soil wedges (Mokwa, 1999), in a similar way to the behaviour of skirted foundations (Bransby and Randolph, 1998).

Both lateral pile analysis and bearing capacity analysis is required for analyzing the hybrid system as an individual foundation unit. The lateral response of piles is well reported in the literature and various methods of analysis have been proposed by numerous researchers. Reese *et al.* (1974), Duncan *et al.* (1994) and Zhang *et al.* (2005) have reported the results of their investigation for the case of laterally loaded single piles. Also, Randolph (1971) developed a very useful method of analysis for analysing piles and pile groups. The effect of the addition of pile caps has also been reported by Broms (1954) and Poulos (1971), as well as Matlock and Reese (1960) for the particular case of single piles with double pinned head condition. Where the plate diameter is relatively small, the system is similar to a single capped pile, for which methods have been developed for analysing the influence of the pile and pile cap under axial loading (Poulos and Randolph, 1983), and the effect of the pile cap on the lateral performance of single piles has also been investigated by others (Kim *et al.*, 1979), (Mokwa and Duncan, 2001: 2003), (Maharaj, 2003).

Also, the bearing capacity problem has been thoroughly investigated under different loading conditions relevant to offshore foundations, see for example references Houlsby and Puzrin (1999), and Gourvenec and Randolph (2003).

2 RECENT RESEARCH

A single gravity study carried out on the hybrid system in sand (Stone *et al.*, 2007) suggested that the additional rotation restraint provided by the footing can result in a stiffer lateral response of the pile and greater ultimate lateral load. The degree of restraint at the pile head was dependent on the size of the footing, the initial contact between the soil and the footing and the stiffness of the soil beneath the footing. Observations of heaved and displaced soil in front of the edge of the footing also suggested that a degree of passive soil resistance is likely to be generated under the lateral movement and rotation of the footing.

A comprehensive series of single gravity tests carried out on the hybrid system in sand where the elements affecting the overall performance of the foundation system was investigated in depth was reported by Arshi (2011), and Arshi and Stone (2011, 2012a, 2012b). It was reported that the size for the footing has a direct effect on the overall lateral bearing capacity of the foundation system. Furthermore it was reported that the ratio between the vertical and horizontal load has a significant effect on the lateral performance of the foundation system where larger vertical loads tend to improve the lateral bearing capacity of the hybrid system. The connection between the footing and the pile was also investigated where it was suggested that the hybrid foundation system tends to be more effective if vertical movements are allowed at the pile-footing connection. This movement allows the footing to act independently from the pile where the positive contact between the footing and the soil underneath is solely controlled by the vertical load acting on the footing.

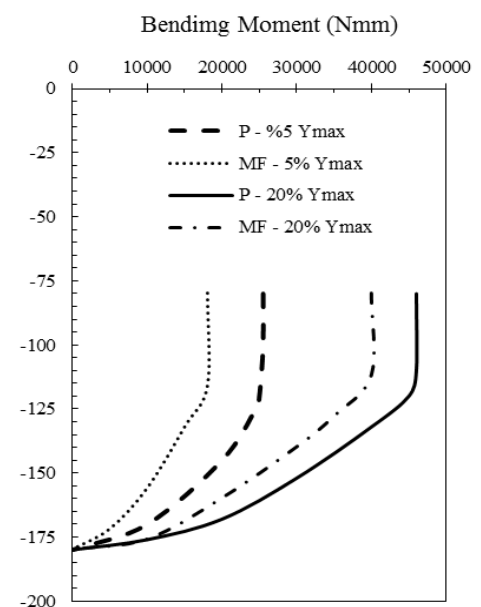


Figure 2. Bending moment distribution comparison (Arshi *et al.* 2013). Note that P, MF and Ymax refer to pile only, monopole-footing and deflection at 1 pile diameter, respectively.

The results of a series of more comprehensive single gravity tests together with preliminary centrifuge tests in sand were carried out and the results were reported by Arshi *et al.* (2013). In the case of single gravity tests, skirts with different lengths were added to the footing. The tests were conducted in sand and the results indicated that the presence of the skirts has a relatively significant contribution on the lateral load capacity of the system. The results show that adding the skirts to the footing and increasing the skirt length tends to increase the lateral bearing capacity of the foundation system by about 50% in

comparison to a non-skirted hybrid system. It is also apparent that footings with very short skirts do not tend to show any ‘apparent’ additional advantage to that without the skirt. Furthermore, bending moment versus depth plots were extracted from instrumented piles tested in centrifuge at 50g, for piles with and without the footings (see Figure 2) and indicated the additional capacity enhanced by the addition of the footing.

3 CENTRIFUGE TESTS

The soil used for the tests was a rounded to sub-rounded fine grained, uniformly graded, quartz sand with an average particle size of 0.25mm (Fraction D from David Ball Ltd.). The maximum and minimum void ratios were determined to be 1.06 and 0.61 respectively. These correspond to dry unit weights of 12.6 and 16.5 kN/m³. The critical state friction angle, determined from direct shear testing, was 32 degrees. The sample were prepared by dry pluviation of sand into a 320mm diameter 180mm deep circular tub, and the tub was then placed mounted into a square strongbox.

The model foundation system was fabricated from a 10mm diameter thin-walled, open-ended steel tube ($t=0.5$ mm). The bearing plate was 80mm diameter (4m prototype) and formed from a 5mm thick aluminium plate with a clamping arrangement allowing the location of the plate to be varied in relation to the pile, i.e. the length of pile protruding below the plate can be adjusted. This is equivalent to a 0.5m diameter, 4m long pile with a 4m diameter footing.

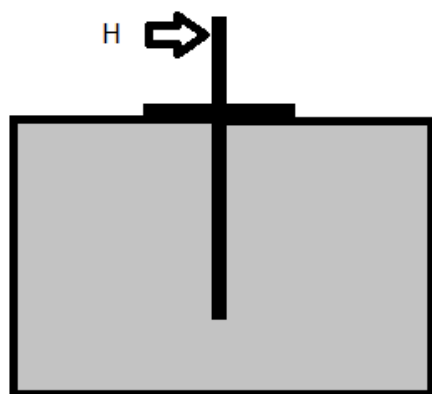


Figure 3. Loading arrangement for centrifuge tests. The lateral load H was purely horizontal.

All the centrifuge model tests were conducted on the GT6/0.75 geotechnical beam centrifuge at the University of Brighton, Brighton.

The samples were prepared by air pulvation of sand with a unit weight of 16.5 kN/m³, void ratio of 0.89 and a relative density of 94%. On completion of

pouring the sand bed, the strongbox was mounted onto the centrifuge platform.

The installation method consisted of pushing the pile by hand to about 40% of its desired penetration depth and then final driving of the pile by light tapping with a hammer to the desired depth of installation. The footing was then slid along the pile down to the soil surface, care was taken to ensure that the bearing plate was in firm contact with the soil surface on completion of installation. For tests when only the vertical capacity of the hybrid system was required, the bearing plate was fixed to the pile shaft some 5-10mm clear of the soil surface.

Vertical load of the model foundation was provided via placing weights right on top of the footing. Lateral loading was provided using a steel wire looped around the pile at 80mm from the mudline in order to create rather high bending moments, and was connected to a load actuator. A linear variable differential transformer (LVDT) was used to record the lateral displacement at the pile head. All the centrifuge tests were conducted at 50 gravities.

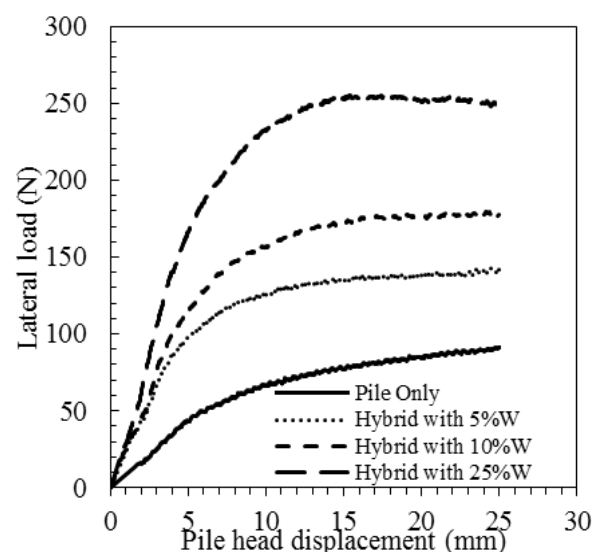


Figure 4. Load vs. deflection test results at 50g

The results of the centrifuge tests showing the lateral load deflection response of the pile against hybrid system are presented in Figure 4. Here all tests are carried out with a constant pile length (80mm) and the results here show the obvious advantage of the addition of the plate. It is worthwhile noting that the lateral response of the single piles is almost linearly increasing with deflection, and deciding the value of the ultimate load is often down to interpretation and deflection based in practice. However, the addition of the footing to the pile makes this behaviour at higher loads rather more distinct and similar to the overall response of an eccentrically loaded circular

footing. This, in return, makes choosing the value of the ultimate load less of a challenge.

The impact of the lateral bearing capacity of the hybrid system, previously reported in single gravity tests by Arshi and Stone (2012a; 2012b) and Arshi *et al.* (2013) was examined here in the centrifuge. In order to fully assess this, first the ultimate bearing capacity of the footing was estimated experimentally. Then 5%, 10% and 25% of that capacity was applied vertically as a dead load to the footing prior to the application the lateral load. The benefits of the presence as well as the magnitude of pre loading is well illustrated in Figure 4 where the ultimate lateral loads increase by 136%, 175% and 252%. At low deflections (equivalent to 5% of piles diameter) this increase is 92%, 140% and 357%, respectively for 5%, 10% and 25% bearing loads. This is indicative of the importance of the presence and magnitude of bearing load.

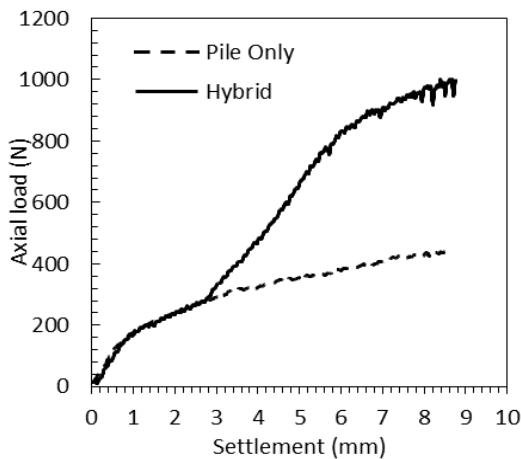


Figure 5. Response of the hybrid system under axial load at 50g

Another significant advantage of the hybrid system, as apparent from Figure 4, is the increase in secant stiffness. This becomes particularly important at small deflections (less than 5% of piles diameter) where the initial stiffness increases by 100% when the footing is added to the pile. The results show that this increase is independent of the magnitude of bearing load at deflecting equivalent to 5% of piles diameter (in particular 10% pile diameter deflection) and minimum bearing load is required in order to maintain this initial stiffness.

In order to examine the relationship between load-deflection initial stiffness and the contribution that the addition of footing makes in terms of initial stiffness, the hybrid system was tested under purely axial load and was compared against the monopile. For the case of the hybrid test, the footing was set about 3mm from mudline in order to see how the slope of the gradient of the settlement graph changes when the footing starts to have contact with soil and

the results are presented in Figure 5. This is almost identical up until about 3mm settlement for both the pile only and hybrid however after 3mm the advantage of the addition of plate is apparent. This suggests that axial bearing capacity is predominantly dominated by the footing component.

4 3D FINITE ELEMENT MODELLING

The 3D finite element analyses were performed using Imperial College Finite Element Program (ICFEP; Potts and Zdravkovic, 1999) which involved scaling up the centrifuge tests and modelling the equivalent prototype.

The aim here was to replicate the centrifuge tests in prototype dimensions and compare the load versus deflection response of the 3D FE results with the centrifuge tests (scaled to prototype). The foundation system was modelled as a prototype installed in the middle of a 30m diameter and 30m long soil model. The construction sequence followed exactly the same steps as the centrifuge tests and lateral load was applied incrementally in order to produce the load versus deflection response. The constitutive model used for modelling all soil units was the non-linear elasto-plastic Mohr-Coulomb model. Jardine *et al.* (1986) small strain stiffness model was utilised for taking into account nonlinearity below yield. This model takes into account the variation of normalised shear and bulk stiffnesses, with deviatoric and volumetric strains. The input parameters including the small strain stiffness model parameters used were the ones recommended by Zdravkovic *et al.* (2005) for Thanet sand that was used for the centrifuge tests.

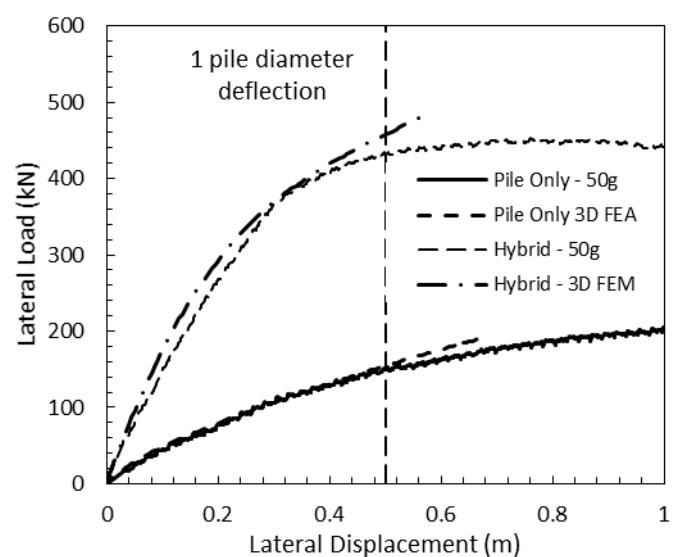


Figure 6. Centrifuge and ICFEP test results

Due to geometric and loading symmetry, only half of the foundation system was modelled as a 3D prob-

lem, which was done as a means of increasing the efficiency of the calculation.

The results of the load-deflection test are shown in Figure 6. As apparent from the figure, for both pile only and hybrid cases, the results shows a very good match between the centrifuge and 3D model tests. The red line on the graph marks deflection at one pile diameter (0.5m) and up until this point the match between the centrifuge and numerical tests are 97% for the pile test and 92% for the hybrid test, both of which show an extremely good match. It is important to note that 98% match between the centrifuge and numerical models at defections smaller than 5% of piles diameter.

Furthermore, the deflections along pile length for the Hybrid test is shown in Figure 7 which shows 2.8m to be the point of rotation. Comparing this with the point of rotation for the pile only test, for a given load, the presence of the footing tends to reduce the movements along the pile and movements associated with the flow of soil near mudline. This may be considered an advantage (as less soil movement takes place for a given load) in cases where minimising load associated movements has to be kept at minimum. Also, it was observed that increasing the magnitude of vertical load acting on the footing has a further movement-associated effect where for a given lateral load, higher dead loads lead to smaller deflections long the pile.

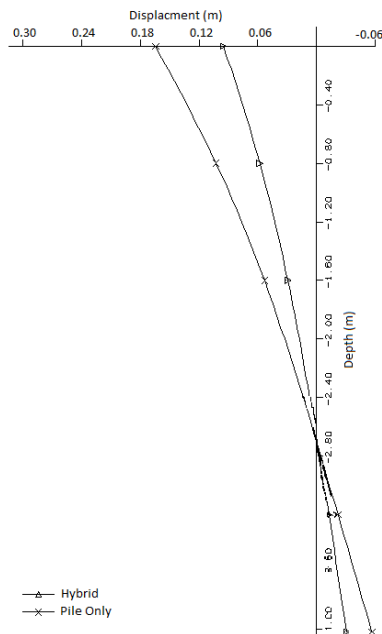


Figure 7. Displacement profile long the pile from ICFEP

Figure 8 shows stress contours for total mean stress at one pile diameter deflection (0.5m). The results here illustrate the reduced contact area and the rotation of the footing about its centroid. This centroid was found to be half of the radius of the footing which also agrees well with the results reported by Stone *et al.* (2007) as well as the empirical relationship developed and used for the 2D analysis and de-

sign charts developed reported by Arshi *et al.* (2013).

5 CONCLUSION

Centrifuge tests coupled with 3D finite element analyses showed that the addition of a circular footing to the pile leads to a significant improvement in the lateral bearing capacity of the foundation system. This is a result of the provision of a high rotational stiffness that leads to higher bearing pressure under half of the circular footing. Also the addition of the footing leads to a reduction of soil and pile movements associated with the lateral loads at mudline. Another very important factor that controls the magnitude of the lateral bearing capacity is the value of deadweight and it was illustrated that this value could be kept at minimum (equivalent to 5% of the bearing capacity of the footing applied vertically) for conditions where deflections are up to 5% of pile diameter.

The results presented in this paper further verifies the huge potential benefit of this system. For typical offshore piles this design method helps increasing the lateral capacity of the pile in sand without increasing pile diameter nor its penetration depth.

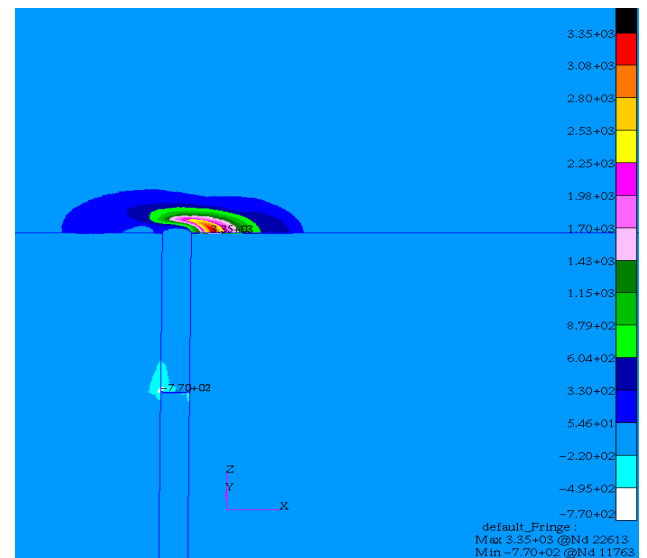


Figure 8. Stress contour from 3D model tests

6 REREFENCES

- Arshi HS. (2011). Structural behavior and performance of skirted hybrid monopile-footing foundations for offshore oil and gas facilities. *Proceedings of the Institution of Structural Engineers: Young Researchers Conference '11*. London: IStructE Publications, 8.
- Arshi HS and Stone KJL. (2011). An investigation of a rock socketed pile with an integral bearing plate founded over weak rock. *Proceedings of*

- the 15th European Conference of Soil Mechanics and Geotechnical Engineering. Amsterdam: Ios Pr Inc, 705 – 711. ISBN 1607508001
- Arshi HS and Stone KJL. (2012). Lateral resistance of hybrid monopile-footing foundations in cohesionless soils for offshore wind turbines. *Proceedings of the 7th International Conference on Offshore Site Investigation and Geotechnics*. London: Society for Underwater Technology, 519 – 526. ISBN 0906940532
- Arshi HS and Stone KJL. (2012) Increasing the lateral resistance of offshore monopile foundations: hybrid monopile-footing foundation system. In: *Proceedings of the 3rd International Conference on Engineering, project and production management, Brighton, September 10th – 11th 2012*. Brighton: University of Brighton, pp. 217-226. ISBN 9781905593866
- Arshi HS, Stone KJL, Vaziri M, Newson T, El-Marasi M, Taylor RN and Goody R. (2013). Physical model testing of hybrid monopile-footing foundation system in sand for offshore structures. In: *Proceeding of the 19th International Conference on Soil Mechanics and Geotechnical Engineering*, Paris, Sep 2nd 2013. Pp. 2307-2310. ISBN 9782859784744
- Bransby MF and Randolph MF. (1998). Combined loading of skirted foundations. *Géotechnique*. 48(5), 637–655.
- Broms BB. (1964). Lateral resistance of piles in cohesionless soils. *ASCE Journal of the Soil Mechanics and Foundation Division*. 90(SM3), 123-156.
- Duncan JM, Evans LT and Ooi PS. (1994). Lateral load analysis of single piles and drilled shafts. *ASCE Journal of Geotechnical Engineering*. 120(6), 1018-1033.
- El-Marassi M, Newson T, El-Naggar H and Stone KJL. (2008). Numerical modelling of the performance of a hybrid monopiled-footing foundation. *Proceedings of the 61st Canadian Geotechnical Conference, GeoEdmonton 2008*. Edmonton, (Paper No. 480), 97 – 104.
- Gourvenec S and Randolph M. (2003). Effect of strength non-homogeneity on the shape of failure envelopes for combined loading of strip and circular foundations on clay. *Géotechnique*. 53(6), 575–586.
- Houlsby GT and Puzrin AM. (1999). The bearing capacity of a strip footing on clay under combined loading. *Proc. R. Soc. London Ser. A*. 455, 893–916.
- Jardine RJ, Potts DM and Fourie AB. (1986). Studies of the influence of non-linear stress-strain characteristics in soil-structure interaction. *Geotechnique*. 36(3). 377-396.
- Kim JB, Singh LP and Brungraber RJ. (1979). Pile cap soil interaction from full scale lateral load tests. *ASCE Journal of Geotechnical Engineering*. 105(5), 643-653.
- Maharaj DK. (2003). Load-deflection response of laterally loaded single pile by nonlinear finite element analysis. *EJEG*.
- Matlock H and Reese LC. (1960). Generalized solutions for laterally loaded piles. *ASCE Journal of Soil Mechanics and Foundations Division*. 86(SM5), 63-91.
- Mokwa RL. (1999). Investigation of the Resistance of Pile Caps to Lateral Loading. *Ph.D Thesis*. Virginia Polytechnic Institute, Blacksburg, Virginia.
- Mokwa RL and Duncan JM. (2001). Experimental evaluation of lateral-load resistance of pile caps. *ASCE Journal of Geotechnical and Geoenvironmental Engineering*. 127(2), 185 - 192.
- Mokwa RL and Duncan JM. (2003). Rotational restraint of pile caps during lateral loading. *ASCE Journal of Geotechnical and Geoenvironmental Engineering*. 129(9), 829 - 837.
- Potts DM and Zdravcokic L. (1999). Finite element analysis in geotechnical engineering: theory. London, Thomas Telford.
- Poulos HG. (1971). Behaviour of laterally loaded piles: Part I-single piles. *ASCE Journal of the Soil Mechanics and Foundations Division*. 97(SM5), 711-731.
- Poulos HG and Randolph MF. (1983). Pile group analysis: a study of two methods. *ASCE Journal of Geotechnical Engineering*. 109(3), 355-372.
- Powrie W, and Daly MP. (2007). Centrifuge modelling of embedded retaining wall with stabilising bases. *Geotechnique*. 57(6), 485-497.
- Randolph MF. (1981). The response of flexible piles to lateral loading. *Géotechnique*. 31(2), 247-259.
- Reese LC, Cox WR and Koop FD. (1974). Analysis of laterally loaded piles in sand. *Offshore Technology Conference*. Vol. II (Paper No. 2080), 473-484.
- Stone KJL, Newson TA and Sandon J. (2007). An investigation of the performance of a ‘hybrid’ monopile-footing foundation for offshore structures. *Proceedings of 6th International on Offshore Site Investigation and Geotechnics*. London: SUT, 391-396.
- Stone KJL, Newson TA and El Marassi, M. (2010). An investigation of a monopiled-footing foundation. *International Conference on Physical Modelling in Geotechnics, ICPMG2010*. Rotterdam: Balkema, 829-833.
- Stone KJL, Newson TA, El Marassi M, El Naggar H, Taylor RN, and Goodey RA (2011). An investigation of the use of bearing plate to enhance the bearing capacity of monopile foundations. *International Conference on Frontiers in Offshore Geotechnics II - ISFOG*. London: Taylor and Francis Group, 623-628.
- Zdravkovic L, Potts DM and St. John HD. (2005). Modelling of a 3D excavation in finite element analysis. *Geotechnique*. Vol. 55(7), 497-513.
- Zhang L, Silva F and Grismala R. (2005) Ultimate lateral resistance to piles in cohesionless soils. *Journal of Geotechnical and Geoenvironmental Engineering*. Vol. 131(1), 78–83.

8. REFERENCES

- Arshi HS. (2011). Structural behavior and performance of skirted hybrid monopile-footing foundations for offshore oil and gas facilities. *Proceedings of the Institution of Structural Engineers: Young Researchers Conference '11*. London: IStructE Publications, 8.
- Arshi HS and Stone KJL. (2011). An investigation of a rock socketed pile with an integral bearing plate founded over weak rock. *Proceedings of the 15th European Conference of Soil Mechanics and Geotechnical Engineering*. Amsterdam: Ios Pr Inc, 705 – 711. ISBN 1607508001
- Arshi HS and Stone KJL. (2012). Lateral resistance of hybrid monopile-footing foundations in cohesionless soils for offshore wind turbines. *Proceedings of the 7th International Conference on Offshore Site Investigation and Geotechnics*. London: Society for Underwater Technology, 519 – 526. ISBN 0906940532
- Arshi HS and Stone KJL. (2012) Increasing the lateral resistance of offshore monopole foundations: hybrid monopile-footing foundation system. *In: Proceedings of the 3rd International Conference on Engineering, project and production management, Brighton, September 10th – 11th 2012*. Brighton: University of Brighton, pp. 217-226. ISBN 9781905593866
- Arshi HS, Stone KJL, Vaziri M, Newson T, El-Marasi M, Taylor RN and Goody R. (2013). Physical model testing of hybrid monopile-footing foundation system in sand for offshore structures. *In: Proceeding of the 19th International Conference on Soil Mechanics and Geotechnical Engineering*, Paris, Sep 2nd 2013. Pp. 2307-2310. ISBN 9782859784744
- Bransby MF and Randolph MF. (1998). Combined loading of skirted foundations. *Géotechnique*. 48(5), 637–655.
- Broms BB. (1964). Lateral resistance of piles in cohesionless soils. *ASCE Journal of the Soil Mechanics and Foundation Division*. 90(SM3), 123-156.
- Carder, D.R & Brookes N.J (1993). Discussion. In *Retaining Structures* (ed. C.R.I Clayton), London, Thomas Telford, 498-501.
- Carder, D.R., Watson, G.V.R., Chandler R.J & Powrie W (1999) Long term performance of an embedded retaining wall with a stabilizing base. *Proc. Instn. Civ. Engrs Geotech. Engng* 137, No. 2, 63-74.
- Chalkidis A (2005) Model study of a hybrid foundation system. Final year project, University of Brighton.
- Duncan JM, Evans LT and Ooi PS. (1994). Lateral load analysis of single piles and drilled shafts. *ASCE Journal of Geotechnical Engineering*. 120(6), 1018-1033.
- El-Marassi M, Newson T, El-Naggar H and Stone KJL. (2008). Numerical modelling of the performance of a hybrid monopiled-footing foundation. *Proceedings of the 61st Canadian Geotechnical Conference, GeoEdmonton 2008*. Edmonton, (Paper No. 480), 97 – 104.
- Gourvenec S and Randolph M. (2003). Effect of strength non-homogeneity on the shape of failure envelopes for combined loading of strip and circular foundations on clay. *Géotechnique*. 53(6), 575–586.

-
- Houlsby GT and Puzrin AM. (1999). The bearing capacity of a strip footing on clay under combined loading. *Proc. R. Soc. London Ser. A*. 455, 893–916.
- Jardine RJ, Potts DM and Fourie AB. (1986). Studies of the influence of non-linear stress-strain characteristics in soil-structure interaction. *Geotechnique*. 36(3). 377-396.
- Kim JB, Singh LP and Brungraber RJ. (1979). Pile cap soil interaction from full scale lateral load tests. *ASCE Journal of Geotechnical Engineering*. 105(5), 643-653.
- Maharaj DK. (2003). Load-deflection response of laterally loaded single pile by nonlinear finite element analysis. *EJEG*.
- Matlock H and Reese LC. (1960). Generalized solutions for laterally loaded piles. *ASCE Journal of Soil Mechanics and Foundations Division*. 86(SM5), 63-91.
- Mokwa RL. (1999). Investigation of the Resistance of Pile Caps to Lateral Loading. *Ph.D Thesis*. Virginia Polytechnic Institute, Blacksburg, Virginia.
- Mokwa RL and Duncan JM. (2001). Experimental evaluation of lateral-load resistance of pile caps. *ASCE Journal of Geotechnical and Geoenvironmental Engineering*. 127(2), 185 - 192.
- Mokwa RL and Duncan JM. (2003). Rotational restraint of pile caps during lateral loading. *ASCE Journal of Geotechnical and Geoenvironmental Engineering*. 129(9), 829 - 837.
- Potts DM and Zdravcokic L. (1999). Finite element analysis in geotechnical engineering: theory. London, Thomas Telford.
- Poulos HG. (1971). Behaviour of laterally loaded piles: Part I-single piles. *ASCE Journal of the Soil Mechanics and Foundations Division*. 97(SM5), 711-731.
- Poulos HG and Randolph MF. (1983). Pile group analysis: a study of two methods. *ASCE Journal of Geotechnical Engineering*. 109(3), 355-372.
- Poulos HG and Davis E (1980) *Pile Foundation Analysis and Design*, Wiley and Sons.
- Poulos HG and Davis E (1974) *Elastic Solutions for Soil and Rock*.
- Powrie W, and Daly MP. (2007). Centrifuge modelling of embedded retaining wall with stabilising bases. *Geotechnique*. 57(6), 485-497.
- Randolph MF. (1981). The response of flexible piles to lateral loading. *Geotechnique*. 31(2), 247-259.
- Reese LC, Cox WR and Koop FD. (1974). Analysis of laterally loaded piles in sand. *Offshore Technology Conference*. Vol. II (Paper No. 2080), 473-484.
- Stone KJL, Newson TA and Sandon J. (2007). An investigation of the performance of a 'hybrid' monopole-footing foundation for offshore structures. *Proceedings of 6th International on Offshore Site Investigation and Geotechnics*. London: SUT, 391-396.
- Stone KJL, Newson TA and El Marassi, M. (2010). An investigation of a monopiled-footing foundation. *International Conference on Physical Modelling in Geotechnics, ICPMG2010*. Rotterdam: Balkema, 829-833.

Stone KJL, Newson TA, El Marassi M, El Nagggar H, Taylor RN, and Goodey RA (2011). An investigation of the use of bearing plate to enhance the bearing capacity of monopile foundations. *International Conference on Frontiers in Offshore Geotechnics II - ISFOG*. London: Taylor and Francis Group, 623-628.

Stone K.J.L and D.M Wood (1992) "Effects of Dilatancy and Particle Size Observed in Model Tests on Sand", *Soils and Foundations*, Vol 32, No. 4, 43-57.

Stone KJL 1988 Modelling of rupture Development in soils, PhD University of Cambridge.

Zdravkovic L, Potts DM and St. John HD. (2005). Modelling of a 3D excavation in finite element analysis. *Geotechnique*. Vol. 55(7), 497-513.

Zhang L, Silva F and Grismala R. (2005) Ultimate lateral resistance to piles in cohesionless soils. *Journal of Geotechnical and Geoenvironmental Engineering*. Vol. 131(1), 78–83.

Ganendra D, Potts DM, 1995, Application of the Fourier series aided finite element method to elasto-plastic problems, *4th Int. Conf. Computational Plasticity*, Barcelona, Publisher: Pinewood Press, Pages: 201-212

9. TABLES

Table 4.1. Details of 1g monopile tests

Model ID	D (mm)	Z (mm)	d (mm)	D/d	V (N)	P-F Connectivity
P.F40.W1.FX	10	150	40	0.25	10	Coupled
P.F40.W1.FR	10	150	40	0.25	10	Decoupled
P.F40.W2.FX	10	150	40	0.25	50	Coupled
P.F40.W2.FR	10	150	40	0.25	50	Decoupled
P.F60.W1.FX	10	150	60	0.17	10	Coupled
P.F60.W1.FR	10	150	60	0.17	10	Decoupled
P.F60.W2.FX	10	150	60	0.17	50	Coupled
P.F60.W2.FR	10	150	60	0.17	50	Decoupled
P.F80.W1.FX	10	150	80	0.125	10	Coupled
P.F80.W1.FR	10	150	80	0.125	10	Decoupled
P.F80.W2.FX	10	150	80	0.125	50	Coupled
P.F80.W2.FR	10	150	80	0.125	50	Decoupled
P.F40.W5.FR.L80	10	80	40	0.25	50	Decoupled
P.F40.W5.FR.L120	10	120	40	0.25	50	Decoupled
P.F60.W5.FR.L60	10	60	60	0.17	50	Decoupled
P.F60.W5.FR.L120	10	120	60	0.17	50	Decoupled
P.F60.W5.FR.L180	10	180	60	0.17	50	Decoupled
P.F80.W5.FR.L80	10	80	80	0.125	50	Decoupled
P.F80.W5.FR.L160	10	160	80	0.125	50	Decoupled
P.F80.W5.FR.L200	10	200	80	0.125	50	Decoupled

Details of skirted 1g monopile-footing tests

Model ID	D (mm)	Z (mm)	d (mm)	D/d	ts (mm)	l (mm)	l/d	V (N)	P-F Connectivity
P.F40.S1.W1.FX	10	150	40	0.25	1	12	0.3	10	Coupled
P.F40.S1.W1.FR	10	150	40	0.25	1	12	0.3	10	Decoupled
P.F40.S2.W1.FX	10	150	40	0.25	1	24	0.6	10	Coupled
P.F40.S2.W1.FR	10	150	40	0.25	1	24	0.6	10	Decoupled
P.F40.S3.W1.FX	10	150	40	0.25	1	36	0.9	10	Coupled
P.F40.S3.W1.FR	10	150	40	0.25	1	36	0.9	10	Decoupled
P.F40.S1.W5.FX	10	150	40	0.25	1	12	0.3	50	Coupled
P.F40.S1.W5.FR	10	150	40	0.25	1	12	0.3	50	Decoupled
P.F40.S2.W5.FX	10	150	40	0.25	1	24	0.6	50	Coupled
P.F40.S2.W5.FR	10	150	40	0.25	1	24	0.6	50	Decoupled
P.F40.S3.W5.FX	10	150	40	0.25	1	36	0.9	50	Coupled
P.F40.S3.W5.FR	10	150	40	0.25	1	36	0.9	50	Decoupled
P.F60.S1.W1.FX	10	150	60	0.17	1	18	0.3	10	Coupled
P.F60.S1.W1.FR	10	150	60	0.17	1	18	0.3	10	Decoupled
P.F60.S2.W1.FX	10	150	60	0.17	1	36	0.6	10	Coupled
P.F60.S2.W1.FR	10	150	60	0.17	1	36	0.6	10	Decoupled
P.F60.S3.W1.FX	10	150	60	0.17	1	54	0.9	10	Coupled
P.F60.S3.W1.FR	10	150	60	0.17	1	54	0.9	10	Decoupled
P.F60.S1.W5.FX	10	150	60	0.17	1	18	0.3	50	Coupled
P.F60.S1.W5.FR	10	150	60	0.17	1	18	0.3	50	Decoupled
P.F60.S2.W5.FX	10	150	60	0.17	1	36	0.6	50	Coupled
P.F60.S2.W5.FR	10	150	60	0.17	1	36	0.6	50	Decoupled
P.F60.S3.W5.FX	10	150	60	0.17	1	54	0.9	50	Coupled
P.F60.S3.W5.FR	10	150	60	0.17	1	54	0.9	50	Decoupled
P.F80.S1.W1.FX	10	150	80	0.125	1	24	0.3	10	Coupled
P.F80.S1.W1.FR	10	150	80	0.125	1	24	0.3	10	Decoupled
P.F80.S2.W1.FX	10	150	80	0.125	1	48	0.6	10	Coupled
P.F80.S2.W1.FR	10	150	80	0.125	1	48	0.6	10	Decoupled
P.F80.S3.W1.FX	10	150	80	0.125	1	72	0.9	10	Coupled
P.F80.S3.W1.FR	10	150	80	0.125	1	72	0.9	10	Decoupled
P.F80.S1.W5.FX	10	150	80	0.125	1	24	0.3	50	Coupled
P.F80.S1.W5.FR	10	150	80	0.125	1	24	0.3	50	Decoupled
P.F80.S2.W5.FX	10	150	80	0.125	1	48	0.6	50	Coupled
P.F80.S2.W5.FR	10	150	80	0.125	1	48	0.6	50	Decoupled
P.F80.S3.W5.FX	10	150	80	0.125	1	72	0.9	50	Coupled
P.F80.S3.W5.FR	10	150	80	0.125	1	72	0.9	50	Decoupled

Pile only tests

Model ID	Z (mm)	D (mm)	V (N)
P.W0	150	10	0
P.W1	150	10	10
P.W5	150	10	50
P.W5.L60	60	10	50
P.W5.L80	80	10	50
P.W5.L120	120	10	50
P.W5.L180	180	10	50
P.W5.L200	200	10	50

Table 4.2. Details of footing tests

Model ID	d (mm)	e (mm)
F40.M	40	0
F60.M	60	0
F80.M	80	0
F40.E1	40	9.50
F40.E2	40	16
F60.E1	60	9
F60.E2	60	17
F60.E3	60	26
F80.E1	80	9
F80.E2	80	21
F80.E3	80	33.50

Table 4.3. Skirted footing tests

ID	ts (mm)	l (mm)	d (mm)	l/d
F40.S01.M	1	12	40	0.3
F40.S02.M	1	24	40	0.6
F40.S03.M	1	36	40	0.9
F60.S01.M	1	18	60	0.3
F60.S02.M	1	36	60	0.6
F60.S03.M	1	54	60	0.9
F80.S01.M	1	24	80	0.3
F80.S02.M	1	48	80	0.6
F80.S03.M	1	72	80	0.9

Table 5.1: Summary of centrifuge tests

Test ID C - coupled D - decoupled	Pile embed- ment (mm)	Plate diameter (mm)	Plate/pile fixity
C/40/60/1	40	60	Coupled
C/40/60/5	40	60	Coupled
C/40/60/10	40	60	Coupled
C/40/60/25	40	60	Coupled
C/40/80/0	40	80	Coupled
C/40/80/5	40	80	Coupled
C/40/80/10	40	80	Coupled
C/40/80/25	40	80	Coupled
D/40/60/0	40	60	Decoupled
D/40/60/5	40	60	Decoupled
D/40/60/10	40	60	Decoupled
D/40/60/25	40	60	Decoupled
D/40/80/0	40	80	Decoupled
D/40/80/5	40	80	Decoupled
D/40/80/10	40	80	Decoupled
D/40/80/25	40	80	Decoupled
C/80/40/3	80	40	Coupled
C/80/40/5	80	40	Coupled
C/80/40/10	80	40	Coupled
C/80/40/25	80	40	Coupled
C/80/60/1	80	60	Coupled
C/80/60/5	80	60	Coupled
C/80/60/10	80	60	Coupled
C/80/60/25	80	60	Coupled
C/80/80/1	80	80	Coupled
C/80/80/5	80	80	Coupled
C/80/80/10	80	80	Coupled
C/80/80/25	80	80	Coupled
D/80/40/3	80	40	Decoupled

D/80/40/5	80	40	Decoupled
D/80/40/10	80	40	Decoupled
D/80/40/25	80	40	Decoupled
D/80/60/1	80	60	Decoupled
C/80/60/5	80	60	Decoupled
C/80/60/10	80	60	Decoupled
C/80/60/25	80	60	Decoupled
C/80/80/1	80	80	Decoupled
C/80/80/5	80	80	Decoupled
C/80/80/10	80	80	Decoupled
C/80/80/25	80	80	Decoupled

Estimated from axial load test

Table 5.2

Test ID	Pile embed-ment (mm)	Plate diameter (mm)	Total load on system (N)	Load carried by pile (N)*	Load carried by plate (N)	Initial plate bearing pressure (kPa)	Percentage of ultimate bearing pressure (%)
Series 1: Coupled Hybrid Tests							
(Coupled/pile length/plate diameter/% pre-stress)							
C/40/60/1	40	60	276	250	26	9	1
C/40/60/5	40	60	371	250	121	43	5
C/40/60/10	40	60	492	250	242	85	10
C/40/60/25	40	60	854	250	604	214	25
C/40/80/0	40	80	291	250	41	8	1
C/40/80/5	40	80	465	250	215	43	5
C/40/80/10	40	80	679	250	429	85	10
C/40/80/25	40	80	1323	250	1073	214	25
Series 1: Decoupled Hybrid Tests							
(Decoupled/pile length/plate diameter/% pre-stress)							
D/40/60/0	40	60	276	250	26	9	1
D/40/60/5	40	60	371	250	121	43	5
D/40/60/10	40	60	492	250	242	85	10
D/40/60/25	40	60	854	250	604	214	25

D/40/80/0	40	80	291	250	41	8	1
D/40/80/5	40	80	465	250	215	43	5
D/40/80/10	40	80	655	250	415	83	10
D/40/80/25	40	80	1323	250	1073	214	25
Series 2: Coupled Hybrid Tests							
(Coupled/pile length/plate diameter/% pre-stress)							
C/80/40/3	80	40	566	535	31	25	3
C/80/40/5	80	40	589	535	54	43	5
C/80/40/10	80	40	642	535	107	85	10
C/80/40/25	80	40	803	535	268	214	25
C/80/60/1	80	60	561	535	26	9	1
C/80/60/5	80	60	656	535	121	43	5
C/80/60/10	80	60	777	535	242	85	10
C/80/60/25	80	60	1139	535	604	214	25
C/80/80/1	80	80	576	535	41	8	1
C/80/80/5	80	80	750	535	215	43	5
C/80/80/10	80	80	964	535	429	85	10
C/80/80/25	80	80	1608	535	1073	214	25
Series 2: Decoupled Hybrid Tests							
(Decoupled/pile length/plate diameter/% pre-stress)							

D/80/40/3	80	40	31	535	31	25	3
D/80/40/5	80	40	54	535	54	43	5
D/80/40/10	80	40	107	535	107	85	10
D/80/40/25	80	40	268	535	268	214	25
D/80/60/1	80	60	26	535	26	9	1
C/80/60/5	80	60	121	535	121	43	5
C/80/60/10	80	60	242	535	242	85	10
C/80/60/25	80	60	604	535	604	214	25
C/80/80/1	80	80	41	535	41	8	1
C/80/80/5	80	80	215	535	215	43	5
C/80/80/10	80	80	415	535	415	83	10
C/80/80/25	80	80	1073	535	1073	214	25

Estimated from axial load test (refer to figure **)

